

000 CERTIFYING THE FULL YOLO PIPELINE: A PROBA- 001 002 003 004 005 006 007 008 009 010 011 012 013 014 015 016 017 018 019 020 021 022 023 024 025 026 027 028 029 030 031 032 033 034 035 036 037 038 039 040 041 042 043 044 045 046 047 048 049 050 051 052 053 054 055 056 057 058 059 060 061 062 063 064 065 066 067 068 069 070 071 072 073 074 075 076 077 078 079 080 081 082 083 084 085 086 087 088 089 090 091 092 093 094 095 096 097 098 099 100 101 102 103 104 105 106 107 108 109 110 111 112 113 114 115 116 117 118 119 120 121 122 123 124 125 126 127 128 129 130 131 132 133 134 135 136 137 138 139 140 141 142 143 144 145 146 147 148 149 150 151 152 153 154 155 156 157 158 159 160 161 162 163 164 165 166 167 168 169 170 171 172 173 174 175 176 177 178 179 180 181 182 183 184 185 186 187 188 189 190 191 192 193 194 195 196 197 198 199 200 201 202 203 204 205 206 207 208 209 210 211 212 213 214 215 216 217 218 219 220 221 222 223 224 225 226 227 228 229 230 231 232 233 234 235 236 237 238 239 240 241 242 243 244 245 246 247 248 249 250 251 252 253 254 255 256 257 258 259 260 261 262 263 264 265 266 267 268 269 270 271 272 273 274 275 276 277 278 279 280 281 282 283 284 285 286 287 288 289 290 291 292 293 294 295 296 297 298 299 300 301 302 303 304 305 306 307 308 309 310 311 312 313 314 315 316 317 318 319 320 321 322 323 324 325 326 327 328 329 330 331 332 333 334 335 336 337 338 339 340 341 342 343 344 345 346 347 348 349 350 351 352 353 354 355 356 357 358 359 360 361 362 363 364 365 366 367 368 369 370 371 372 373 374 375 376 377 378 379 380 381 382 383 384 385 386 387 388 389 390 391 392 393 394 395 396 397 398 399 400 401 402 403 404 405 406 407 408 409 410 411 412 413 414 415 416 417 418 419 420 421 422 423 424 425 426 427 428 429 430 431 432 433 434 435 436 437 438 439 440 441 442 443 444 445 446 447 448 449 450 451 452 453 454 455 456 457 458 459 460 461 462 463 464 465 466 467 468 469 470 471 472 473 474 475 476 477 478 479 480 481 482 483 484 485 486 487 488 489 490 491 492 493 494 495 496 497 498 499 500 501 502 503 504 505 506 507 508 509 510 511 512 513 514 515 516 517 518 519 520 521 522 523 524 525 526 527 528 529 530 531 532 533 534 535 536 537 538 539 540 541 542 543 544 545 546 547 548 549 550 551 552 553 554 555 556 557 558 559 559 560 561 562 563 564 565 566 567 568 569 569 570 571 572 573 574 575 576 577 578 579 579 580 581 582 583 584 585 586 587 588 589 589 590 591 592 593 594 595 596 597 598 599 599 600 601 602 603 604 605 606 607 608 609 609 610 611 612 613 614 615 616 617 618 619 619 620 621 622 623 624 625 626 627 628 629 629 630 631 632 633 634 635 636 637 638 639 639 640 641 642 643 644 645 646 647 648 649 649 650 651 652 653 654 655 656 657 658 659 659 660 661 662 663 664 665 666 667 668 669 669 670 671 672 673 674 675 676 677 678 679 679 680 681 682 683 684 685 686 687 688 689 689 690 691 692 693 694 695 696 697 698 699 699 700 701 702 703 704 705 706 707 708 709 709 710 711 712 713 714 715 716 717 718 719 719 720 721 722 723 724 725 726 727 728 729 729 730 731 732 733 734 735 736 737 738 739 739 740 741 742 743 744 745 746 747 748 749 749 750 751 752 753 754 755 756 757 758 759 759 760 761 762 763 764 765 766 767 768 769 769 770 771 772 773 774 775 776 777 778 779 779 780 781 782 783 784 785 786 787 788 789 789 790 791 792 793 794 795 796 797 798 799 799 800 801 802 803 804 805 806 807 808 809 809 810 811 812 813 814 815 816 817 818 819 819 820 821 822 823 824 825 826 827 828 829 829 830 831 832 833 834 835 836 837 838 839 839 840 841 842 843 844 845 846 847 848 849 849 850 851 852 853 854 855 856 857 858 859 859 860 861 862 863 864 865 866 867 868 869 869 870 871 872 873 874 875 876 877 878 879 879 880 881 882 883 884 885 886 887 888 889 889 890 891 892 893 894 895 896 897 898 899 899 900 901 902 903 904 905 906 907 908 909 909 910 911 912 913 914 915 916 917 918 919 919 920 921 922 923 924 925 926 927 928 929 929 930 931 932 933 934 935 936 937 938 939 939 940 941 942 943 944 945 946 947 948 949 949 950 951 952 953 954 955 956 957 958 959 959 960 961 962 963 964 965 966 967 968 969 969 970 971 972 973 974 975 976 977 978 979 979 980 981 982 983 984 985 986 987 988 989 989 990 991 992 993 994 995 996 997 998 999 1000 1001 1002 1003 1004 1005 1006 1007 1008 1009 1009 1010 1011 1012 1013 1014 1015 1016 1017 1018 1019 1019 1020 1021 1022 1023 1024 1025 1026 1027 1028 1029 1029 1030 1031 1032 1033 1034 1035 1036 1037 1038 1039 1040 1041 1042 1043 1044 1045 1046 1047 1048 1049 1049 1050 1051 1052 1053 1054 1055 1056 1057 1058 1059 1059 1060 1061 1062 1063 1064 1065 1066 1067 1068 1069 1069 1070 1071 1072 1073 1074 1075 1076 1077 1078 1079 1079 1080 1081 1082 1083 1084 1085 1086 1087 1088 1089 1089 1090 1091 1092 1093 1094 1095 1096 1097 1098 1098 1099 1099 1100 1101 1102 1103 1104 1105 1106 1107 1108 1109 1109 1110 1111 1112 1113 1114 1115 1116 1117 1118 1119 1119 1120 1121 1122 1123 1124 1125 1126 1127 1128 1129 1129 1130 1131 1132 1133 1134 1135 1136 1137 1138 1139 1139 1140 1141 1142 1143 1144 1145 1146 1147 1148 1149 1149 1150 1151 1152 1153 1154 1155 1156 1157 1158 1159 1159 1160 1161 1162 1163 1164 1165 1166 1167 1168 1169 1169 1170 1171 1172 1173 1174 1175 1176 1177 1178 1179 1179 1180 1181 1182 1183 1184 1185 1186 1187 1188 1189 1189 1190 1191 1192 1193 1194 1195 1196 1197 1198 1198 1199 1199 1200 1201 1202 1203 1204 1205 1206 1207 1208 1209 1209 1210 1211 1212 1213 1214 1215 1216 1217 1218 1219 1219 1220 1221 1222 1223 1224 1225 1226 1227 1228 1229 1229 1230 1231 1232 1233 1234 1235 1236 1237 1238 1239 1239 1240 1241 1242 1243 1244 1245 1246 1247 1248 1249 1249 1250 1251 1252 1253 1254 1255 1256 1257 1258 1259 1259 1260 1261 1262 1263 1264 1265 1266 1267 1268 1269 1269 1270 1271 1272 1273 1274 1275 1276 1277 1278 1279 1279 1280 1281 1282 1283 1284 1285 1286 1287 1288 1289 1289 1290 1291 1292 1293 1294 1295 1296 1297 1298 1298 1299 1299 1300 1301 1302 1303 1304 1305 1306 1307 1308 1309 1309 1310 1311 1312 1313 1314 1315 1316 1317 1318 1319 1319 1320 1321 1322 1323 1324 1325 1326 1327 1328 1329 1329 1330 1331 1332 1333 1334 1335 1336 1337 1338 1339 1339 1340 1341 1342 1343 1344 1345 1346 1347 1348 1349 1349 1350 1351 1352 1353 1354 1355 1356 1357 1358 1359 1359 1360 1361 1362 1363 1364 1365 1366 1367 1368 1369 1369 1370 1371 1372 1373 1374 1375 1376 1377 1378 1379 1379 1380 1381 1382 1383 1384 1385 1386 1387 1388 1389 1389 1390 1391 1392 1393 1394 1395 1396 1397 1398 1398 1399 1399 1400 1401 1402 1403 1404 1405 1406 1407 1408 1409 1409 1410 1411 1412 1413 1414 1415 1416 1417 1418 1419 1419 1420 1421 1422 1423 1424 1425 1426 1427 1428 1429 1429 1430 1431 1432 1433 1434 1435 1436 1437 1438 1439 1439 1440 1441 1442 1443 1444 1445 1446 1447 1448 1449 1449 1450 1451 1452 1453 1454 1455 1456 1457 1458 1459 1459 1460 1461 1462 1463 1464 1465 1466 1467 1468 1469 1469 1470 1471 1472 1473 1474 1475 1476 1477 1478 1479 1479 1480 1481 1482 1483 1484 1485 1486 1487 1488 1489 1489 1490 1491 1492 1493 1494 1495 1496 1497 1498 1498 1499 1499 1500 1501 1502 1503 1504 1505 1506 1507 1508 1509 1509 1510 1511 1512 1513 1514 1515 1516 1517 1518 1519 1519 1520 1521 1522 1523 1524 1525 1526 1527 1528 1529 1529 1530 1531 1532 1533 1534 1535 1536 1537 1538 1539 1539 1540 1541 1542 1543 1544 1545 1546 1547 1548 1549 1549 1550 1551 1552 1553 1554 1555 1556 1557 1558 1559 1559 1560 1561 1562 1563 1564 1565 1566 1567 1568 1569 1569 1570 1571 1572 1573 1574 1575 1576 1577 1578 1579 1579 1580 1581 1582 1583 1584 1585 1586 1587 1588 1589 1589 1590 1591 1592 1593 1594 1595 1596 1597 1598 1598 1599 1599 1600 1601 1602 1603 1604 1605 1606 1607 1608 1609 1609 1610 1611 1612 1613 1614 1615 1616 1617 1618 1619 1619 1620 1621 1622 1623 1624 1625 1626 1627 1628 1629 1629 1630 1631 1632 1633 1634 1635 1636 1637 1638 1639 1639 1640 1641 1642 1643 1644 1645 1646 1647 1648 1649 1649 1650 1651 1652 1653 1654 1655 1656 1657 1658 1659 1659 1660 1661 1662 1663 1664 1665 1666 1667 1668 1669 1669 1670 1671 1672 1673 1674 1675 1676 1677 1678 1679 1679 1680 1681 1682 1683 1684 1685 1686 1687 1688 1689 1689 1690 1691 1692 1693 1694 1695 1696 1697 1698 1698 1699 1699 1700 1701 1702 1703 1704 1705 1706 1707 1708 1709 1709 1710 1711 1712 1713 1714 1715 1716 1717 1718 1719 1719 1720 1721 1722 1723 1724 1725 1726 1727 1728 1729 1729 1730 1731 1732 1733 1734 1735 1736 1737 1738 1739 1739 1740 1741 1742 1743 1744 1745 1746 1747 1748 1749 1749 1750 1751 1752 1753 1754 1755 1756 1757 1758 1759 1759 1760 1761 1762 1763 1764 1765 1766 1767 1768 1769 1769 1770 1771 1772 1773 1774 1775 1776 1777 1778 1779 1779 1780 1781 1782 1783 1784 1785 1786 1787 1788 1789 1789 1790 1791 1792 1793 1794 1795 1796 1797 1798 1798 1799 1799 1800 1801 1802 1803 1804 1805 1806 1807 1808 1809 1809 1810 1811 1812 1813 1814 1815 1816 1817 1818 1819 1819 1820 1821 1822 1823 1824 1825 1826 1827 1828 1829 1829 1830 1831 1832 1833 1834 1835 1836 1837 1838 1839 1839 1840 1841 1842 1843 1844 1845 1846 1847 1848 1849 1849 1850 1851 1852 1853 1854 1855 1856 1857 1858 1859 1859 1860 1861 1862 1863 1864 1865 1866 1867 1868 1869 1869 1870 1871 1872 1873 1874 1875 1876 1877 1878 1879 1879 1880 1881 1882 1883 1884 1885 1886 1887 1888 1889 1889 1890 1891 1892 1893 1894 1895 1896 1897 1898 1898 1899 1899 1900 1901 1902 1903 1904 1905 1906 1907 1908 1909 1909 1910 1911 1912 1913 1914

054 Verifying object detection networks with these methods, however, presents additional challenges
 055 beyond the large parameter scales:

056 (1) **Post-Processing Stage:** Critical post-processing steps, such as Non-Maximum Suppression
 057 (NMS) (Neubeck & Van Gool, 2006), generally fall outside the scope of current formal verification
 058 methods (Cohen et al., 2024; Elboher et al., 2024);

059 (2) **Large Input-Output Spaces:** The dimensionality of the detection
 060 inputs and outputs even renders PAC-based methods (Li et al., 2022)
 061 (Li et al., 2022; Blohm et al., 2025; Haussler & Welzl, 1987) computationally infeasible.

062 Due to these limitations, even recent verification methods specifically designed for object detection
 063 (Cohen et al., 2024; Elboher et al., 2024) are restricted to simplified models or do not account
 064 for complex operations such as NMS. To address this gap, we propose a PAC-based **Object Detection**
 065 **Probabilistic Verification** (ODPV) framework for YOLO networks under OD threats. To our knowledge, **this is the first framework that effectively verifies the robustness of the original object**
 066 **detection networks at a practical scale**. Although PAC verification cannot provide deterministic
 067 guarantees, it currently offers the most practical means to validate YOLO in a reasonable time.

069 Our methodology includes three main components: (1) estimating output ranges under input pertur-
 070 bations, (2) formally verifying NMS within the estimated output space, and (3) iteratively refining
 071 verification results. We implement our approach and evaluate it on standard benchmarks. Our main
 072 contributions are as follows.

073 (1) We formally define the PAC verification problem of the **object disappearance-OD** threat in object
 074 detection and propose a novel verification approach to address it.

075 (2) We implement a complete verification process that includes the NMS step, which has been under-
 076 explored in previous work, and provide probabilistic guarantees for each step.

077 (3) We conduct experiments on widely used networks and datasets to evaluate our proposed method.
 078 We demonstrate that our method requires fewer samples to achieve comparable probabilistic guar-
 079 antees and tighter certified Intersection-over-Union (IoU) bounds.

080 In summary, we are the first to address the challenges of verifying large-scale detection networks
 081 and to provide an efficient probabilistic verification method.

083 **Remark 1.** *We emphasize an important distinction: Our work differs from randomized smoothing
 084 in the type of guarantee it provides (Cohen et al., 2019; Yang et al., 2020). Randomized smoothing
 085 establishes robustness for modified, "smoothed" classifiers, not the original detector. In contrast,
 086 we leave the network unchanged and provide statistical guarantees for the original model.*

088 2 RELATED WORK

091 **Object detection.** Early detectors relied on hand-crafted features such as HOG (Dalal & Triggs,
 092 2005) and sliding windows (Viola & Jones, 2001), but lacked adaptability. CNN-based approaches
 093 transformed feature extraction; R-CNN variants (Girshick et al., 2014; Ren, 2015) combined region
 094 proposals with deep learning methods. More recent approaches such as YOLO (Redmon, 2016;
 095 Redmon & Farhadi, 2017; Farhadi & Redmon, 2018; Bochkovskiy et al., 2020b) and SSD (Liu
 096 et al., 2016; 2017) achieved real-time detection in complex scenarios.

097 **Verification techniques for Neural Networks.** Formal verification determines whether a property
 098 holds under given input constraints. State-of-the-art tools (Katz et al., 2017; 2019; Zhang et al.,
 099 2022a; 2018) employ Branch-and-Bound, combining relaxations (Singh et al., 2019; Bak, 2021),
 100 bound propagation (Wang et al., 2018b; Weng et al., 2018; Wang et al., 2018a; Gowal et al., 2019),
 101 and constraint solving (Khedr et al., 2021; Ehlers, 2017; Henriksen & Lomuscio, 2020; Kouvaras &
 102 Lomuscio, 2021). However, for large networks such as YOLO (with $640 \times 480 \times 3$ inputs), even
 103 basic bound propagation may require more than 5000 GB of memory, rendering formal verification
 104 infeasible in practice. To address scalability, probabilistic verification estimates the likelihood of
 105 property satisfaction. Sampling-based methods (Webb et al., 2019; Cardelli et al., 2019; Mangal
 106 et al., 2019; Anderson & Sojoudi, 2023) provide probabilistic estimates, but may miss rare cases,
 107 thereby creating gaps between analysis and actual robustness. DeepPAC (Li et al., 2022) approxi-
 108 mutes local network behavior with linear equations and high-confidence error bounds, but it requires
 109 prohibitively large sample sizes for models such as YOLO. Techniques like median smoothing (Chi-



108
109
110
111
112
113
114
115
116
117
118
119
120
121
122
123
124
125
126
127
128
129
130
131
132
133
134
135
136
137
138
139
140
141
142
143
144
145
146
147
148
149
150
151
152
153
154
155
156
157
158
159
160
161

Figure 1: (First Stage) The network tries to find all boxes that may contain objects. A subset of these boxes is shown here.



Figure 2: (Second Stage) Final output boxes selected by NMS include the corresponding label and its confidence score.

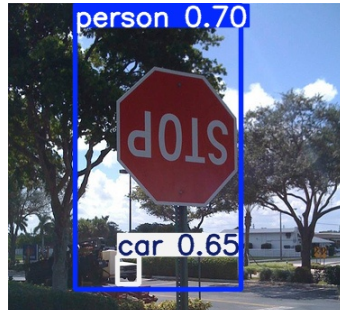


Figure 3: Under imperceptible input perturbations, YOLO can no longer recognize these objects.

ang et al., 2020) certify robustness for a modified, "smoothed" detector, whereas our approach directly verifies the original network.

Verification of Object Detection. Current efforts mainly focus on small or simplified detectors. (Cohen et al., 2024) propagate bounds to certify Intersection-over-Union (IoU), while (Elboher et al., 2024) encode IoU into networks for existing verifiers. Both approaches ignore the NMS step and fail to scale to real-world detectors. Comprehensive verification of complete detection pipelines remains an open problem.

3 PRELIMINARIES

This section outlines the key stages of YOLO object detection, as shown in Fig. 1- 3 with an image from the COCO validation dataset (Lin et al., 2014) and defines the threat of object disappearance.

3.1 KEY STAGES OF YOLO OBJECT DETECTION

Bounding Box Prediction (First Stage). The YOLO network $F : \mathbb{R}^{d_0} \rightarrow \mathbb{R}^{d_L}$ processes an input \mathbf{x} (with dimension d_0) to generate an output $\mathbf{y} = F(\mathbf{x})$ (with dimension d_L). The output \mathbf{y} can be reformulated as a set of bounding boxes $\{box_i\}_{i=1}^{n_{\mathbf{x}}}$, where $n_{\mathbf{x}}$ is a constant determined by the fixed input dimension. Each bounding box box_i is represented as $(x_i, y_i, w_i, h_i, c_i, p_{i1}, p_{i2}, \dots, p_{in})$. Here, (x_i, y_i) denotes the box's center coordinates, (w_i, h_i) its width and height, c_i its confidence score, and p_{ij} the probability of the object belonging to class j (for $j \in [n]$, where n is the total number of classes). The class of box_i is assigned as $\text{Class}(box_i) = \arg \max_{j \in [n]} p_{ij}$. These boxes collectively identify possible object locations in the input image, as Figure 1 illustrates.

Non-Maximum Suppression (Second Stage). Let $\mathbf{y} = F(\mathbf{x})$ be the output tensor from the first stage. The second stage processes \mathbf{y} by using an operator N to select a subset of bounding boxes $\{box_{i_j}\}_{j \in [n_{\mathbf{x}}]} \subseteq \mathbf{y} = \{box_i\}_{i=1}^{n_{\mathbf{x}}}$, forming the final YOLO output (Figure 2). The standard operator N is Non-Maximum Suppression (NMS) (Neubeck & Van Gool, 2006) in YOLO, which uses \mathbf{y} and predefined thresholds $\eta, \iota \in (0, 1)$ to select the final output. For simplicity, we denote this as $N(\mathbf{y})$, as η and ι are fixed, so we omit them. NMS selects boxes based on the following three rules:

- (n1): If $i_j \in [n_{\mathbf{x}}]$ and $box_{i_j} \in N(\mathbf{y})$, then it must satisfy $c_{i_j} \geq \iota$;
- (n2): If $i_j \in [n_{\mathbf{x}}]$ satisfies $box_{i_j} \notin N(\mathbf{y})$ and $c_{i_j} \geq \iota$, then there must exist a $box_{i_k} \in N(\mathbf{y})$ such that $\text{Class}(box_{i_j}) = \text{Class}(box_{i_k})$ and $c_{i_j} \leq c_{i_k}$, $\text{IoU}(box_{i_j}, box_{i_k}) \geq \eta$;
- (n3): If $i_j, i_k \in [n_{\mathbf{x}}]$ such that $box_{i_j}, box_{i_k} \in N(\mathbf{y})$ and $\text{Class}(box_{i_j}) = \text{Class}(box_{i_k})$, then it must satisfy $\text{IoU}(box_{i_j}, box_{i_k}) < \eta$.

The $\text{IoU}(box_1, box_2) = \frac{\text{Area}(box_1 \cap box_2)}{\text{Area}(box_1 \cup box_2)}$ measures overlap between two boxes, where $\text{Area}(box_1 \cap box_2)$ and $\text{Area}(box_1 \cup box_2)$ denote the intersection and union areas. The NMS-selected subset is unique and we focus on its properties, as implementation details are beyond our scope.

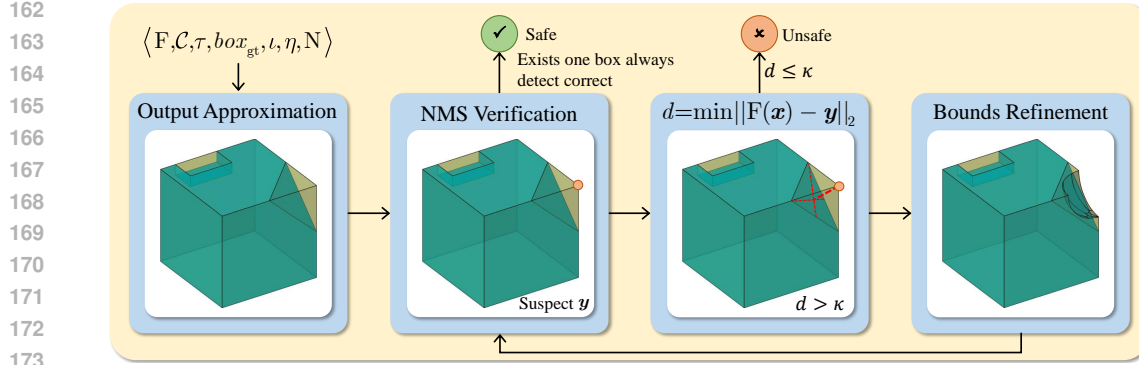


Figure 4: Our verification framework for object detection networks. The green cube represents the network’s **true but unknown output space** under input constraints. The yellow cube is the **over-approximated region** calculated by our method, which is probabilistically guaranteed to contain the true output space. Part 3 of our framework (Refinement) progressively shrinks the yellow region by identifying and excluding areas that do not intersect with the true output space, thereby tightening the verification bounds.

3.2 OBJECT DISAPPEARANCE THREAT ON OBJECT DETECTION

An object detection model successfully detects an object O in the image x if there exists at least one $box_i \in N(F(x))$ satisfying: $\text{Class}(box_i) = \text{Class}(box_{gt})$ and $\text{IoU}(box_i, box_{gt}) \geq \tau$, where τ is a predefined IoU threshold and box_{gt} is O ’s ground truth bounding box. We define the **object disappearance (OD) threat** as follows:

Object Disappearance (OD) Threat Definition. Given ground truth box box_{gt} , perturbation radius ε , IoU threshold τ , and class $\text{Class}(box_{gt})$, OD occurs if there exists a perturbation δ with $\|\delta\|_p \leq \varepsilon$ such that

$$\max_{box_i \in N(F(x+\delta))} \left[\text{IoU}(box_i, box_{gt}) \cdot \mathbb{I}(\text{Class}(box_i) = \text{Class}(box_{gt})) \right] < \tau.$$

where $\mathbb{I}(\cdot)$ denotes an indicator function (returns 1 if true, 0 otherwise).

4 VERIFICATION FRAMEWORK FOR OBJECT DETECTION

In this section, we introduce the verification target and our verification approach.

First, we formally define the OD PAC-Verification problem.

Definition 1 (OD PAC-Verification Problem). Given input constraints \mathcal{C} , IoU threshold τ , error rate $\alpha \in [0, 1]$ and significance level $\beta \in [0, 1]$ and ground truth box box_{gt} , verify whether with confidence at least $1 - \beta$, the following holds:

$$P_{x \sim \mathcal{C}} (\exists box_i \in N(F(x)) \text{ s.t. } [\text{IoU}(box_i, box_{gt}) \geq \tau \wedge \text{Class}(box_i) = \text{Class}(box_{gt})]) \geq 1 - \alpha$$

If true, the system is deemed PAC-safe in \mathcal{C} under τ . This definition reduces to the OD Formal Verification Problem when $\alpha = 0, \beta = 0$. [Here we use \$x \sim \mathcal{C}\$ to denote that \$x\$ is sampled from a distribution over the input constraint set \$\mathcal{C}\$.](#)

Then, we propose a three-part verification framework (see Alg. 1 and Fig. 4) to solve it:

Part 1: Network Output Approximation. For input $x^{(0)}$ and constraint \mathcal{C} , approximate the output set $\{F(x)\}_{x \in \mathcal{C}}$ with a regular region \mathcal{Z} (hyperrectangles/hyperspheres) such that: $\{F(x)\}_{x \in \mathcal{C}} \subseteq \mathcal{Z}$.

Part 2: NMS Verification. Verify whether, for all $y \in \mathcal{Z}$, there exists a $box_i \in N(y)$ that satisfies the OD safety property (Definition 1). If this holds, the detector is safe. Otherwise, identify a y that violates the IoU or class-matching condition.

Part 3: Counterexample Validation and Refinement. Compute $d_{\min} = \min_{x \in \mathcal{C}} \|F(x) - y\|_2$. If $d_{\min} \leq \kappa$ (with $\kappa \geq 0$ as a tolerance), the system is unsafe. Otherwise, refine \mathcal{Z} by excluding

216 **Algorithm 1** Verification framework for the OD PAC-Verification problem

217

218 **Require:**

219 The network F ; the input constraints \mathcal{C} ; the threshold in OD verification problem τ ; the thresh-

220 old for Part Three κ ; the number of refinement steps T ; the ground truth bounding box box_{gt} .

221 **Ensure:**

222 Whether YOLO is safe under OD attack.

223 1: Get \mathcal{Z} over-approximating $\{F(\mathbf{x})\}_{\mathbf{x} \in \mathcal{C}}$ ▷ Part One

224 2: **repeat**

225 3: **if** $\forall \mathbf{y} \in \mathcal{Z}, \exists box_i \in N(\mathbf{y})$ such that $IoU(box_i, box_{gt}) \geq \tau \wedge \text{Class}(box_i) = q$ **then**

226 4: **return** Safe. ▷ $q = \text{Class}(box_{gt})$, Part Two

227 5: **else**

228 6: Get $\mathbf{y}' \in \mathcal{Z}$ violating the specified property ▷ Part Two

229 7: $d_{\min} = \min_{\mathbf{x} \in \mathcal{C}} \|F(\mathbf{x}) - \mathbf{y}'\|_2$ ▷ Part Three

230 8: $\mathcal{Z} = \mathcal{Z} \setminus \mathcal{B}_2(\mathbf{y}', d_{\min})$ ▷ Part Three

231 9: **end if**

232 10: **until** $d_{\min} \leq \kappa$ or refine T steps

233 11: **return** Unsafe ▷ Part Three

234 **Algorithm 2 Algorithm for Part 1:** Network Output Approximation (Part 1)

235

236 **Require:**

237 The neural network F ; the input constraints \mathcal{C} , $\mathbf{N}_1, \mathbf{N}_2 \in \mathbb{Z}^{\pm}$, $\mathbf{N}_1, \mathbf{N}_2 \in \mathbb{Z}^+$, a threshold ζ .

238 **Ensure:**

239 The bounding box \mathcal{Z} .

240 1: $\{\mathbf{x}^{(i)}\}_{i=1}^{N_1} \leftarrow$ Randomly select N_1 points in \mathcal{C} . ▷ Find the \mathbf{v}_{\max}

241 2: **for** $j \in [d_L]$ **do** ▷ Find the \mathbf{v}_{\max}

242 3: $(\mathbf{v}_{\max})_j \leftarrow \max\{\max_i\{|F(\mathbf{x}^{(i)})_j - F(\mathbf{x}^{(0)})_j|\}, \zeta\}$ ▷ Use ζ to prevent division by zero

243 4: **end for**

244 5: $\{\mathbf{z}^{(i)}\}_{i=1}^{N_2} \leftarrow$ Randomly select N_2 points in \mathcal{C} . ▷ Find the c_1

245 6: $c_1 \leftarrow \max_{i \in [N_2], j \in [d_L]} \frac{|F(\mathbf{z}^{(i)}) - F(\mathbf{x}^{(0)})|_j}{(\mathbf{v}_{\max})_j}$. ▷ Find the c_1

246 7: **return** $\mathcal{Z} \leftarrow \{F(\mathbf{x}^{(0)}) + \epsilon : |\epsilon| \leq c_1 \mathbf{v}_{\max}\}$.

247

248

249

250 $\mathcal{B}_2(\mathbf{y}, d_{\min}) = \{\mathbf{y}' : \|\mathbf{y} - \mathbf{y}'\|_2 < d_{\min}\}$ as the regular region we obtained may be larger than the

251 actual output space $\{F(\mathbf{x})\}_{\mathbf{x} \in \mathcal{C}}$, and then go back to Part 2. Note that we limit Part 3 iterations for

252 high-dimensional outputs to prevent computational overload.

253

254 **Remark 2.** Because our goal is PAC verification, each of the three steps is implemented using

255 probabilistic methods with probability guarantees, rather than exact computation, as shown in the

256 next section.

257

258

259 5 VERIFICATION METHOD FOR YOLO OBJECT DETECTION

260

261

262 We illustrate the application of the verification framework from Section 4 to YOLO object detection.

263 Because of YOLO’s complexity and scale, formal verification becomes intractable; therefore, we

264 adopt PAC verification, i.e. black-box verification via sampling. Proofs for Propositions, Lemmas,

265 and Theorems are provided in the Appendix.

266 We define the input constraint as $\mathcal{C} = \{\mathbf{x} : \|\mathbf{x} - \mathbf{x}^{(0)}\|_p \leq \varepsilon\}$ for a given sample $\mathbf{x}^{(0)}$, norm

267 $p \in \mathbb{Z}^+ \cup \{\infty\}$, and perturbation radius $\varepsilon \in (0, 1)$. We consider a probability distribution over

268 the input set \mathcal{C} , and write $\mathbf{x} \sim \mathcal{C}$ to denote that \mathbf{x} is a sample drawn from this distribution. For

269 convenience, we define the comparison $\mathbf{a} \leq \mathbf{b}$ for vectors $\mathbf{a}, \mathbf{b} \in \mathbb{R}^n$ to mean $\forall j \in [n] : a_j \leq b_j$,

where a_j is the j -th component of \mathbf{a} . Similarly, scalar-vector multiplication is defined element-wise.

270 **Algorithm 3** **Algorithm for Part 2:** NMS Verification ([Part 2](#))

271 **Require:** $\{\{box_i^k\}_{i=1}^{n_x}\}_{k \in \Delta}$ reinterpreted from \mathcal{Z} ; IoU threshold τ ; ground truth bounding box box_{gt} .

272 **Ensure:** Either a non-empty safe set $Q(\mathcal{Z}, \tau, box_{gt})$, or an unsafe witness $z \in \mathcal{Z}$.

273 1: $Q \leftarrow \emptyset$.

274 2: **for** $i \in [n_x]$ **do**

275 3: Calculate $\tau_1(i, \mathcal{Z}, box_{gt})$ and $\tau_2(i, \mathcal{Z}, box_{gt})$

276 4: $\tau(i, \mathcal{Z}, box_{gt}) \leftarrow \min(\tau_1(i, \mathcal{Z}, box_{gt}), \tau_2(i, \mathcal{Z}, box_{gt}))$ ▷ Appendix I

277 5: **if** $\tau(i, \mathcal{Z}, box_{gt}) > \tau$ **then** $Q \leftarrow Q \cup \{i\}$ ▷ Lemma 2

278 6: **end if** ▷ Lemma 1

279 7: **end for**

280 8: **if** $Q \neq \emptyset$ **then return** (Safe, Q)

281 9: **else** $i \leftarrow \arg \max_{i \in [n_x]} \{\tau(i, \mathcal{Z}, box_{gt})\}$

282 10: **end if**

283 11: **return** (Unsafe, z) ▷ $z \in \mathcal{Z}$ such that its corresponding box i leads to the value $\tau(i, \mathcal{Z}, box_{gt})$

286

287 **5.1 IMPLEMENTATION PART 1 ON YOLO**

288 Consider a network $F : \mathbb{R}^{d_0} \rightarrow \mathbb{R}^{d_L}$ and an input constraint \mathcal{C} . In Part 1 of our approach, we aim to determine the range of $\{F(\mathbf{x})\}_{\mathbf{x} \in \mathcal{C}}$ with a probabilistic guarantee. We first find a constant $c_1 \in \mathbb{R}^+$ and a vector $\mathbf{v}_{\max} \in \mathbb{R}^{d_L}$ such that $\forall \mathbf{x} \in \mathcal{C}, c_1 \mathbf{v}_{\max} \geq |F(\mathbf{x}) - F(\mathbf{x}^{(0)})|$ holds element-wise. Then let $\mathcal{Z} = \{F(\mathbf{x}^{(0)}) + \epsilon : |\epsilon| \leq c_1 \mathbf{v}_{\max}\}$, and it is easy to see that $\{F(\mathbf{x})\}_{\mathbf{x} \in \mathcal{C}} \subset \mathcal{Z}$.

289 As shown in Algorithm 2, we first randomly select N_1 samples from \mathcal{C} , and define $(\mathbf{v}_{\max})_j =$
290 $\max_i \{|F(\mathbf{x}^{(i)})_j - F(\mathbf{x}^{(0)})_j|\}, \zeta\}$, where $\zeta > 0$ is a small constant to ensure all components
291 are positive. When finding c_1 , directly solving the problem $c_1 = \min_{c \geq 0} c$ s.t. $c \in \bigcap_{\mathbf{x} \in \mathcal{C}} \{|F(\mathbf{x}) -$
292 $F(\mathbf{x}^{(0)})| \leq c \mathbf{v}_{\max}\}$ is infeasible. Since each constraint is convex for c , by the RCP_N (Campi et al.,
293 2009), we can get c_1 by randomly selecting N_2 samples $\{\mathbf{x}^{(i)}\}_{i=1}^{N_2}$ from \mathcal{C} , then we calculate c_1 by
294 the following optimization problem:

295
$$c_1 = \min_{c \geq 0} c \quad \text{s.t.} \quad |F(\mathbf{x}^{(i)}) - F(\mathbf{x}^{(0)})| \leq c \mathbf{v}_{\max}, \quad \forall i \in [N_2]. \quad (1)$$

296 **Proposition 1** (probabilistic guarantee for Part 1). *For any $N_1 > 1$, let \mathbf{v}_{\max} be a vector with positive components (e.g., as estimated from N_1 samples in Algorithm 2). If c_1 is computed based on this \mathbf{v}_{\max} using $N_2 \geq [\frac{2 \ln 1/\beta}{\alpha} + 2 + \frac{2 \ln 2/\alpha}{\alpha}]$ samples as described in Algorithm 2, then with probability $1 - \beta$, we have: $P_{\mathbf{x} \sim \mathcal{C}} (|F(\mathbf{x}) - F(\mathbf{x}^{(0)})| \leq c_1 \cdot \mathbf{v}_{\max}) \geq 1 - \alpha$, which implies $P_{\mathbf{x} \sim \mathcal{C}} (F(\mathbf{x}) \in \mathcal{Z}) \geq 1 - \alpha$.*

297 **Remark 3.** The probabilistic guarantee imposes no special requirements on N_1 . We select \mathbf{v}_{\max} in this way because a larger N_1 yields a tighter approximation of the true output range (Appendix D).

311 **5.2 IMPLEMENTATION PART 2 ON NMS**

312 To better illustrate the NMS verification, we use an infinite index set Δ to enumerate all possible values in \mathcal{Z} , i.e., $\mathcal{Z} = \{\mathbf{z}^k\}_{k \in \Delta}$, where each $\mathbf{z}^k \in \mathcal{Z}$ is a possible output vector. Each \mathbf{z}^k can be interpreted as a set of boxes $\{box_i^k\}_{i=1}^{n_x}$ according to the YOLO output format. We assume that box_i^k can be written $box_i^k = (x_i^k, y_i^k, w_i^k, h_i^k, c_i^k, p_{i1}^k, p_{i2}^k, \dots, p_{in}^k)$. To soundly verify the NMS, we first define the safe set $Q(\mathcal{Z}, \tau, box_{gt})$, which contains indices of boxes that satisfy the NMS conditions.

313 **Definition 2** (Safe Set). The safe set $Q(\mathcal{Z}, \tau, box_{gt}) \subseteq [n_x]$ and $i \in Q(\mathcal{Z}, \tau, box_{gt})$ if and only if:

- 314 (1): $\forall k \in \Delta$, $\text{Class}(box_i^k) = \text{Class}(box_{gt})$, $c_i^k \geq \iota$ and $\text{IoU}(box_i^k, box_{gt}) \geq \tau$;
315 (2): $\nexists k \in \Delta, n \in [n_x] \setminus \{i\}$ such that $c_n^k \geq \iota$, $\text{Class}(box_n^k) = \text{Class}(box_{gt})$, $c_n^k \geq c_i^k$,
316 $\text{IoU}(box_i^k, box_n^k) \geq \eta$, and $\text{IoU}(box_{gt}, box_n^k) < \tau$.

323 Then we can soundly verify the NMS by checking whether the safe set is empty.

324 **Proposition 2** (NMS Soundness Verification). *For given \mathcal{Z} , τ , and box_{gt} , if $Q(\mathcal{Z}, \tau, box_{gt}) \neq \emptyset$,
325 then for $\forall k \in \Delta : \exists box_i \in N(\mathbf{z}^k)$, s.t. $IoU(box_i, box_{gt}) \geq \tau \wedge \text{Class}(box_i) = \text{Class}(box_{gt})$.*
326

327 According to this proposition, verification reduces to calculating the safe set. To calculate the safe
328 set, we need the following key metric:

329 **Definition 3** (Safe IoU Threshold). The Safe IoU Threshold $\tau(i, \mathcal{Z}, box_{gt}) := \inf\{\tau' \in [0, 1] | i \notin Q(\mathcal{Z}, \tau', box_{gt})\}$, where \inf is the infimum operator.
330
331

332 The following lemmas about $\tau(i, \mathcal{Z}, box_{gt})$ can help us compute the safe set $Q(\mathcal{Z}, \tau, box_{gt})$.
333

334 **Lemma 1** (Threshold Properties). $\tau < \tau(i, \mathcal{Z}, box_{gt}) \Rightarrow i \in Q(\mathcal{Z}, \tau, box_{gt})$

335 We can obtain $\tau(i, \mathcal{Z}, box_{gt})$ by solving the following optimization problem:
336

337 **Lemma 2** (Threshold Computation). *The threshold can be calculated as $\tau(i, \mathcal{Z}, box_{gt}) = \min\{\tau_1(i, \mathcal{Z}, box_{gt}), \tau_2(i, \mathcal{Z}, box_{gt})\}$, where:*
338

$$\begin{aligned} \tau_1(i, \mathcal{Z}, box_{gt}) &= \min_{k \in \Delta} IoU(box_i^k, box_{gt}) \cdot \mathbb{I}(\text{Class}(box_i^k) = q) \cdot \mathbb{I}(c_i^k \geq \iota), q = \text{Class}(box_{gt}) \\ \tau_2(i, \mathcal{Z}, box_{gt}) &= \begin{cases} \min_{k \in \Delta, n \neq i} IoU(box_n^k, box_{gt}) & \text{if } \exists(k, n) \text{ s.t. } \mathcal{C}_{kn} = 1 \\ 1 & \text{otherwise} \end{cases} \end{aligned}$$

344 where constraint $\mathcal{C}_{kn} \equiv \mathbb{I}(c_n^k \geq \iota) \cdot \mathbb{I}(\text{Class}(box_n^k) = q) \cdot \mathbb{I}(IoU(box_i^k, box_n^k) \geq \eta) \cdot \mathbb{I}(c_n^k \geq c_i^k)$.
345

346 Appendix I shows how we encode the optimization problem in line 3 of Algorithm 3 as a mixed-
347 integer quadratic program (MIQP) and use the Gurobi solver to solve it.
348

349 5.3 IMPLEMENTATION PART 3 ON YOLO

350 Part 3 of our framework refines the initial output approximation \mathcal{Z} . When Part 2 detects a potential
351 counterexample $\mathbf{y} \in \mathcal{Z}$, in part 3, we need to check whether \mathbf{y} is actually reachable by \mathbf{F} for some
352 $\mathbf{x} \in \mathcal{C}$. This is done by computing $d_{\min} = \min_{\mathbf{x} \in \mathcal{C}} \|\mathbf{F}(\mathbf{x}) - \mathbf{y}\|_2$.

353 Due to the high dimensionality, even if $\mathbf{y} \in \{\mathbf{F}(\mathbf{x})\}_{\mathbf{x} \in \mathcal{C}}$, the d_{\min} derived from the sampled outputs
354 converges to zero very slowly as the sample size increases, so directly estimating d_{\min} simply by
355 taking the minimum distance from a set of sampled outputs $\{\mathbf{F}(\mathbf{x}^{(i)})\}$ to \mathbf{y} may be unreliable.
356

357 To address this, we introduce Algorithm 4, a two-step procedure for estimating d_{\min} with proba-
358 bility guarantees. **Step One (Estimating \mathbf{C})**: This step aims to characterize the local variability of
359 the function \mathbf{F} within the input constraint set \mathcal{C} . It computes a constant C by repeatedly sampling
360 pairs of points and observing the ratio $\frac{B'_i}{A'_i - B'_i}$. **Step Two (Estimating d_{\min} using \mathbf{C})**: Using the
361 constant C and a new set of M_2 samples, this step estimates d_{\min} for the specific target vector \mathbf{y} .
362 The formula $d_{\min} \leftarrow \max\left\{\frac{B_m - C(A_m - B_m)}{1+2C}, 0\right\}$ leverages C to provide a more conservative estimate
363 of the minimum distance than B_m (the minimum observed distance from the M_2 samples) alone.
364

365 Let $V(\mathbf{y}, d_{\min}) = P_{\mathbf{x} \sim \mathcal{C}}(\mathbf{F}(\mathbf{x}) \in \mathcal{B}_2(\mathbf{y}, d_{\min}))$, and $V(\mathbf{y}, 0) = 0$. We use $V(\mathbf{y}, d_{\min})$ to measure
366 the intersection between $\mathcal{B}_2(\mathbf{y}, d_{\min})$ and $\{\mathbf{F}(\mathbf{x})\}_{\mathbf{x} \in \mathcal{C}}$. We show that with high probability, the
367 $V(\mathbf{y}, d_{\min})$ is very small.

368 **Theorem 1** (probabilistic guarantee for Part 3). *For any $\alpha, \beta, \delta, \epsilon \in (0, 1)$ satisfying $(1-2\epsilon)^M - \delta >$
369 0 and $N \cdot ((1-2\epsilon)^M - \delta) > \frac{2}{\alpha} \ln(\frac{1}{\beta}) + 2 + \frac{2}{\alpha} \ln(\frac{2}{\alpha})$, with the algorithm 4, for any \mathbf{y} , with probability
370 at least $1 - e^{-2N\delta^2} - \beta - 2(1-\epsilon)^{M_2}$ over steps one and two, we have $V(\mathbf{y}, d_{\min}) \leq \alpha$.*
371

372 **Remark 4.** Take $N = 3000, M = 10, M_2 = 2000$, and $\epsilon = 1/200, \delta = 0.1, \alpha, \beta = 0.0099$, then
373 $1 - e^{-2N\delta^2} - \beta \geq 0.99$ and $1 - \alpha - 2(1-\epsilon)^{M_2} \geq 0.99$.

374 We also provide a sound refinement algorithm for small networks, shown in Appendix K.
375

376 5.4 THE PROBABILISTIC GUARANTEE FOR THE ENTIRE ALGORITHM

377 We prove that the whole algorithm implemented above has a probabilistic guarantee as follows, by
378 combining proposition 1, 2 and theorem 1:

378 **Algorithm 4** [Algorithm for Part 3](#): Counterexample Validation and Refinement [\(Part 3\)](#)379 **Require:**380 The neural network F ; the input constraints \mathcal{C} , $\mathbf{N}, \mathbf{M}, \mathbf{M}_2 \in \mathbb{Z}^+$, $N, M, M_2 \in \mathbb{Z}^+$, a vector \mathbf{y} .381 **Ensure:**

```

382     Estimate  $d_{\min} = \min_{\mathbf{x} \in \mathcal{C}} \|\mathbf{y} - F(\mathbf{x})\|_2$ .
383     1:  $C \leftarrow 0$ ;  $\{\mathbf{x}^{(i)}\}_{i=1}^N \leftarrow$  Randomly select  $N$  samples from  $\mathcal{C}$                                 ▷ Step One
384     2: for  $i \in [N]$  do
385         3:  $\{\mathbf{x}^{(i,j)}\}_{j=1}^M \leftarrow$  Randomly select  $M$  samples from  $\mathcal{C}$  again                                ▷ Step One
386         4:  $A'_i \leftarrow \max_{j \in [M]} \|F(\mathbf{x}^{(i,j)}) - F(\mathbf{x}^{(i)})\|_2$ ,  $B'_i \leftarrow \min_{j \in [M]} \|F(\mathbf{x}^{(i,j)}) - F(\mathbf{x}^{(i)})\|_2$ 
387         5:  $C \leftarrow \max\{C, \frac{B'_i}{A'_i - B'_i}\}$                                               ▷ Step One
388     6: end for
389     7:  $\{\mathbf{x}^{(i)}\}_{i=1}^{M_2} \leftarrow$  Select  $M_2$  samples from  $\mathcal{C}$                                 ▷ Step Two
390     8: Let  $A_m \leftarrow \max_{i \in [M_2]} \|F(\mathbf{x}^{(i)}) - \mathbf{y}\|_2$ ,  $B_m \leftarrow \min_{i \in [M_2]} \|F(\mathbf{x}^{(i)}) - \mathbf{y}\|_2$       ▷ Step Two
391     9: return  $d_{\min} \leftarrow \max\left\{\frac{B_m - C(A_m - B_m)}{1 + 2C}, 0\right\}$                                 ▷ Step Two
392
393
394
395
```

Theorem 2. *Using the notation from the three algorithms above. Given $\alpha, \beta, \delta, \epsilon \in (0, 1)$ satisfying $(1 - 2\epsilon)^M - \delta > 0$, $N \cdot ((1 - 2\epsilon)^M - \delta) > \frac{2}{\alpha} \ln(\frac{1}{\beta}) + 2 + \frac{2}{\alpha} \ln(\frac{2}{\alpha})$ and $N_2 \geq [\frac{2 \ln 1/\beta}{\alpha} + 2 + \frac{2 \ln 2/\alpha}{\alpha}]$. Then, after executing the algorithms defined above, with any κ in part 3, if for a sample \mathbf{x} , these algorithms output ‘safe’ after T refinement turns, then with probability at least $1 - T(e^{-2N\delta^2} + \beta + 2(1 - \epsilon)^{M_2}) - \beta$ of parts one and three, we have $P_{\mathbf{x} \sim \mathcal{C}}(\mathbf{x} \text{ is safe}) > 1 - (1 + T)\alpha$.*

If we take $N_1 = 30,000$, $N_2 = 5,000$, $N = 3,000$, $M = 10$, $M_2 = 2,000$, $\alpha = \beta = 0.0099$, $\epsilon = 1/200$, $\delta = 0.1$, we can achieve a 98% probabilistic guarantee with 98% confidence using only 37,000 samples, which means with at least 98% confidence, the probability of an OD event occurring under the given perturbation distribution is at most 2%.

Remark 5. Note all our theoretical guarantees depend only on the i.i.d. assumption and hold for any sampling distribution, not just uniform.

409 **6 EXPERIMENTS**

411 Our experiment consists of the evaluations of the bounds accuracy and the safety guarantee. Detailed
412 experimental settings and more experimental results are provided in Appendix N to Appendix T.

414 **Basic setting.** Our experiments used the medium and large versions of the YOLOv3, YOLOv5,
415 YOLOv8 and YOLO11 models by Ultralytics (Jocher et al., 2023). We conduct verification on
416 the COCO dataset (Lin et al., 2014), a widely used benchmark for object detection, and randomly
417 select 100 validation images containing more than 520 objects. We use a uniform distribution for
418 sampling, which is a common choice in the literature (Li et al., 2022; Cohen et al., 2024). The IoU
419 threshold $\tau \in \{0.5, 0.7\}$, the constants in NMS are $\eta = 0.45$ and $\iota = 0.25$, which are commonly
420 used in object detection tasks. In Appendix X we also evaluate our method under other perturbation
421 distributions (e.g., Gaussian, Salt and Pepper) on different threat models (e.g., False Appearance).
422 We set $\zeta = 0.001$ (Alg. 2) and $\kappa = 0.01$ (Alg. 4). The perturbation radius is set to $\frac{1}{255}$ or $\frac{2}{255}$.
423 Larger radii make the network overly fragile, enabling counterexamples to be found with very few
424 samples, and thus eliminating meaningful differences between methods.

425 **Baseline Selection.** By Theorem 2, our method achieves a 98% probabilistic guarantee with 98%
426 confidence using only **37,000** samples. In contrast, RCP_N requires over **56011,000,000** samples,
427 while DeepPAC (Li et al., 2022) requires over **100,000,000** samples and needs to solve LPs with
428 more than 10^{12} variables to achieve the same guarantee (see Appendix N), making both approaches
429 impractical. Formal verification methods are also infeasible: existing tools (Cohen et al., 2024;
430 Elboher et al., 2024) handle only 2-3 convolutional layers with 2-3 linear layers, far below the scale
431 of YOLO, and cannot address its complex architecture or NMS. Therefore, **direct comparisons**
432 with DeepPAC, RCP_N , and formal verification are **not feasible**. Instead, we use RCP_N with 10^6
433 samples (yielding weaker guarantees) as a baseline.

432 Table 1: Comparison of our method with RCP_N . Δ_{PGD} denotes the mean absolute difference of
 433 IoU lower bounds relative to the PGD attack. Bold values indicate the best performance.

434

ε	method	model	time	Δ_{PGD}		model	time	Δ_{PGD}	
				$\tau = 0.5$	$\tau = 0.7$			$\tau = 0.5$	$\tau = 0.7$
$\frac{1}{255}$	Ours	v3spp	109.0	0.49	0.45	v8m	50.7	0.48	0.44
	RCP_N		563.5	0.55	0.53		455.0	0.52	0.52
	Ours	RCP_N	106.3	0.48	0.41		49.6	0.53	0.45
	RCP_N		562.9	0.58	0.54		454.7	0.59	0.55
$\frac{2}{255}$	Ours	v3	108.5	0.52	0.46	v8x	132.3	0.49	0.46
	RCP_N		561.0	0.57	0.55		591.3	0.55	0.54
	Ours	RCP_N	105.0	0.48	0.42		129.0	0.51	0.44
	RCP_N		560.3	0.60	0.55		590.6	0.61	0.57
$\frac{1}{255}$	Ours	v5m	43.6	0.42	0.39	11m	59.1	0.48	0.43
	RCP_N		445.5	0.47	0.47		468.8	0.53	0.52
	Ours	RCP_N	42.8	0.48	0.42		58.0	0.50	0.43
	RCP_N		444.4	0.55	0.50		467.8	0.57	0.53
$\frac{2}{255}$	Ours	v5x	131.5	0.48	0.44	11x	147.2	0.49	0.45
	RCP_N		593.8	0.54	0.54		618.1	0.54	0.54
	Ours	RCP_N	128.4	0.52	0.45		141.9	0.50	0.44
	RCP_N		593.2	0.60	0.57		616.5	0.62	0.57

454

455 Table 2: Guarantee evaluation of our method with $\tau = 0.5$ and $\varepsilon = \frac{1}{255}, \varepsilon \in \{\frac{1}{255}, \frac{2}{255}\}$ under 10^6
 456 uniform perturbations. TPR/FPR: True/False Positive Rate. TNR/FNR: True/False Negative Rate.
 457 A detection is considered positive if verified robust by our method, and negative otherwise. Certified
 458 Robust Accuracy (CRA): percentage of detections verified robust that are indeed robust. Average
 459 Bounds Improvement (ABI): average gain in certified IoU lower bounds.

460

model	ε	TPR (%)	FPR (%)	TNR (%)	FNR (%)	CRA (%)	ABI
yolo11x	1/255	94.9	2.9	97.1	5.1	98.9	0.10
	2/255	85.2	1.4	98.6	14.8	99.4	0.17
yolo11m	1/255	95.0	3.0	97.0	5.0	98.6	0.10
	2/255	93.1	1.1	98.9	6.9	99.4	0.11
yolov8x	1/255	95.1	0.0	100.0	4.9	100.0	0.09
	2/255	89.7	0.6	99.4	10.3	99.7	0.14
yolov8m	1/255	97.3	2.6	97.4	2.7	98.9	0.08
	2/255	93.9	2.4	97.6	6.1	98.8	0.11
yolov5xu	1/255	94.8	0.7	99.3	5.2	99.7	0.09
	2/255	90.6	0.6	99.4	9.4	99.7	0.13
yolov5mu	1/255	96.0	2.9	97.1	4.0	98.6	0.10
	2/255	92.4	0.5	99.5	7.6	99.7	0.11
yolov3-sppu	1/255	95.6	0.0	100.0	4.4	100.0	0.08
	2/255	87.4	0.0	100.0	12.6	100.0	0.15
yolov3u	1/255	95.7	1.3	98.7	4.3	99.4	0.09
	2/255	85.8	0.0	100.0	14.2	100.0	0.16

480

481

482

483 **Bounds Accuracy.** Table 1 compares our method with RCP_N , showing that our approach is both
 484 faster and more accurate. In particular, it achieves a smaller mean absolute difference between IoU
 485 lower bounds and the worst-case input found by the PGD attack (Δ_{PGD}), indicating tighter certified
 bounds. Figure 5 further confirms this, as our bounds remain consistently closer to those of PGD.

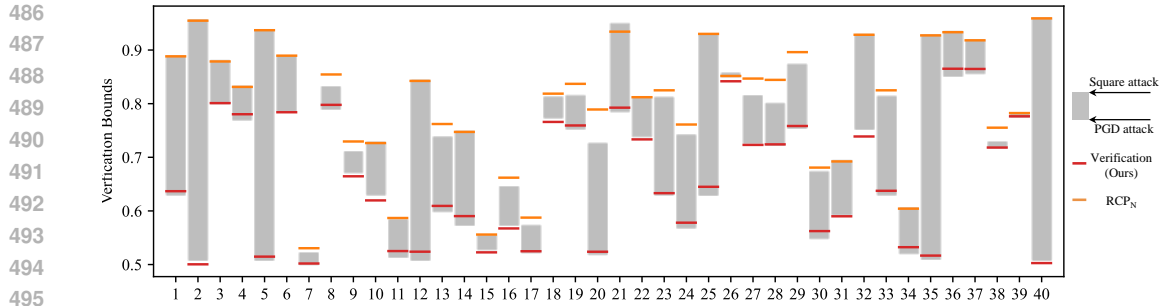


Figure 5: **IoU-lower** Lower bounds of the IoU between detected boxes and their corresponding ground truth ground-truth boxes under our method, RCP_N , the square attack, and the PGD attack. Results are computed on YOLO11x with $\epsilon = \frac{1}{255}$ and $\tau = 0.5$. Each x-axis tick corresponds to an object in the COCO dataset.

Safety Guarantee. Table 2 further shows results under 10^6 uniform perturbations: the certified robust accuracy (CRA) exceeds 98%, and the false positive rate (FPR) remains very low, consistent with theory. The true positive rate (TPR) is lower, as expected since our certification is stricter than empirical robustness. Finally, the average bounds improvement (ABI) confirms that our method yields tighter certified IoU lower bounds.

Additional Experiments. We further evaluate (i) the effect of Part 3 (Appendix P), (ii) an ablation study on hyperparameters (Appendix T), (iii) real-world applications (Appendix R), and (iv) a comparison with median smoothing (Appendix S).

7 CONCLUSION

This paper presents a novel probabilistic framework for verifying framework to provide provable probabilistic guarantees for YOLO-based object detection systems against object disappearance attacks, specific threats (e.g., Object Disappear, False Appearance) under various perturbation distributions, a key step toward trustworthy deployment. Our contributions are threefold: (i) a formal definition of the OD verification problem, (ii) a practical three-stage methodology that explicitly incorporates formal analysis of Non-Maximum Suppression (NMS) NMS, and (iii) strong probabilistic guarantees for the full pipeline. Experiments on multiple YOLO architectures and the COCO dataset distributions show that our approach delivers reliable safety assurances and achieves tighter certified IoU bounds with far greater sample efficiency than prior methods.

Limitations and Future Directions: Our method relies on an assumed distribution of input perturbations, a limitation inherent to the PAC framework. Developing verification methods for other types of attacks remains an important direction for future work. Another valuable direction involves leveraging adversarial attack strategies to further refine Stages 1 and 3, alongside investigating more efficient methods for interval estimation and refinement.

REFERENCES

- Brendon G. Anderson and Somayeh Sojoudi. Data-driven certification of neural networks with random input noise. *IEEE Transactions on Control of Network Systems*, 10(1):249–260, 2023. doi: 10.1109/TCNS.2022.3199148.
- Stanley Bak. nnenum: Verification of ReLU neural networks with optimized abstraction refinement. In *Proceedings of the 13th International Symposium on NASA Formal Methods (NFM)*, pp. 19–36. Springer, 2021.
- Teodora Baluta, Zheng Leong Chua, Kuldeep S. Meel, and Prateek Saxena. Scalable quantitative verification for deep neural networks. In *2021 IEEE/ACM 43rd International Conference on Software Engineering (ICSE)*, pp. 312–323, 2021. doi: 10.1109/ICSE43902.2021.00039.
- Peter Blohm, Patrick Indri, Thomas Gärtner, and SAGAR MALHOTRA. Probably approximately global robustness certification. In *Forty-second International Conference on Machine Learning, 2025*. URL <https://openreview.net/forum?id=UKH1XpiFMy>.

- 540 Alexey Bochkovskiy, Chien-Yao Wang, and Hong-Yuan Mark Liao. Yolov4: Optimal speed and
 541 accuracy of object detection. *CoRR*, abs/2004.10934, 2020a. URL <https://arxiv.org/abs/2004.10934>.
- 543
- 544 Alexey Bochkovskiy, Chien-Yao Wang, and Hong-Yuan Mark Liao. Yolov4: Optimal speed and
 545 accuracy of object detection, 2020b.
- 546
- 547 David Boetius, Stefan Leue, and Tobias Sutter. Solving probabilistic verification problems of neural
 548 networks using branch and bound. In *Forty-second International Conference on Machine Learn-
 549 ing*, 2025. URL <https://openreview.net/forum?id=suZ1pNdKrV>.
- 550
- 551 Christopher Brix, Stanley Bak, Changliu Liu, and Taylor T. Johnson. The fourth international veri-
 552 fication of neural networks competition (vnn-comp 2023): Summary and results, 2023.
- 553
- 554 Christopher Brix, Stanley Bak, Taylor T. Johnson, and Haoze Wu. The fifth international verification
 555 of neural networks competition (vnn-comp 2024): Summary and results, 2024. URL <https://arxiv.org/abs/2412.19985>.
- 556
- 557 Marco C Campi, Simone Garatti, and Maria Prandini. The scenario approach for systems and control
 558 design. *Annual Reviews in Control*, 33(2):149–157, 2009.
- 559
- 560 Luca Cardelli, Marta Kwiatkowska, Luca Laurenti, and Andrea Patane. Robustness guarantees for
 561 bayesian inference with gaussian processes. In *Proceedings of the AAAI conference on artificial
 562 intelligence*, volume 33, pp. 7759–7768, 2019.
- 563
- 564 Nicholas Carlini and David A. Wagner. Towards evaluating the robustness of neural networks. In
 565 *2017 IEEE Symposium on Security and Privacy, SP 2017, San Jose, CA, USA, May 22-26, 2017*,
 566 pp. 39–57. IEEE Computer Society, 2017. doi: 10.1109/SP.2017.49. URL <https://doi.org/10.1109/SP.2017.49>.
- 567
- 568 Yanbo Chen and Weiwei Liu. A theory of transfer-based black-box attacks: explanation and impli-
 569 cations. *Advances in Neural Information Processing Systems*, 36, 2024.
- 570
- 571 Ping-yeh Chiang, Michael Curry, Ahmed Abdelkader, Aounon Kumar, John Dickerson, and Tom
 572 Goldstein. Detection as regression: Certified object detection with median smoothing. *Advances
 573 in Neural Information Processing Systems*, 33:1275–1286, 2020.
- 574
- 575 Jung Im Choi and Qing Tian. Adversarial attack and defense of yolo detectors in autonomous
 576 driving scenarios. In *2022 IEEE Intelligent Vehicles Symposium (IV)*, pp. 1011–1017, 2022. doi:
 577 10.1109/IV51971.2022.9827222.
- 578
- 579 Jeremy Cohen, Elan Rosenfeld, and Zico Kolter. Certified adversarial robustness via randomized
 580 smoothing. In *international conference on machine learning*, pp. 1310–1320. PMLR, 2019.
- 581
- 582 Noémie Cohen, Mélanie Ducoffe, Ryma Boumazouza, Christophe Gabreau, Claire Pagetti, Xavier
 583 Pucel, and Audrey Galametz. Verification for object detection–ibp iou. *arXiv preprint
 arXiv:2403.08788*, 2024.
- 584
- 585 N. Dalal and B. Triggs. Histograms of oriented gradients for human detection. In *2005 IEEE Com-
 586 puter Society Conference on Computer Vision and Pattern Recognition (CVPR’05)*, volume 1, pp.
 587 886–893 vol. 1, 2005. doi: 10.1109/CVPR.2005.177.
- 588
- 589 Yinpeng Dong, Fangzhou Liao, Tianyu Pang, Hang Su, Jun Zhu, Xiaolin Hu, and Jianguo Li. Boost-
 590 ing adversarial attacks with momentum. In *2018 IEEE Conference on Computer Vision and
 591 Pattern Recognition, CVPR 2018, Salt Lake City, UT, USA, June 18-22, 2018*, pp. 9185–9193.
 592 Computer Vision Foundation / IEEE Computer Society, 2018. doi: 10.1109/CVPR.2018.00957.
- 593
- 594 Ruediger Ehlers. Formal verification of piece-wise linear feed-forward neural networks. In *Au-
 595 tomated Technology for Verification and Analysis: 15th International Symposium, ATVA 2017,
 596 Pune, India, October 3–6, 2017, Proceedings 15*, pp. 269–286. Springer, 2017.
- 597
- 598 Yizhak Y. Elboher, Avraham Raviv, Yael Leibovich Weiss, Omer Cohen, Roy Assa, Guy Katz, and
 599 Hillel Kugler. Formal verification of deep neural networks for object detection, 2024. URL
 600 <https://arxiv.org/abs/2407.01295>.

- 594 Ali Farhadi and Joseph Redmon. Yolov3: An incremental improvement. In *Computer vision and*
 595 *pattern recognition*, volume 1804, pp. 1–6. Springer Berlin/Heidelberg, Germany, 2018.
- 596
- 597 Ross Girshick. Fast r-cnn. In *2015 IEEE International Conference on Computer Vision (ICCV)*, pp.
 598 1440–1448, 2015. doi: 10.1109/ICCV.2015.169.
- 599
- 600 Ross Girshick, Jeff Donahue, Trevor Darrell, and Jitendra Malik. Rich feature hierarchies for ac-
 601 curate object detection and semantic segmentation. In *Proceedings of the IEEE conference on*

602 *computer vision and pattern recognition*, pp. 580–587, 2014.

603

604 Ian J. Goodfellow, Jonathon Shlens, and Christian Szegedy. Explaining and harnessing adversarial
 605 examples. In Yoshua Bengio and Yann LeCun (eds.), *3rd International Conference on Learning*

606 *Representations, ICLR 2015, San Diego, CA, USA, May 7-9, 2015, Conference Track Proceed-
 607 ings*, 2015. URL <http://arxiv.org/abs/1412.6572>.

608

609 Sven Gowal, Krishnamurthy Dj Dvijotham, Robert Stanforth, Rudy Bunel, Chongli Qin, Jonathan
 610 Uesato, Relja Arandjelovic, Timothy Mann, and Pushmeet Kohli. Scalable verified training for
 611 provably robust image classification. In *Proceedings of the IEEE/CVF International Conference*

612 *on Computer Vision*, pp. 4842–4851, 2019.

613

614 David Haussler and Emo Welzl. ε -nets and simplex range queries. *Discrete & Computational*

615 *Geometry*, 2:127–151, 1987. URL [https://api.semanticscholar.org/CorpusID:
 616 27638326](https://api.semanticscholar.org/CorpusID:27638326).

617

618 Patrick Henriksen and Alessio Lomuscio. Efficient neural network verification via adaptive refine-
 619 ment and adversarial search. In *ECAI 2020*, pp. 2513–2520. IOS Press, 2020.

620

621 Jung Im Choi and Qing Tian. Adversarial attack and defense of yolo detectors in autonomous driving
 622 scenarios. In *2022 IEEE Intelligent Vehicles Symposium (IV)*, pp. 1011–1017. IEEE, 2022.

623

624 Glenn Jocher, Jing Qiu, and Ayush Chaurasia. Ultralytics YOLO. In *github*, January 2023. URL
<https://github.com/ultralytics/ultralytics>.

625

626 Guy Katz, Clark Barrett, David L Dill, Kyle Julian, and Mykel J Kochenderfer. Reluplex: An
 627 efficient smt solver for verifying deep neural networks. In *Proceedings of the 29th International*

628 *Conference on Computer Aided Verification (CAV)*, pp. 97–117. Springer, 2017.

629

630 Guy Katz, Derek A. Huang, Duligur Ibeling, Kyle Julian, Christopher Lazarus, Rachel Lim, Parth
 631 Shah, Shantanu Thakoor, Haoze Wu, Aleksandar Zeljic, David L. Dill, Mykel J. Kochenderfer,
 632 and Clark W. Barrett. The marabou framework for verification and analysis of deep neural net-
 633 works. In Isil Dillig and Serdar Tasiran (eds.), *Computer Aided Verification - 31st International*

634 *Conference, CAV 2019, New York City, NY, USA, July 15-18, 2019, Proceedings, Part I*, volume 11561 of *Lecture Notes in Computer Science*, pp. 443–452. Springer, 2019. doi: 10.1007/
 635 978-3-030-25540-4\26. URL https://doi.org/10.1007/978-3-030-25540-4_26.

636

637 Haitham Khedr, James Ferlez, and Yasser Shoukry. Peregrinn: Penalized-relaxation greedy neural
 638 network verifier. In *Computer Aided Verification: 33rd International Conference, CAV 2021,
 639 Virtual Event, July 20–23, 2021, Proceedings, Part I* 33, pp. 287–300. Springer, 2021.

640

641 Suhas Kotha, Christopher Brix, J Zico Kolter, Krishnamurthy Dvijotham, and Huan Zhang. Provably
 642 bounding neural network preimages. *Advances in Neural Information Processing Systems*, 36:
 643 80270–80290, 2023.

644

645 Panagiotis Kouvaros and Alessio Lomuscio. Towards scalable complete verification of ReLU neural
 646 networks via dependency-based branching. In *IJCAI*, pp. 2643–2650, 2021.

647

648 Huichen Li, Xiaojun Xu, Xiaolu Zhang, Shuang Yang, and Bo Li. Qeba: Query-efficient boundary-
 649 based blackbox attack. In *Proceedings of the IEEE/CVF conference on computer vision and*

650 *pattern recognition*, pp. 1221–1230, 2020.

651

652 Renjue Li, Pengfei Yang, Cheng-Chao Huang, Youcheng Sun, Bai Xue, and Lijun Zhang. Towards
 653 practical robustness analysis for dnns based on pac-model learning. In *Proceedings of the 44th*

654 *International Conference on Software Engineering*, pp. 2189–2201, 2022.

- 648 Zuoxin Li, Lu Yang, and Fuqiang Zhou. Fssd: feature fusion single shot multibox detector. *arXiv*
 649 *preprint arXiv:1712.00960*, 2017.
- 650
- 651 Tao Lin, Lijia Yu, Gaojie Jin, Renjue Li, Peng Wu, and Lijun Zhang. Out-of-bounding-box triggers:
 652 A stealthy approach to cheat object detectors. In Aleš Leonardis, Elisa Ricci, Stefan Roth, Olga
 653 Russakovsky, Torsten Sattler, and Gü̈l Varol (eds.), *Computer Vision – ECCV 2024*, pp. 269–287,
 654 Cham, 2025. Springer Nature Switzerland. ISBN 978-3-031-72848-8.
- 655 Tsung-Yi Lin, Michael Maire, Serge Belongie, James Hays, Pietro Perona, Deva Ramanan, Piotr
 656 Dollár, and C Lawrence Zitnick. Microsoft coco: Common objects in context. In *Computer*
 657 *Vision–ECCV 2014: 13th European Conference, Zurich, Switzerland, September 6–12, 2014,*
 658 *Proceedings, Part V 13*, pp. 740–755. Springer, 2014.
- 659 Wei Liu, Dragomir Anguelov, Dumitru Erhan, Christian Szegedy, Scott Reed, Cheng-Yang Fu, and
 660 Alexander C Berg. Ssd: Single shot multibox detector. In *Computer Vision–ECCV 2016: 14th*
 661 *European Conference, Amsterdam, The Netherlands, October 11–14, 2016, Proceedings, Part I*
 662 *14*, pp. 21–37. Springer, 2016.
- 663 Yanpei Liu, Xinyun Chen, Chang Liu, and Dawn Song. Delving into transferable adversarial exam-
 664 ples and black-box attacks. In *5th International Conference on Learning Representations, ICLR*
 665 *2017, Toulon, France, April 24–26, 2017, Conference Track Proceedings*. OpenReview.net, 2017.
 666 URL <https://openreview.net/forum?id=Sys6GJqx1>.
- 667 Aleksander Madry, Aleksandar Makelov, Ludwig Schmidt, Dimitris Tsipras, and Adrian Vladu.
 668 Towards deep learning models resistant to adversarial attacks. In *6th International Conference*
 669 *on Learning Representations, ICLR 2018, Vancouver, BC, Canada, April 30 - May 3, 2018,*
 670 *Conference Track Proceedings*. OpenReview.net, 2018. URL <https://openreview.net/forum?id=rJzIBfZAb>.
- 671
- 672 Ravi Mangal, Aditya V. Nori, and Alessandro Orso. Robustness of neural networks: a probabilis-
 673 tic and practical approach. In *Proceedings of the 41st International Conference on Software*
 674 *Engineering: New Ideas and Emerging Results, ICSE-NIER ’19*, pp. 93–96. IEEE Press, 2019.
 675 doi: 10.1109/ICSE-NIER.2019.00032. URL [https://doi.org/10.1109/ICSE-NIER.](https://doi.org/10.1109/ICSE-NIER.2019.00032)
 676 2019.00032.
- 677
- 678 P. Massart. The Tight Constant in the Dvoretzky-Kiefer-Wolfowitz Inequality. *The Annals of*
 679 *Probability*, 18(3):1269 – 1283, 1990. doi: 10.1214/aop/1176990746. URL <https://doi.org/10.1214/aop/1176990746>.
- 680
- 681 Michael Naaman. On the tight constant in the multivariate dvoretzky-kiefer-wolfowitz inequality.
 682 *Statistics & Probability Letters*, 173:109088, 2021. ISSN 0167-7152. doi: <https://doi.org/10.1016/j.spl.2021.109088>. URL <https://www.sciencedirect.com/science/article/pii/S016771522100050X>.
- 683
- 684 Alexander Neubeck and Luc Van Gool. Efficient non-maximum suppression. In *18th international*
 685 *conference on pattern recognition (ICPR’06)*, volume 3, pp. 850–855. IEEE, 2006.
- 686
- 687 Sangdon Park, Osbert Bastani, Nikolai Matni, and Insup Lee. PAC confidence sets for deep neural
 688 networks via calibrated prediction. In *8th International Conference on Learning Representations,*
 689 *ICLR 2020, Addis Ababa, Ethiopia, April 26–30, 2020*. OpenReview.net, 2020. URL <https://openreview.net/forum?id=BJxVI04YvB>.
- 690
- 691 J Redmon. You only look once: Unified, real-time object detection. In *Proceedings of the IEEE*
 692 *conference on computer vision and pattern recognition*, 2016.
- 693
- 694 Joseph Redmon and Ali Farhadi. Yolo9000: better, faster, stronger. In *Proceedings of the IEEE*
 695 *conference on computer vision and pattern recognition*, pp. 7263–7271, 2017.
- 696
- 697 Shaoqing Ren. Faster r-cnn: Towards real-time object detection with region proposal networks.
 698 *arXiv preprint arXiv:1506.01497*, 2015.
- 699
- 700 Gagandeep Singh, Timon Gehr, Markus Püschel, and Martin Vechev. An abstract domain for cer-
 701 *tifying neural networks. Proceedings of the ACM on Programming Languages*, 3(POPL):1–30,
 2019.

- 702 Hoang-Dung Tran, Sungwoo Choi, Hideki Okamoto, Bardh Hoxha, Georgios Fainekos, and Daniil
 703 Prokhorov. Quantitative verification for neural networks using probstars. In *Proceedings of the*
 704 *26th ACM International Conference on Hybrid Systems: Computation and Control, HSCC '23*,
 705 New York, NY, USA, 2023. Association for Computing Machinery. ISBN 9798400700330. doi:
 706 10.1145/3575870.3587112. URL <https://doi.org/10.1145/3575870.3587112>.
 707
- 708 Paul Viola and Michael Jones. Rapid object detection using a boosted cascade of simple features.
 709 In *Proceedings of the 2001 IEEE computer society conference on computer vision and pattern*
 710 *recognition. CVPR 2001*, volume 1, pp. I–I. Ieee, 2001.
 711
- 712 Shiqi Wang, Kexin Pei, Justin Whitehouse, Junfeng Yang, and Suman Jana. Efficient formal safety
 713 analysis of neural networks. *Advances in neural information processing systems*, 31, 2018a.
 714
- 715 Shiqi Wang, Kexin Pei, Justin Whitehouse, Junfeng Yang, and Suman Jana. Formal security analysis
 716 of neural networks using symbolic intervals. In *27th USENIX Security Symposium (USENIX*
 717 *Security 18)*, pp. 1599–1614, 2018b.
 718
- 719 Stefan Webb, Tom Rainforth, Yee Whye Teh, and M. Pawan Kumar. Statistical verification of
 720 neural networks. In *International Conference on Learning Representations*, 2019. URL <https://openreview.net/forum?id=S1xcx3C5FX>.
 721
- 722 Lily Weng, Huan Zhang, Hongge Chen, Zhao Song, Cho-Jui Hsieh, Luca Daniel, Duane Boning,
 723 and Inderjit Dhillon. Towards fast computation of certified robustness for ReLu networks. In
 724 *International Conference on Machine Learning*, pp. 5276–5285. PMLR, 2018.
 725
- 726 Lily Weng, Pin-Yu Chen, Lam Nguyen, Mark Squillante, Akhilan Boopathy, Ivan Oseledets, and
 727 Luca Daniel. Proven: Verifying robustness of neural networks with a probabilistic approach. In
 728 *International Conference on Machine Learning*, pp. 6727–6736. PMLR, 2019.
 729
- 730 Kaidi Xu, Huan Zhang, Shiqi Wang, Yihan Wang, Suman Jana, Xue Lin, and Cho-Jui Hsieh. Fast
 731 and complete: Enabling complete neural network verification with rapid and massively parallel
 732 incomplete verifiers. In *9th International Conference on Learning Representations, ICLR 2021,*
 733 *Virtual Event, Austria, May 3-7, 2021*. OpenReview.net, 2021. URL <https://openreview.net/forum?id=nVZtXBI6LNn>.
 734
- 735 Greg Yang, Tony Duan, J Edward Hu, Hadi Salman, Ilya Razenshteyn, and Jerry Li. Randomized
 736 smoothing of all shapes and sizes. In *International conference on machine learning*, pp. 10693–
 737 10705. PMLR, 2020.
 738
- 739 Huan Zhang, Tsui-Wei Weng, Pin-Yu Chen, Cho-Jui Hsieh, and Luca Daniel. Efficient neural
 740 network robustness certification with general activation functions. *Advances in neural information*
 741 *processing systems*, 31, 2018.
 742
- 743 Huan Zhang, Shiqi Wang, Kaidi Xu, Linyi Li, Bo Li, Suman Jana, Cho-Jui Hsieh, and J. Zico Kolter.
 744 General cutting planes for bound-propagation-based neural network verification. In *NeurIPS*,
 745 2022a.
 746
- 747 Huan Zhang, Shiqi Wang, Kaidi Xu, Yihan Wang, Suman Jana, Cho-Jui Hsieh, and Zico Kolter. A
 748 branch and bound framework for stronger adversarial attacks of ReLU networks. In *International*
 749 *Conference on Machine Learning*, pp. 26591–26604. PMLR, 2022b.
 750
- 751 Zhong-Qiu Zhao, Peng Zheng, Shou-tao Xu, and Xindong Wu. Object detection with deep learning:
 752 A review. *IEEE transactions on neural networks and learning systems*, 30(11):3212–3232, 2019.
 753
- 754 Zhengxia Zou, Keyan Chen, Zhenwei Shi, Yuhong Guo, and Jieping Ye. Object detection in 20
 755 years: A survey. *Proceedings of the IEEE*, 111(3):257–276, 2023.

756 **A APPENDIX**
757758 This appendix provides more related work, supplementary discussions, proofs, and experiments to
759 support the main text. We organize the appendix as follows:
760

- 761 • **Section B:** Summarizes additional related work.
762
- 763 • **Section C:** Provides the proof of Proposition 1 (probabilistic guarantee for part 1).
764
- 765 • **Section D:** Explains the role of sample size in Part 1 Step 1 and its effect on v_{\max} .
766
- 767 • **Section E:** Gives the proof of Proposition 2 (NMS Soundness Verification).
768
- 769 • **Section F:** Proves Lemma 1 (threshold properties).
770
- 771 • **Section G:** Proves Lemma 2 (explicit threshold computation formulas).
772
- 773 • **Section H:** Defines and estimates the verification bound for object detection and provides
774 proofs for Lemmas 4 and 5.
775
- 776 • **Section I:** Details the verification procedure for Non-Maximum Suppression, including
777 abstract box construction and IoU bound computation.
778
- 779 • **Section J:** Proves Theorem 1 (probabilistic guarantee for Part 3).
780
- 781 • **Section K:** We propose a strict sound gradient-based refinement algorithm to implement
782 Part Three on small-scale networks(Theorem 4).
783
- 784 • **Section L:** Provides the proof of Theorem 4 based on dual formulations.
785
- 786 • **Section M:** Gives the proof of Theorem 2, combining probabilistic guarantees across all
787 parts.
788
- 789 • **Section N:** Reports detailed experimental settings, sample number calculations, and server
790 configuration.
791
- 792 • **Section O:** Discuss the efficiency of the NMS verification process.
793
- 794 • **Section P:** Shows the effectiveness of Part 3 refinement for YOLO and CNNs.
795
- 796 • **Section Q:** Shows time-verified box comparison between our method and RCP_N .
797
- 798 • **Section R:** Demonstrates our method's effectiveness on real-world images.
799
- 800 • **Section S:** Compares our method against median smoothing under Gaussian noise.
801
- 802 • **Section T:** Presents an ablation study on parameters η and ι .
803
- 804 • **Section U:** Discusses the broader impact of our verification method.
805
- 806 • **Section V :** LLM Usage Statement.
807
- 808 • **Section W:** Lists and explains all hyperparameters used in our algorithms.
809
- 810 • **Section X:** Provides details on how to adapt our method to other attacks beyond OD attacks.
811

796 **B ADDITIONAL RELATED WORK**
797798 **Adversarial attacks**
799

800 **Adversarial attacks.** Adversarial methods induce misclassification through imperceptible perturbations. White-box attacks exploit gradient information (Goodfellow et al., 2015; Madry et al., 2018; Carlini & Wagner, 2017) and can be adapted to OD attacks (Choi & Tian, 2022; Li et al., 2020). Black-box attacks use transferability (Chen & Liu, 2024) or query-based optimization (Li et al., 2020); these are more practical but may be computationally costly. Using adversarial attacks in isolation only demonstrates non-robustness if the attack is successful, whereas our method provides a rigorous probabilistic certificate of robustness. A network that is robust with high probability under common perturbations(e.g. sensor noise) is acceptable for practical deployment, whereas the strict requirement of complete robustness in a neighborhood often leads to a significant drop in network performance. Thus focus is on providing probabilistic robustness under realistic perturbations such as sensor noise rather than adversarial attacks (which often represent worst-case scenarios).

810 **Bound Estimate Methods.** There are several classical methods for estimating
 811 probabilistic output bounds of neural networks, including DKW-based confidence
 812 regions (Massart, 1990; Naaman, 2021), ERM-based hyper-rectangles, and
 813 ϵ -nets (Haussler & Welzl, 1987; Blohm et al., 2025). While these methods are theoretically robust,
 814 their sample complexity typically scales with the output dimension d_L (e.g., $\tilde{O}(d_L/\epsilon)$ for ϵ -nets).
 815 Given the extremely high-dimensional output space of YOLO networks, dimension-dependent
 816 bounds like those from ϵ -nets or DKW would be computationally infeasible. We therefore focus
 817 on dimension-independent PAC bounds, making estimation feasible even for high-dimensional
 818 outputs.

819 **PAC with Attack.** There are several PAC verification methods that incorporate adversarial attacks
 820 to refine the estimated output bounds (Blohm et al., 2025; Li et al., 2022; Baluta et al., 2021). For
 821 example, Blohm et al. (2025) evaluates the robustness of individual points via a local robustness
 822 oracle (such as PGD or LiRPA) and leverages ϵ -net sampling methods to provide high-probability
 823 statistical guarantees for global robustness. Combining attacks with PAC verification is an
 824 interesting direction, we will explore this in future work.

826 C THE PROOF OF PROPOSITION 1

827 **Proposition** (probabilistic guarantee for part 1). *For any $N_1 > 1$, let \mathbf{v}_{\max} be a vector with
 828 positive components (e.g., as estimated from N_1 samples in Algorithm 2). If c_1 is computed
 829 based on this \mathbf{v}_{\max} using $N_2 \geq [\frac{2 \ln 1/\beta}{\alpha} + 2 + \frac{2 \ln 2/\alpha}{\alpha}]$ samples as described in Algorithm 2,
 830 then with probability $1 - \beta$, we have: $\mathbb{P}_{\mathbf{x} \sim \mathcal{C}} (|F(\mathbf{x}) - F(\mathbf{x}^{(0)})| \leq c_1 \cdot \mathbf{v}_{\max}) \geq 1 - \alpha$, which
 831 implies $\mathbb{P}_{\mathbf{x} \sim \mathcal{C}} (F(\mathbf{x}) \in \mathcal{Z}) \geq 1 - \alpha$.*

832 This proposition can be directly obtained by classic method RCP_N , which is introduced below.

833 C.1 CLASSIC METHOD FOR PROBABILITY SAMPLING.

834 We begin by introducing a well-known method, result from the RCP_N method (Campi et al., 2009),
 835 which forms the basis of our approach in this section. Consider the following optimization problem
 836 with possibly infinite constraints:

837 an infinite number of constraints:

$$\min_{\mathbf{x} \in \mathbb{R}^d} \mathbf{a}^\top \mathbf{x} + b \quad \text{s.t.} \quad \mathbf{x} \in \bigcap_{\delta \in \Delta} \mathcal{X}_\delta, \quad (2)$$

838 Where where Δ is a index set an index set, and $\mathcal{X}_\delta \subseteq \mathbb{R}^d$ is the denotes the constraint set
 839 corresponding to the index δ th constraint set.

840 Since the constraints are infinite there are infinitely many constraints, we can not solve the problem
 841 directly. Thus we consider sample the constraints $\{\delta_i\}_{i=1}^N$ from Δ , and estimate the possibility
 842 that the optimal value of the optimization problem equation 3 with the constraints $\{\mathcal{X}_{\delta_i}\}_{i=1}^N$ is the
 843 optimal value of the problem equation 2 with the constraints $\{\mathcal{X}_\delta\}_{\delta \in \Delta}$.

844 according to a probability distribution \mathcal{Q} on Δ , and consider the sampled problem equation 3. We
 845 are interested in quantifying how likely it is that the optimal solution of the sampled problem is
 846 (almost) feasible for the original problem.

$$\min_{\mathbf{x} \in \mathbb{R}^d} \mathbf{a}^\top \mathbf{x} + b \quad \text{s.t.} \quad \mathbf{x} \in \bigcap_{\substack{\delta_i, i \in [N] \\ i \in [N]}} \mathcal{X}_{\delta_i}. \quad (3)$$

847 When \mathcal{X}_δ is convex for every $\delta \in \Delta$, we have that: the following result. If \mathcal{Q} is a distribution
 848 defined on Δ , and $N \geq [\frac{2 \ln(1/\beta)}{\alpha} + 2d + \frac{2d \ln(2/\alpha)}{\alpha}]$, then with probability

$$849 N \geq \left[\frac{2 \ln(1/\beta)}{\alpha} + 2d + \frac{2d \ln(2/\alpha)}{\alpha} \right],$$

864 then, with probability at least $1 - \beta$ of $\{\delta_i\}_{i=1}^N \sim Q$ over the i.i.d. samples $\{\delta_i\}_{i=1}^N \sim Q^N$, if the
 865 following optimization problem equation 3 has a unique solution x_{\min} , such this solution x_{\min}
 866 satisfies $P_{\delta \sim \Delta}(x_{\min} \in \mathcal{X}_{\delta}) \geq 1 - \alpha$.

867

$$868 \quad P_{\delta \sim Q}(x_{\min} \in \mathcal{X}_{\delta}) \geq 1 - \alpha.$$

869

870

A classic application for of RCP_N is to find the minimum (or maximum) value compute a high-probability upper bound of a function f when input in a constraint $f(t)$ over a domain Δ , which can be written as \vdash . This can be formulated as an optimization problem with a decision variable $x \in \mathbb{R}$ (i.e., dimension $d = 1$):

871

$$872 \quad \min_{x \in \mathbb{R}} x \quad \text{s.t. } x \geq f(t), \forall t \in \Delta. \quad (4)$$

873

874

875 By applying the RCP_N result with $d = 1$, we know that when $N \geq \lceil \frac{2 \ln(1/\beta)}{\alpha} + 2d + \frac{2d \ln(2/\alpha)}{\alpha} \rceil$
 876 and we select if we draw N samples $\{t_i\}_{i=1}^N$ in from Δ , then with probability according to Q , where
 877

878

879

$$880 \quad N \geq \left\lceil \frac{2 \ln(1/\beta)}{\alpha} + 2 + \frac{2 \ln(2/\alpha)}{\alpha} \right\rceil,$$

881

882

883 then, with probability at least $1 - \beta$, there are $P_{t \sim \Delta}(f(t) \leq \max_i f(t_i)) \geq 1 - \alpha$. over the
 884 sampling, we have $P_{t \sim Q}(f(t) \leq \max_{i=1 \dots N} f(t_i)) \geq 1 - \alpha$.

885

886

D ABOUT THE EFFECT ANALYSIS OF THE SAMPLE NUMBER SIZE EFFECT IN PART 1 STEP 1

887

888

In this section, we will demonstrate why we choose justify the choice of v_{\max} as show in the algorithm 2. Then main result is that we want presented in Algorithm 2. The main objective is to ensure that the range \mathcal{Z} we obtained by algorithm should not far beyond the real obtained by Algorithm 2 does not significantly exceed the actual range $\{F(x)\}_{x \in \mathcal{C}}$.

889

890

And algorithm 2 can guarantee such thing under some assumption as shown in the below: Algorithm 2 guarantees this property under certain assumptions, as detailed in the following proposition.

891

892

Proposition 3. Let $|(F(x))_i - (F(x^{(0)}))_i| \sim N_i$ when $x \sim \mathcal{C}$, and $v_i \in \mathbb{R}_+$ is the minimum value such that $P_{x \sim N_i}(x \leq v_i) = 1$.

893

894

If $\alpha_1^i \leq \alpha_2^i \leq 1$ and β_1, β_2 satisfy that: $P_{x \sim N_i}(x \leq \alpha_1^i v_i) = \beta_1$ and $P_{x \sim N_i}(x \leq \alpha_2^i v_i) = \beta_2$ for any $i \in [d_L]$.

895

896

Let $z_i = (c_1 v_{\max})_i$ where c_1 and v_{\max} are obtained by algorithm 2, then we have that: $\frac{z_j}{v_j} \leq \max_i \left\{ \frac{\alpha_2^i}{\alpha_1^i} \right\} \alpha_2^j$ for any $j \in [d_L]$ with probability $1 - d_L(1 + \beta_1^{N_1} - \beta_2^{N_1}) - d_L(1 + \beta_1^{N_2} - \beta_2^{N_2})$.

897

898

Proof. Easy to see that, for any $i \in [d_L]$, for the random selected Observe that for any coordinate $i \in [d_L]$, given the N_1 points $\{x_j\}$ in randomly selected points $\{x_k\}$ from \mathcal{C} in algorithm 2, there are $P(\alpha_1^i v_i \geq \max_j (x_j)_i \geq \alpha_1^i v_i) \geq \beta_1^{N_1} + \beta_2^{N_1}$ for any $i \in [d_L]$. So with probability $1 - d_L(1 + \beta_1^{N_1} - \beta_2^{N_1})$, there are $\alpha_2^i v_i \geq \max_j (x_j)_i \geq \alpha_1^i v_i$ stand for any $i \in [d_L]$ Algorithm 2, we have:

899

900

$$901 \quad P\left(\alpha_2^i v_i \geq \max_k (x_k)_i \geq \alpha_1^i v_i\right) \geq \beta_2^{N_1} - \beta_1^{N_1}.$$

902

903

904 Applying the union bound, with probability $1 - d_L(1 - (\beta_2^{N_1} - \beta_1^{N_1})) = 1 - d_L(1 + \beta_1^{N_1} - \beta_2^{N_1})$,
 905 the condition $\alpha_2^i v_i \geq \max_k (x_k)_i \geq \alpha_1^i v_i$ holds for all $i \in [d_L]$.

906

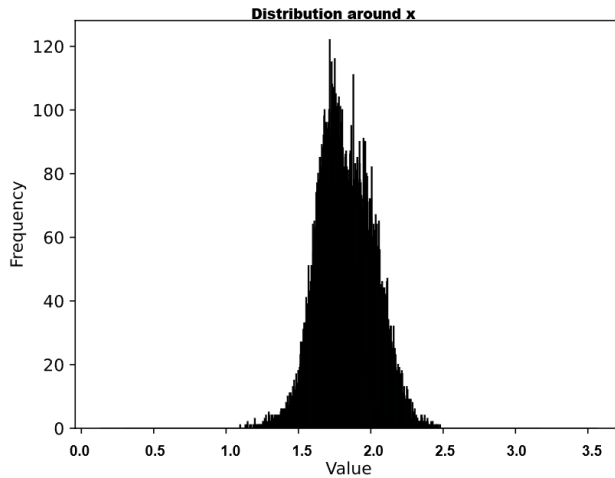
907

908 SimilarSimilarly, for the N_2 points $\{x'_j\}$ random selected in the algorithm $\{x'_k\}$ randomly selected in
 909 Algorithm 2, with probability $1 - d_L(1 + \beta_1^{N_2} - \beta_2^{N_2})$, there are $\alpha_2^i v_i \geq \max_j (x'_j)_i \geq \alpha_1^i v_i$ stand

910

911

918
919
920
921
922
923
924
925
926
927
928
929
930
931
932
933



934
935
936
937
938
939
940
941
942
943
944
945
946
947
948
949
950
951
952
953
954
955
956
957
958
959
960
961
962
963
964
965
966
967
968
969
970
971

Figure 6: This is a picture about the distribution around a sample x . When we take $\alpha_1 = 2.3/3.5$ and $\alpha_2 = 2.8/3.5$, by such figure, we have that $\beta_1 \leq 0.99$ but $\beta_2 \approx 1$. Thus $(\alpha_2/\alpha_1)\alpha_2 \approx 0.97$. Hence, if there are $N_1 = N_2 = 3000$, then $1 - d_L(1 + \beta_1^{N_1} - \beta_2^{N_1}) - d_L(1 + \beta_1^{N_2} - \beta_2^{N_2}) \geq 0.99$ when $d_L \leq 10^7$.

for any $i \in [d_L]$, $1 - d_L(1 + \beta_1^{N_2} - \beta_2^{N_2})$, the condition $\alpha_2^i v_i \geq \max_k (x'_k)_i \geq \alpha_1^i v_i$ holds for all $i \in [d_L]$.

Hence, based on the algorithm 2, we know that $c_1 \leq \max_i \{\alpha_2^i / \alpha_1^i\}$ when the above results hold for any $i \in [d_L]$. Hence, there are $(c_1 v_{\max})_j \leq \max_i \{\frac{\alpha_2^i}{\alpha_1^i}\} \alpha_2^j v_j$ any $j \in [d_L]$, which is what we want construction in Algorithm 2, if the above events occur, we have $c_1 \leq \max_i \{\alpha_2^i / \alpha_1^i\}$. Therefore, for any $j \in [d_L]$, implies:

$$(c_1 v_{\max})_j \leq \max_i \left\{ \frac{\alpha_2^i}{\alpha_1^i} \right\} \alpha_2^j v_j,$$

which completes the proof. \square

Based on our observations of many numerous neural network outputs, we have found that the outputs of neural networks find that the output values are highly likely to be concentrated in a certain within a specific region. An example is given in the figure provided in Figure 6. Based on this, there can be $\alpha_1 \approx \alpha_2$ but $1 \approx \beta_2$ and $1 \gg \beta_1$. Hence, because $\alpha_1 \approx \alpha_2$, we know observation, it is possible that $\alpha_1 \approx \alpha_2$ while $\beta_2 \approx 1$ and $\beta_1 \ll 1$. Consequently, since $\alpha_1 \approx \alpha_2$, we can infer that each dimension of \mathcal{Z} will not far extend significantly beyond v_i , because $1 \approx \beta_2$ and $1 \gg \beta_1$, we know $1 - d_L(1 + \beta_1^{N_1} - \beta_2^{N_1}) - d_L(1 + \beta_1^{N_2} - \beta_2^{N_2}) \approx 1$, which is what we want. Furthermore, since $\beta_2 \approx 1$ and $\beta_1 \ll 1$, the probability term satisfies:

$$1 - d_L(1 + \beta_1^{N_1} - \beta_2^{N_1}) - d_L(1 + \beta_1^{N_2} - \beta_2^{N_2}) \approx 1.$$

However, in reality practice, we cannot accurately estimate α_i and β_i , so. Therefore, the choice of N_1 is mainly determined by experiments. The above theorem is only used to support primarily determined empirically. The theorem above serves to theoretically justify the accuracy of the region \mathcal{Z} we found obtained when N_1 is sufficiently large.

972 E THE PROOF OF PROPOSITION 2
973
974

Proposition (NMS Soundness Verification). *For given \mathcal{Z} , τ , and box_{gt} , if $Q(\mathcal{Z}, \tau, box_{gt}) \neq \emptyset$, then for $\forall k \in \Delta : \exists box_i \in N(z^k)$, s.t. $IoU(box_i, box_{gt}) \geq \tau \wedge \text{Class}(box_i) = \text{Class}(box_{gt})$.*

975 We give a lemma at first present a lemma.
976977 **Lemma 3.** *For a given $z \in \mathcal{Z}$, if there is no $box_i \in N(z)$ satisfies that $IoU(box_i, box_{gt}) \geq \tau$ and $\text{Class}(box_i) = q$, where $q = \text{Class}(box_{gt})$, then:*978 *For any $box_i \in z$ with $c_i \geq \iota$, $\text{Class}(box_i) = q$ and $IoU(box_i, box_{gt}) \geq \tau$, there exists another $box_j \in z$ such that $c_j \geq \iota$, $\text{Class}(box_j) = \text{Class}(box_i)$, $c_i \leq c_j$, $IoU(box_j, box_{gt}) < \tau$ and $IoU(box_i, box_j) \geq \eta$.*
979980 *Proof.* Assume that there exists a $box_i \in z$ with $c_i \geq \iota$, $\text{Class}(box_i) = \text{Class}(box_{gt})$, and $IoU(box_i, box_{gt}) \geq \tau$. By assumption, there must be the assumption of the lemma, it implies that $box_i \notin N(z)$. According to981 According to condition (n2) in Section 3.1, there must exist a $box_j \in N(z)$ such that $IoU(box_i, box_j) \geq \eta$, $c_i \leq c_j$, and $\text{Class}(box_i) = \text{Class}(box_j) = \text{Class}(box_{gt})$. By condition 982 (n1) in See Section 3.1, $box_j \in N(z)$ implies that $c_j \geq \iota$.
983984 However, by the assumptions, there is no $box_j \in N(z)$ that satisfies $\text{Class}(box_j) = q$ 985 $\text{Class}(box_i) = \text{Class}(box_{gt})$, and $IoU(box_j, box_{gt}) \geq \tau$, and. Since we have shown that 986 $\text{Class}(box_j) = \text{Class}(box_{gt})$ above, so we can get it follows that $IoU(box_j, box_{gt}) < \tau$. This 987 completes the proof. \square
988989 Using such a this lemma, we can directly get the proposition prove Proposition 2.
990991 *Proof.* Assume that $Q(\mathcal{Z}, \tau, box_{gt}) \neq \emptyset$ but for some $k \in \Delta$ such, the stated result does not hold.992 Based on condition (1) of the definition of $Q(\mathcal{Z}, \tau, box_{gt})$, let $i \in Q(\mathcal{Z}, \tau, box_{gt})$, then based on the lemma. Then, based on Lemma 3, we know that there exists another 993 $box_j \in z^k$ such that $c_j^k \geq \iota$, $\text{Class}(box_j^k) = \text{Class}(box_i^k)$, $c_i^k \leq c_j^k$, $IoU(box_j, box_{gt}) < \tau$, 994 and $IoU(box_i, box_j) \geq \eta$, which is a contradiction with the. This contradicts condition (2) of the 995 definition of $Q(\mathcal{Z}, \tau, box_{gt})$.
996997 So the assumption is wrong and we get the result. Thus, the assumption leads to a contradiction, and 998 the result follows. \square
9991000 F THE PROOF OF LEMMA 1
1001

Lemma (Threshold Properties). $\tau < \tau(i, \mathcal{Z}, box_{gt}) \Rightarrow i \in Q(\mathcal{Z}, \tau, box_{gt})$

1002 *Proof.* Firstly, we show that when $\tau' > \tau$, we have $Q(\mathcal{Z}, \tau', box_{gt}) \subset Q(\mathcal{Z}, \tau, box_{gt})$. Because if 1003 First, we demonstrate that for any $\tau' > \tau$, the inclusion $Q(\mathcal{Z}, \tau', box_{gt}) \subset Q(\mathcal{Z}, \tau, box_{gt})$ holds. 1004 Indeed, if an index i satisfied the satisfies Condition (1) in definition 2 with Definition 2 with a 1005 threshold τ' , then it also satisfied the it necessarily satisfies Condition (1) in definition 2 with any 1006 threshold $\tau < \tau'$ under with any lower threshold $\tau < \tau'$, assuming the input constraints and ground 1007 truth unchanged. Similar for remain unchanged. A similar argument applies to Condition (2) in 1008 definition 2. Then we get the Definition 2. This establishes the monotonicity result.
10091010 So if $\tau < \tau(i, \mathcal{Z}, box_{gt})$. Now, suppose for the sake of contradiction that $\tau < \tau(i, \mathcal{Z}, box_{gt})$ and 1011 $i \notin Q(\mathcal{Z}, \tau, box_{gt})$, then $i \notin Q(\mathcal{Z}, \tau', box_{gt})$ for any $\tau' > \tau$ by the preceding result, which implies 1012 $\tau > \tau(i, \mathcal{Z}, box_{gt})$ according $i \notin Q(\mathcal{Z}, \tau, box_{gt})$. By the monotonicity established above, this 1013 implies that $i \notin Q(\mathcal{Z}, \tau', box_{gt})$ for any $\tau' > \tau$. According to the definition of $\tau(i, \mathcal{Z}, box_{gt})$,
1014

1026 but this is contradiction to $\tau < \tau(i, \mathcal{Z}, box_{gt})$. So the assumption is wrong, and we prove the
 1027 lemma. $\tau(i, \mathcal{Z}, box_{gt})$, this entails $\tau \geq \tau(i, \mathcal{Z}, box_{gt})$, which contradicts the initial hypothesis that
 1028 $\tau < \tau(i, \mathcal{Z}, box_{gt})$. Thus, the assumption leads to a contradiction, which completes the proof. \square
 1029

1030 G THE PROOF OF LEMMA 2

1033 **Lemma** (Threshold Computation). *The threshold can be calculated as $\tau(i, \mathcal{Z}, box_{gt}) =$
 1034 $\min\{\tau_1(i, \mathcal{Z}, box_{gt}), \tau_2(i, \mathcal{Z}, box_{gt})\}$, where:*

$$1036 \tau_1(i, \mathcal{Z}, box_{gt}) = \min_{k \in \Delta} \text{IoU}(box_i^k, box_{gt}) \cdot \mathbb{I}(\text{Class}(box_i^k) = q) \cdot \mathbb{I}(c_i^k \geq \iota), q = \text{Class}(box_{gt})$$

$$1038 \tau_2(i, \mathcal{Z}, box_{gt}) = \begin{cases} \min_{k \in \Delta, n \neq i} \text{IoU}(box_n^k, box_{gt}) & \text{if } \exists(k, n) \text{ s.t. } \mathcal{C}_{kn} = 1 \\ 1 & \text{otherwise} \end{cases}$$

1041 where constraint $\mathcal{C}_{kn} \equiv \mathbb{I}(c_n^k \geq \iota) \cdot \mathbb{I}(\text{Class}(box_n^k) = q) \cdot \mathbb{I}(\text{IoU}(box_i^k, box_n^k) \geq \eta) \cdot \mathbb{I}(c_n^k \geq$
 1042 $c_i^k)$.

1044 *Proof.* There are $\tau(i, \mathcal{Z}, box_{gt}) \leq \min\{\tau_1(i, \mathcal{Z}, box_{gt}), \tau_2(i, \mathcal{Z}, box_{gt})\}$.

1046 It is easy to see that when $\tau' > \tau_1(i, \mathcal{Z}, box_{gt})$,

1047 We prove the equality by showing both directions of the inequality.

1049 **Part 1: Proof of $\tau(i, \mathcal{Z}, box_{gt}) \leq \min\{\tau_1, \tau_2\}$.**

1050 Observe that if $\tau' \geq \tau_1(i, \mathcal{Z}, box_{gt})$, index i will not in safe set $Q(\mathcal{Z}, \tau', box_{gt})$ because
 1051 violate is not contained in the safe set $Q(\mathcal{Z}, \tau', box_{gt})$ because it violates Condition (1) in
 1052 definition 2. When $\tau' > \tau_2(i, \mathcal{Z}, box_{gt})$, even if Definition 2. Similarly, if $\tau' > \tau_2(i, \mathcal{Z}, box_{gt})$,
 1053 index i satisfies (1), i will not in safe set $Q(\mathcal{Z}, \tau', box_{gt})$ because violate is excluded from
 1054 the safe set $Q(\mathcal{Z}, \tau', box_{gt})$ because it violates Condition (2) in definition 2. So there are
 1055 $\tau(i, \mathcal{Z}, box_{gt}) \leq \min\{\tau_1(i, \mathcal{Z}, box_{gt}), \tau_2(i, \mathcal{Z}, box_{gt})\}$, even if Condition (1) is satisfied.
 1056 Consequently, the threshold must satisfy:

$$1058 \tau(i, \mathcal{Z}, box_{gt}) \leq \min\{\tau_1(i, \mathcal{Z}, box_{gt}), \tau_2(i, \mathcal{Z}, box_{gt})\}.$$

1060 There are $\tau(i, \mathcal{Z}, box_{gt}) \geq \min\{\tau_1(i, \mathcal{Z}, box_{gt}), \tau_2(i, \mathcal{Z}, box_{gt})\}$. **Part 2: Proof of**
 1061 $\tau(i, \mathcal{Z}, box_{gt}) \geq \min\{\tau_1, \tau_2\}$.

1063 Easy to see that when $\tau' < \tau_1(i, \mathcal{Z}, box_{gt})$, Note that when $\tau' < \tau_1(i, \mathcal{Z}, box_{gt})$, index i must
 1064 satisfied the satisfy Condition (1) in definition 2 for such τ' ; when $\tau' < \tau_2(i, \mathcal{Z}, box_{gt})$, Definition 2.
 1065 Likewise, when $\tau' < \tau_2(i, \mathcal{Z}, box_{gt})$, index i must satisfied the satisfy Condition (2) in definition 2
 1066 for such τ' . Therefore, if we choose a threshold $\tau \leq \min\{\tau_1(i, \mathcal{Z}, box_{gt}), \tau_2(i, \mathcal{Z}, box_{gt})\}$, index
 1067 i satisfies both conditions, which implies $i \in Q(\mathcal{Z}, \tau, box_{gt})$. By the definition of the threshold
 1068 $\tau(i, \mathcal{Z}, box_{gt})$, this implies:

$$1069 \tau(i, \mathcal{Z}, box_{gt}) \geq \min\{\tau_1(i, \mathcal{Z}, box_{gt}), \tau_2(i, \mathcal{Z}, box_{gt})\}.$$

1071 So when $\tau < \min\{\tau_1(i, \mathcal{Z}, box_{gt}), \tau_2(i, \mathcal{Z}, box_{gt})\}$, there must be $i \in Q(\mathcal{Z}, \tau, box_{gt})$, which
 1072 implies $\tau(i, \mathcal{Z}, box_{gt}) \geq \min\{\tau_1(i, \mathcal{Z}, box_{gt}), \tau_2(i, \mathcal{Z}, box_{gt})\}$.

1074 So we get the result Combining the results from Part 1 and Part 2, the equality holds. \square

1076 H GET THE VERIFICATION BOUND

1078 In this section, we show how to **Calculate the verification bound** for NMS.

1079 We first define the verification bounds:

1080
1081**Definition 4** (OD Verification Bounding). For constraints \mathcal{C} and box_{gt} , define:1082
1083

$$\min_{\mathbf{x} \in \mathcal{C}} \max_{box_i \in N(\mathbf{x})} \text{IoU}(box_i, box_{gt}) \cdot \mathbb{I}(\text{Class}(box_i) = \text{Class}(box_{gt})),$$

1084
1085

as the OD verification bounding. This quantifies robustness against OD attacks.

1086
1087
1088We need to estimate the verification bound $\min_{z \in \mathcal{Z}} \max_{box_i \in N(z)} \text{IoU}(box_i, box_{gt}) \mathbb{I}(\text{Class}(box_i) = \text{Class}(box_{gt}))$
 $\min_{z \in \mathcal{Z}} \max_{box_i \in N(z)} \text{IoU}(box_i, box_{gt}) \mathbb{I}(\text{Class}(box_i) = \text{Class}(box_{gt}))$ under the input restriction \mathcal{Z} and ground truth box_{gt} , according to definition 4.

1089

To estimate such bound, firstly, we need the following lemma:

1090
1091**Lemma 4.** For any $\mathcal{Z}, \tau, box_{gt}$, there is:1092
1093

$$\min_{z \in \mathcal{Z}} \max_{box_i \in N(z)} \text{IoU}(box_i, box_{gt}) \mathbb{I}(\text{Class}(box_i) = \text{Class}(box_{gt})) \geq \tau \mathbb{I}(|Q(\mathcal{Z}, \tau, box_{gt})| \geq 1)$$

1094
1095
1096
1097So we will try to find the maximum τ that makes $Q(\mathcal{Z}, \tau, box_{gt})$ bigger than 0, but sometimes this maximum value does not exist (can only approach the maximum value arbitrarily), so we look for the following value instead:1098
1099
1100

$$\min_{\tau \in [0, 1]} \tau \text{ s.t. } |Q(\mathcal{Z}, \tau, box_{gt})| = 0, \forall 1 \geq \tau' > \tau \quad (5)$$

1101
1102
1103

We use the following lemma to calculate such minimum value:

Lemma 5. The solution of problem 5 is equal to: $\max_{i \in [n_x]} \tau(i, \mathcal{Z}, box_{gt})$.1104
1105
1106Use such lemma, we just to need calculate $\tau(i, \mathcal{Z}, box_{gt})$ as said before, and then we can estimate the verification bounding.1107
1108

H.1 THE PROOF OF LEMMA 4

1109
1110
1111
1112
1113
1114
1115*Proof.* By the proposition By Proposition 2, if $|Q(\mathcal{Z}, \tau, box_{gt})| \geq 1$, then for any $z \in \mathcal{Z}$, there is a $box_i \in N(z)$ such that $\text{IoU}(box_i, box_{gt}) \geq \tau$ and $\text{Class}(box_i) = \text{Class}(box_{gt})$, which implies $z \in \mathcal{Z}$, there exists a $box_i \in N(z)$ such that $\text{IoU}(box_i, box_{gt}) \geq \tau$ and $\text{Class}(box_i) = \text{Class}(box_{gt})$. This implies that the value of $\min_{z \in \mathcal{Z}} \max_{box_i \in N(z)} \text{IoU}(box_i, box_{gt}) \mathbb{I}(\text{Class}(box_i) = \text{Class}(box_{gt}))$ is greater than or equal to τ , so we get the which yields the desired result. \square 1116
1117
1118

H.2 THE PROOF OF LEMMA 5

1119
1120
1121
1122
1123*Proof.* We have shown that when $\tau' > \tau$, we have $Q(\mathcal{Z}, \tau', box_{gt}) \subset Q(\mathcal{Z}, \tau, box_{gt})$ in Lemma 1.By the definition of $\tau(i, \mathcal{Z}, box_{gt})$ and above result, we know that the safe set $Q(\mathcal{Z}, \tau', box_{gt})$ is \emptyset for any $\tau' > \max_{i \in [n_x]} \tau(i, \mathcal{Z}, box_{gt})$, so the solution of problem 5 is not more than $\max_{i \in [n_x]} \tau(i, \mathcal{Z}, box_{gt})$.1124
1125If τ is the solution of problem 5, then for any $i \in [n_x]$, there must be $i \notin Q(\mathcal{Z}, \tau', box_{gt})$ for any $\tau' \geq \tau$, so $\tau \geq \max_{i \in [n_x]} \tau(i, \mathcal{Z}, box_{gt})$.1126
1127
1128So we prove the lemma. \square 1129
1130
1131

I VERIFICATION PROCESS OF NMS

1132
1133To illustrate Non-Maximum Suppression (NMS) verification, we define constraints as $\mathcal{Z} = \mathcal{H} \setminus \mathcal{S}$. Here, \mathcal{H} constrains the neural network output \mathbf{y} , and \mathcal{S} constrains bounding box parameters. This formulation is equivalent to the original. Algorithm 5 details the NMS verification process.

1134 **Algorithm 5** Soundness Object Disappear Thread Verification for NMS

1135 **Require:** Constraints $\mathcal{Z} = \mathcal{H} \setminus \mathcal{S}$; input \mathbf{x} ; output \mathbf{y} ; ground truth box_{gt} ; confidence threshold ι ;
 1136 IoU threshold τ ; upper bound η .

1137 **Ensure:** Calculate τ_1, τ_2 .

1138 1: $\mathcal{B}_{cand}, \mathcal{B}_{other} \leftarrow \emptyset, \emptyset$

1139 2: $\{\overline{box}_i\}_{i=1}^{n_{\mathbf{x}}} = \text{CONSTRUCT_ABSTRACT_BOX}(\mathcal{Z})$

1140 3: **for all** $\overline{box}_i \in \{\overline{box}_k\}_{k=1}^{n_{\mathbf{x}}}$ **do**

1141 4: $\tau_1(i) \leftarrow 0, \tau_2(i) \leftarrow 1$

1142 5: **if** $\forall k \in [n] \setminus \{\text{Class}(box_{gt})\}, \bar{p}_{i, \text{Class}(box_{gt})} \leq \underline{p}_{i,k}$ **then**

1143 6: **continue** ▷ Skip boxes must not match box_{gt} class

1144 7: **end if**

1145 8: **if** $\underline{c}_i \geq \iota$ **then** ▷ Ensure indicator $\mathbb{I}(c_i \geq \iota) = 1$

1146 9: $\tau_1(i) \leftarrow \text{IOU_LOWER_BOUNDS}(\overline{box}_i, box_{gt})$

1147 10: **if** $\forall k \in [n] \setminus \{\text{Class}(box_{gt})\}, \underline{p}_{i, \text{Class}(box_{gt})} \geq \bar{p}_{i,k}$ **then**

1148 11: $\mathcal{B}_{cand} \leftarrow \mathcal{B}_{cand} \cup \{\overline{box}_i\}$ ▷ Box must match box_{gt} class

1149 12: **else**

1150 13: $\mathcal{B}_{other} \leftarrow \mathcal{B}_{other} \cup \{\overline{box}_i\}$ ▷ Box may match box_{gt} class

1151 14: **end if**

1152 15: **end if**

1153 16: **end for**

1154 17: **for all** $\overline{box}_i \in \mathcal{B}_{cand}$ **do**

1155 18: **for all** $\overline{box}_j \in \mathcal{B}_{other}$ **do**

1156 19: **if** $\bar{c}_j < \underline{c}_i$ **then** ▷ Ensure box_j may suppress box_i

1157 20: **continue** ▷ Skip boxes that cannot suppress box_i

1158 21: **end if**

1159 22: $ub \leftarrow \text{IOU_UPPER_BOUNDS}(\overline{box}_i, \overline{box}_j)$

1160 23: **if** $ub \geq \eta$ **then** ▷ Ensure box_i may suppressed by box_j

1161 24: $lb \leftarrow \text{IOU_LOWER_BOUNDS}(\overline{box}_j, box_{gt})$

1162 25: $\tau_2(i) \leftarrow \min(\tau_2(i), lb)$

1163 26: **end if**

1164 27: **end for**

1165 28: **end for**

1166 29: **return** $\{\tau_1(i)\}_{i=1}^{n_{\mathbf{x}}}, \{\tau_2(i)\}_{i=1}^{n_{\mathbf{x}}}$

Next we show how to construct the abstract box \overline{box} and how to calculate the lower and upper bounds of IoU.

Let \mathbb{B} be the 'box space' (space of individual box structures). An interpretation function $G : \mathbb{R}^{d_L} \rightarrow \{\mathcal{S} \subseteq \mathbb{B} \mid |\mathcal{S}| = n_x\}$ maps y to a set $\{box_i\}_{i=1}^{n_x}$ of n_x bounding boxes, where n_x is a constant determined by the fixed input dimension. A function $S : \mathbb{B} \rightarrow \mathcal{P}(\{1, \dots, d_L\})$ (where \mathcal{P} is the power set) maps each distinct $box_k \in \mathbb{B}$ (that could form part of an output set) to its source indices in y . We then define the regular region \mathcal{Z} as follows:

Definition 5 (Regular Region). A regular region is a subset $\mathcal{Z} \subseteq \mathbb{R}^{d_L}$ defined as $\mathcal{Z} = \mathcal{H} \setminus \mathcal{S}$, where:

- \mathcal{H} is a hyperrectangle (axis-aligned rectangular region) centered at $\mathbf{F}(\mathbf{x}^{(0)})$ with component-wise perturbations bounded by $c_1 v_{\max}$;

$$\mathcal{H} = \left\{ \mathbf{F}(\mathbf{x}^{(0)}) + \boldsymbol{\epsilon} \in \mathbb{R}^{d_L} \mid \forall j \in \{1, \dots, d_L\}, |\epsilon_j| \leq (c_1 \mathbf{v}_{\max})_j \right\}$$

- \mathcal{S} is a union of k hyperspherical zones. Each zone $\mathcal{S}_i = B(c_i, d_i)$ is defined by a center c_i and radius d_i , where c_i is the center of the exclusion zone and d_i is the radius. The union of these zones is given by:

$$\mathcal{S} = \bigcup_{i=1}^k \mathcal{S}_i = \bigcup_{i=1}^k \text{B}(\mathbf{c}_i, d_i), \text{B}(\mathbf{c}_i, d_i) = \{ \mathbf{y} \in \mathbb{R}^{d_L} \mid \|\mathbf{y} - \mathbf{c}_i\|_2^2 \leq d_i^2 \}$$

1188 Note, sometimes we just need part dimension of \mathcal{S}_i . Thus we can extend B to $B(\mathbf{c}_i, d_i, \mathcal{I}_i)$,
 1189 where \mathcal{I}_i is the index set of dimensions in \mathcal{S}_i . Then we have:
 1190
$$B(\mathbf{c}_i, d_i, \mathcal{I}_i) = \{ \mathbf{y} \in \mathbb{R}^{d_L} \mid \|\mathbf{y}_{\mathcal{I}_i} - \mathbf{c}_{i, \mathcal{I}_i}\|_2^2 \leq d_i^2 \}$$

 1191 where $\mathbf{c}_{i, \mathcal{I}_i}$ is the component of \mathbf{c}_i for index set \mathcal{I}_i .

1194 I.1 ABSTRACT BOUNDING BOX CONSTRUCTION AND IOU BOUND COMPUTATION

1195 We use \tilde{x} to represent x is a Gurobi variable, $\tilde{\mathbb{R}}$ to represent real number Gurobi variable space. Let
 1196 $\tilde{\mathbf{y}} \in \tilde{\mathbb{R}}^{d_L}$ be the Gurobi variable vector.
 1197

1198 Then we encode the regular region \mathcal{Z} as a set of constraints. To encode \mathcal{H} , we need to
 1199 get the lower and upper bounds of each parameter of each bounding box. Suppose $\mathcal{H} =$
 1200 $\{ \mathbf{F}(\mathbf{x}^{(0)}) + \epsilon \in \mathbb{R}^{d_L} \mid \forall j \in \{1, \dots, d_L\}, |\epsilon_j| \leq (c_1 \mathbf{v}_{\max})_j \}$, where c_1 and \mathbf{v}_{\max} (Note $\mathbf{v}_{\max} > 0$)
 1201 are obtained from Part 1. Let $\bar{\mathbf{y}} = \mathbf{F}(\mathbf{x}^{(0)}) + c_1 \mathbf{v}_{\max}$ and $\underline{\mathbf{y}} = \mathbf{F}(\mathbf{x}^{(0)}) - c_1 \mathbf{v}_{\max}$. Then we add the
 1202 following constraints to the Gurobi model:

$$\underline{\mathbf{y}} \leq \tilde{\mathbf{y}} \leq \bar{\mathbf{y}}$$

1203 Here, \leq is the component-wise less than or equal to operator.
 1204

1205 Next, we need to add the exclusion zone constraints. For each exclusion zone \mathcal{S}_i , we need to add the
 1206 following constraints:
 1207

$$\sum_{j \in \mathcal{I}_i} (\tilde{\mathbf{y}}_j - (\mathbf{c}_i)_j)^2 \geq d_i^2$$

1208 where $(\mathbf{c}_i)_j$ is the component of \mathbf{c}_i for index j .
 1209

1210 CONSTRUCT_ABSTRACT_Box(\mathcal{Z}) adds these constraints to the Gurobi model. And then reorga-
 1211 nizes $\tilde{\mathbf{y}}$ as an abstract bounding box set $\{\overline{\text{box}}_i\}_{i=1}^{n_{\mathbf{x}}}$, where $n_{\mathbf{x}}$ is the number of bounding boxes.
 1212 Each bounding box $\overline{\text{box}}_i = (\tilde{x}_i, \tilde{y}_i, \tilde{w}_i, \tilde{h}_i, \tilde{c}_i, \{\tilde{p}_{i,j}\}_{j=1}^{n_{\mathbf{x}}})$. Note all the parameters of $\overline{\text{box}}_i$ are from
 1213 $\tilde{\mathbf{y}}$ thus have constraints on them.
 1214

1215 IoU bounds for abstract boxes involve:
 1216

1217 1. **Geometric Constraints:** Box i coordinates are:
 1218

$$\begin{aligned} \tilde{x}_{\min}^i &= \tilde{x}_i - \frac{\tilde{w}_i}{2}, & \tilde{x}_{\max}^i &= \tilde{x}_i + \frac{\tilde{w}_i}{2}, \\ \tilde{y}_{\min}^i &= \tilde{y}_i - \frac{\tilde{h}_i}{2}, & \tilde{y}_{\max}^i &= \tilde{y}_i + \frac{\tilde{h}_i}{2}. \end{aligned}$$

1219 2. **Intersection/Union Area**

$$\begin{aligned} I_w &= \max(0, \min(\tilde{x}_{\max}^i, \tilde{x}_{\max}^j) - \max(\tilde{x}_{\min}^i, \tilde{x}_{\min}^j)), \\ I_h &= \max(0, \min(\tilde{y}_{\max}^i, \tilde{y}_{\max}^j) - \max(\tilde{y}_{\min}^i, \tilde{y}_{\min}^j)), \\ A_{\text{int}} &= I_w \cdot I_h, \\ A_{\text{union}} &= (\tilde{x}_{\max}^i - \tilde{x}_{\min}^i) \cdot (\tilde{y}_{\max}^i - \tilde{y}_{\min}^i) + (\tilde{x}_{\max}^j - \tilde{x}_{\min}^j) \cdot (\tilde{y}_{\max}^j - \tilde{y}_{\min}^j) - A_{\text{int}}. \end{aligned}$$

1220 We use big-M constraints to encode $\max(0, \cdot)$ and $\min(\cdot, \cdot)$ operations in Gurobi. For example, to
 1221 encode $\tilde{A}_{\text{expr}} = \max(0, E)$, where E is an expression, we introduce an auxiliary binary variable
 1222 $\tilde{b} \in \{0, 1\}$ and a sufficiently large constant M . The variable \tilde{A}_{expr} is then constrained by:
 1223

$$\begin{aligned} \tilde{A}_{\text{expr}} &\geq E \\ \tilde{A}_{\text{expr}} &\geq 0 \\ \tilde{A}_{\text{expr}} &\leq E + M \cdot \tilde{b} \\ \tilde{A}_{\text{expr}} &\leq M \cdot (1 - \tilde{b}) \end{aligned}$$

1224 where \tilde{A}_{expr} is a Gurobi variable representing the maximum. The inner terms of I_w and I_h , such as
 1225 $\min(\tilde{x}_{\max}^i, \tilde{x}_{\max}^j)$, are handled similarly using appropriate big-M formulations or Gurobi's built-in
 1226 functions. The constant M must be chosen such that $M \geq \max(U_E, -L_E)$, where U_E and L_E are
 1227 known upper and lower bounds for the expression E .
 1228

- 1242 • If $E \geq 0$, the objective of minimizing \tilde{A}_{int} (or other constraints) will force $\tilde{b} = 0$. The
 1243 constraints become $\tilde{A}_{\text{int}} \geq E$, $\tilde{A}_{\text{int}} \geq 0$, $\tilde{A}_{\text{int}} \leq E$, and $\tilde{A}_{\text{int}} \leq M$. This correctly sets
 1244 $\tilde{A}_{\text{int}} = E$.
 1245 • If $E < 0$, the objective will force $\tilde{b} = 1$. The constraints become $\tilde{A}_{\text{int}} \geq E$, $\tilde{A}_{\text{int}} \geq 0$,
 1246 $\tilde{A}_{\text{int}} \leq E + M$, and $\tilde{A}_{\text{int}} \leq 0$. This correctly sets $\tilde{A}_{\text{int}} = 0$.

1248 3. **Binary Search for IoU bounds:** To find IoU (lower bound of IoU):

```

1249   1:  $\tau_{lb} \leftarrow 0$ ,  $\tau_{ub} \leftarrow 1$ ,  $\epsilon_{\text{search}} \leftarrow 10^{-5}$ 
1250   2: while  $|\tau_{ub} - \tau_{lb}| > \epsilon_{\text{search}}$  do
1251   3:    $\tau_{\text{mid}} \leftarrow (\tau_{lb} + \tau_{ub})/2$ 
1252   4:   Solve  $L_{\text{check}} = \min(A_{\text{int}} - \tau_{\text{mid}} A_{\text{union}})$  by Gurobi
1253   5:   if  $L_{\text{check}} \geq 0$  then  $\tau_{lb} \leftarrow \tau_{\text{mid}}$ 
1254   6:   else  $\tau_{ub} \leftarrow \tau_{\text{mid}}$ 
1255   7:   end if
1256   8: end while
1257   9: return  $\tau_{lb}$ 

```

1258 Checking IoU bounds against a value τ is often done via optimizing $A_{\text{int}} - \tau A_{\text{union}}$, as direct interval
 1259 ratio optimization $A_{\text{int}}/A_{\text{union}}$ is complex for solvers (e.g., Gurobi) without reformulation. For
 1260 instance, to check if $\text{IoU}(\text{box}_i, \text{box}_{\text{gt}}) \geq \tau$ is possible, one can check if $\max(A_{\text{int}} - \tau A_{\text{union}}) \geq 0$.

1261 It's trivial to extend the above algorithm to find τ_{ub} (upper bound of IoU).

1262 The Gurobi solver, when minimizing or maximizing an objective subject to these constraints, returns
 1263 an assignment for \tilde{y} (which corresponds to a specific point $z \in \mathcal{Z}$). If a particular optimization (e.g.,
 1264 a step in the binary search showing $L_{\text{check}} < 0$) demonstrates a property violation, the returned \tilde{y} is
 1265 the concrete instance z that exhibits this violation.

1268 J THE PROOF OF THEOREM 1

1271 **Theorem** (probabilistic guarantee for Part 3). *For any $\alpha, \beta, \delta, \epsilon \in (0, 1)$ satisfying $(1 -$
 1272 $2\epsilon)^M - \delta > 0$ and $N \cdot ((1 - 2\epsilon)^M - \delta) > \frac{2}{\alpha} \ln(\frac{1}{\beta}) + 2 + \frac{2}{\alpha} \ln(\frac{2}{\alpha})$, with this algorithm, for
 1273 any y , with probability exceeding $1 - e^{-2N\delta^2} - \beta - 2(1 - \epsilon)^{M_2}$ over step 1 and step 2, we
 1274 have $V(y, d_{\min}) \leq \alpha$.*

1276 For convenience, name the step one in algorithm 4 as P1, the step two in algorithm 4 as P2, denote
 1277 Step 1 in Algorithm 4 by P1, and Step 2 by P2.

1279 J.1 SITUATION 1

1281 Firstly, we show the situation that when $y \in \{F(x)\}_{x \in \mathcal{C}}$. We Theorem 1 aims to estimate a constant
 1282 C such that, with high probability over the sampling in Part 3,

$$1284 \quad \|F(x) - y\|_2 \leq C \quad \text{for most } x \sim \mathcal{C},$$

1285 whenever y lies in the region \mathcal{Z} . The proof proceeds in three steps:

1. For each sampled point x , we estimate a local interval $[B_{F(x)}, A_{F(x)}]$ that covers, with probability
 1286 at least $1 - 2\epsilon$, the distances $\|F(x') - F(x)\|_2$ to its M neighbors.
2. Using Hoeffding's inequality, we show that with high probability at least $N((1 - 2\epsilon)^M - \delta)$ base
 1289 points have all M neighbors lying within their respective intervals.
3. On this subset, we apply an RCP _{N} -style scenario bound to the function $S_{F(x)}$, yielding an upper
 1293 bound C satisfying $P_{x \sim \mathcal{C}}(S_{F(x)} \leq C) \geq 1 - \alpha$.

1295 J.1 SITUATION 1

1296 We first consider the case where \mathbf{y} is itself realizable as $\mathbf{F}(\mathbf{x})$ for some $\mathbf{x} \in \mathcal{C}$. We have the following
 1297 theorem, which can directly get the theorem 1 when $\mathbf{y} \in \{\mathbf{F}(\mathbf{x})\}_{\mathbf{x} \in \mathcal{C}}$:

1298 **Theorem 3.** For any $\alpha, \beta, \delta, \epsilon \in (0, 1)$ satisfied $(1 - 2\epsilon)^M - \delta > 0$ and $N((1 - 2\epsilon)^M - \delta) >$
 1299 $\frac{2}{\alpha} \ln(\frac{1}{\beta}) + 2 + \frac{2}{\alpha} \ln(\frac{2}{\alpha})$, by this algorithm, if $\mathbf{y} \sim \mathbf{F}(\mathcal{C})$ (that is, the distribution of the network
 1300 output when the input obeys \mathcal{C}), then with probability $1 - e^{-2N\delta^2} - \beta - 2(1 - \epsilon)^{M_2}$ of $P_{1 \cup 2}$, there
 1301 is we have $P_{\mathbf{y}}(B_m - C(A_m - B_m) < 0) \geq 1 - \alpha$.

1303 *Proof.* For any given \mathbf{y} , let $A_{\mathbf{y}}$ satisfy that $P_{\mathbf{x} \sim \mathcal{C}}(\|\mathbf{F}(\mathbf{x}) - \mathbf{y}\|_2 \leq A_{\mathbf{y}}) = 1 - \epsilon$, let $B_{\mathbf{y}}$ satisfy that
 1304 $P_{\mathbf{x} \sim \mathcal{C}}(\|\mathbf{F}(\mathbf{x}) - \mathbf{y}\|_2 \geq B_{\mathbf{y}}) = 1 - \epsilon$. Let $S_{\mathbf{y}} = \frac{B_{\mathbf{y}}}{A_{\mathbf{y}} - B_{\mathbf{y}}}$.

1306 The proof is into four parts:

1308 **Part One: For any i , with probability $(1 - 2\epsilon)^M$ of P1, there are we havee** $\|\mathbf{F}(\mathbf{x}^{(i,j)}) -$
 1309 $\mathbf{F}(\mathbf{x}^{(i)})\|_2 \in [B_{\mathbf{F}(\mathbf{x}^{(i)})}, A_{\mathbf{F}(\mathbf{x}^{(i)})}]$ for all $j \in [M]$.

1310 This is obvious, based on the definition of $B_{\mathbf{F}(\mathbf{x}^{(i)})}$ and $A_{\mathbf{F}(\mathbf{x}^{(i)})}$, we know that
 1311 $P_{\mathbf{x}^{(i,j)} \sim \mathcal{C}}(\|\mathbf{F}(\mathbf{x}^{(i,j)}) - \mathbf{F}(\mathbf{x}^{(i)})\|_2 \in [B_{\mathbf{F}(\mathbf{x}^{(i)})}, A_{\mathbf{F}(\mathbf{x}^{(i)})}]) = 1 - 2\epsilon$. Because each selection of For
 1312 any i , since the samples $\mathbf{x}^{(i,j)}$ is independent, so we get the result are i.i.d.,

$$P\left(\|\mathbf{F}(\mathbf{x}^{(i,j)}) - \mathbf{F}(\mathbf{x}^{(i)})\|_2 \in [B_{\mathbf{F}(\mathbf{x}^{(i)})}, A_{\mathbf{F}(\mathbf{x}^{(i)})}]\right) = 1 - 2\epsilon.$$

1317 Thus all M neighbors lie in the interval with probability $(1 - 2\epsilon)^M$.

1318 **Part Two: With probability $1 - e^{-2N\delta^2}$ of P1, there are we have at least $N((1 - 2\epsilon)^M - \delta)$
 1319 numbers of $i \in [N]$ satisfied that $\|\mathbf{F}(\mathbf{x}^{(i,j)}) - \mathbf{F}(\mathbf{x}^{(i)})\|_2 \in [B_{\mathbf{F}(\mathbf{x}^{(i)})}, A_{\mathbf{F}(\mathbf{x}^{(i)})}]$ for all $j \in [M]$.**

1321 To proof that, we need use Hoeffding inequality. Let

1323 Define indicator variables

$$X_i = \mathbb{I}\left\{\|\mathbf{F}(\mathbf{x}^{(i,j)}) - \mathbf{F}(\mathbf{x}^{(i)})\|_2 \in [B_{\mathbf{F}(\mathbf{x}^{(i)})}, A_{\mathbf{F}(\mathbf{x}^{(i)})}] \forall j \in [M]\right\}.$$

1327 Then X_i is the random variable defined as: $X_i = 1$ if $\|\mathbf{F}(\mathbf{x}^{(i,j)}) - \mathbf{F}(\mathbf{x}^{(i)})\|_2 \in [B_{\mathbf{F}(\mathbf{x}^{(i)})}, A_{\mathbf{F}(\mathbf{x}^{(i)})}]$
 1328 for all $j \in [M]$, or $X_i = 0$. Without a doubt, $\{X_i\}_{i=1}^N$ are i.i.d, and by Part One, there are
 1329 $E(X_i) = (1 - 2\epsilon)^M$.

1331 Then by using Hoeffding inequality, we have that: $P\left(\sum_{i=1}^N X_i / N - (1 - 2\epsilon)^M \leq -\delta\right) \leq e^{-2N\delta^2}$,
 1332 this is what we want. with $E[X_i] = (1 - 2\epsilon)^M$. Applying Hoeffding's inequality yields

$$P\left(\frac{1}{N} \sum_{i=1}^N X_i - (1 - 2\epsilon)^M \leq -\delta\right) \leq e^{-2N\delta^2},$$

1337 implying the desired bound on the number of "good" indices. Then the complement event gives:

$$P\left(\frac{1}{N} \sum_{i=1}^N X_i - (1 - 2\epsilon)^M > -\delta\right) > 1 - e^{-2N\delta^2},$$

1342 i.e., at least $N((1 - 2\epsilon)^M - \delta)$ indices i satisfy the desired property with probability at least
 1343 $1 - e^{-2N\delta^2}$.

1345 **Part Three: With probability $1 - e^{2N\delta^2} - \beta$ of P1, there are $P_{\mathbf{x} \sim \mathcal{C}}(S_{\mathbf{F}(\mathbf{x})} \leq C) \geq 1 - \alpha$.**

1347 We have two simple facts:

1348 Firstly, if $i \in [N]$ such that $\|\mathbf{F}(\mathbf{x}^{(i,j)}) - \mathbf{F}(\mathbf{x}^{(i)})\|_2 \in [B_{\mathbf{F}(\mathbf{x}^{(i)})}, A_{\mathbf{F}(\mathbf{x}^{(i)})}]$ for all $j \in [M]$, then there
 1349 must be $C \geq \frac{B'_i}{A'_i - B'_i} \geq S_{\mathbf{F}(\mathbf{x}^{(i)})}$.

1350 Secondly, for any $N_1 \geq N((1 - 2\epsilon)^M - \delta)$, by using RCP_N to find the maximum of function
 1351 $S_{F(\mathbf{x})}$, we know that with probability $1 - \beta$ for i.i.d selected N_1 samples $\{\mathbf{x}^{(i)}\}_{i=1}^{N_1}$ in \mathcal{C} , then
 1352 $P_{\mathbf{x} \sim \mathcal{C}}(S_{F(\mathbf{x})} \leq \max_{i \in [N_1]} \{S_{F(\mathbf{x}^{(i)})}\}) \geq 1 - \alpha$.
 1353

1354 By the two facts, we can deduce that:

1355 For any $N_1 \in \mathbb{Z}^+$, let $\mathcal{Q}_{N_1} \subset 2^{\mathcal{C}}$ and a $q \in 2^{\mathcal{C}} \cap \mathcal{Q}_{N_1}$ if and
 1356 only if $|q| = N_1$ and $P_{\mathbf{x} \sim \mathcal{C}}(S_{F(\mathbf{x})} \leq \max_{\mathbf{x}^{(p)} \in q} \{S_{F(\mathbf{x}^{(p)})}\}) \geq 1 - \alpha$. Let
 1357 $\mathcal{Q}_k = \{q \subset \mathcal{C} : |q| = k, P_{\mathbf{x} \sim \mathcal{C}}(S_{F(\mathbf{x})} \leq \max_{\mathbf{x}^{(p)} \in q} \{S_{F(\mathbf{x}^{(p)})}\}) \geq 1 - \alpha\}$. According to the
 1358 second fact, when $N_1 \geq N((1 - 2\epsilon)^M - \delta)$, there are $P_{\mathbf{x}^{(i)} \sim \mathcal{C}, i \in [N_1]}(\{\mathbf{x}^{(i)}\} \in \mathcal{Q}_{N_1}) \geq 1 - \beta$.
 1359

1360 Then let $\mathcal{T} = \{\mathbf{x}^{(i)}\}$ mean the set contained all $\mathbf{x}^{(i)}$ such
 1361 that $\|F(\mathbf{x}^{(i,j)}) - F(\mathbf{x}^{(i)})\|_2 \in [B_{F(\mathbf{x}^{(i)})}, A_{F(\mathbf{x}^{(i)})}]$ for all $j \in [M]$. Let
 1362 $\mathcal{T} = \{\mathbf{x}^{(i)} \in \mathcal{C} : \forall j \in [M], \|F(\mathbf{x}^{(i,j)}) - F(\mathbf{x}^{(i)})\|_2 \in [B_{F(\mathbf{x}^{(i)})}, A_{F(\mathbf{x}^{(i)})}]\}$. If $\mathcal{T} \in \cup_{k=1}^{\infty} \mathcal{Q}_k$,
 1363 then by the first fact we have $C > \max_{\mathbf{x}^{(i)} \in \mathcal{T}} S_{F(\mathbf{x}^{(i)})}$, hence we have $P_{\mathbf{x} \sim \mathcal{C}}(S_{F(\mathbf{x})} \leq C) \geq$
 1364 $P_{\mathbf{x} \sim \mathcal{C}}(S_{F(\mathbf{x})} \leq \max_{\mathbf{x}^{(p)} \in \mathcal{T}} \{S_{F(\mathbf{x}^{(p)})}\}) \geq 1 - \alpha$, so we only need to calculate $P_{\text{P1}}(\mathcal{T} \in \cup_{k=1}^{\infty} \mathcal{Q}_k)$.
 1365

1366 We have that:

$$\begin{aligned} & P_{\text{P1}}(\mathcal{T} \in \cup_{k=1}^{\infty} \mathcal{Q}_k) \\ &= \sum_{k=1}^{\infty} P_{\text{P1}}(\mathcal{T} \in \mathcal{Q}_k) \\ &= \sum_{k=1}^N P_{\text{P1}}(\mathcal{T} \in \mathcal{Q}_k) \end{aligned}$$

1370 According to the process of algorithm, which k index i satisfy the condition $\|F(\mathbf{x}^{(i,j)}) - F(\mathbf{x}^{(i)})\|_2 \in$
 1371 $[B_{F(\mathbf{x}^{(i)})}, A_{F(\mathbf{x}^{(i)})}]$ for all $j \in [M]$ is determined by the second time randomize samples in P1, and
 1372 whether these samples are in the set \mathcal{Q}_k is determined by first time randomize samples in P1. These
 1373 two processes are completely independent. So we have that:
 1374

$$\begin{aligned} & P_{\text{P1}}(\mathcal{T} \in \mathcal{Q}_k) \\ &= \sum_{\{t_i\}_{i=1}^k \subset [N]} P_{\text{P1}}(\{\mathbf{x}^{(t_i)}\}_{i=1}^k = \mathcal{T}, \{\mathbf{x}^{(t_i)}\}_{i=1}^k \in \mathcal{Q}_k) \\ &= \sum_{\{t_i\}_{i=1}^k \subset [N]} P_{\text{P1}}(\{\mathbf{x}^{(t_i)}\}_{i=1}^k \in \mathcal{Q}_k) P_{\text{P1}}(\{\mathbf{x}^{(t_i)}\}_{i=1}^k = \mathcal{T}) \end{aligned}$$

1379 Then, there are we have that:

$$\begin{aligned} & P_{\text{P1}}(\mathcal{T} \subset \cup_{k=1}^{\infty} \mathcal{Q}_k) \\ &= \sum_{k=1}^N P_{\text{P1}}(\mathcal{T} \subset \mathcal{Q}_k) \\ &= \sum_{k=1}^N \sum_{\{t_i\}_{i=1}^k \subset [N]} P_{\text{P1}}(\{\mathbf{x}^{(t_i)}\}_{i=1}^k \in \mathcal{Q}_k) \cdot P_{\text{P1}}(\{\mathbf{x}^{(t_i)}\}_{i=1}^k = \mathcal{T}) \\ &\geq \sum_{k=N((1-2\epsilon)^M - \delta)}^N \sum_{\{t_i\}_{i=1}^k \subset [N]} P_{\text{P1}}(\{\mathbf{x}^{(t_i)}\}_{i=1}^k \in \mathcal{Q}_k) \cdot P_{\text{P1}}(\{\mathbf{x}^{(t_i)}\}_{i=1}^k = \mathcal{T}) \\ &\geq (1 - \beta) \sum_{k=N((1-2\epsilon)^M - \delta)}^N \sum_{\{t_i\}_{i=1}^k \subset [N]} P_{\text{P1}}(\{\mathbf{x}^{(t_i)}\}_{i=1}^k = \mathcal{T}) \\ &= (1 - \beta) P_{\text{P1}}(|\mathcal{T}| \geq N((1 - 2\epsilon)^M - \delta)) \\ &\geq (1 - \beta)(1 - e^{-2N\delta^2}) \\ &\geq 1 - \beta - e^{-2N\delta^2} \end{aligned}$$

1391 This is what we want.

1392 **Part Four: For any $x \in \mathcal{C}$, with probability at least $1 - 2(1 - \epsilon)^{M_2}$ of i.i.d selected M_2 samples
 1393 form \mathcal{C} , there are two points z_1, z_2 such that $z_1 \leq B_{F(\mathbf{x})}, z_2 \geq A_{F(\mathbf{x})}$.**

1394 The probability of there is no points z_1 such that $z_1 \leq B_{F(\mathbf{x})}$

1395 In P2, among M_2 i.i.d. samples, the probability that no point lies at distance $\leq B_{F(\mathbf{x})}$ is $(1 - \epsilon)^{M_2}$,
 1396 similar as z_2 . So, and similarly for $\geq A_{F(\mathbf{x})}$. Thus both exist simultaneously with probability
 1397 at most $2(1 - \epsilon)^{M_2}$, these two conditions do not hold simultaneously, this is what we want least
 1398 $1 - 2(1 - \epsilon)^{M_2}$.

1399 **Get the result Conclusion.**

1400 For a $\mathbf{x} \sim \mathcal{C}$, by part three, with probability $1 - e^{-2N\delta^2} - \beta$ of P1, there are $P_{\mathbf{x} \sim \mathcal{C}}(S_{F(\mathbf{x})} \leq C) \geq$
 1401 $1 - \alpha$.

1404 When x satisfied $S_{F(x)} \leq C$, and the Part Four is stand in the P2, then there are $B_m - C(A_m - B_m) \leq B_{F(x)} - C(A_{F(x)} - B_{F(x)}) \leq 0$.
 1405
 1406
 1407 Combine them, this is what we want.

1408 □
 1409
 1410

J.2 SITUATION 2

1411 Now, we show how to proof the theorem 1 when $\mathbf{y} \notin \{F(x)\}_{x \in \mathcal{C}}$.
 1412

1413 *Proof.* The proof is a continuation of the previous proof of theorem 3.
 1414

1415 Let p satisfy that $P_{x \sim \mathcal{C}}(S_{F(x)} \leq p) = 1 - \alpha$ and $\mathcal{Q} = \{x \in \mathcal{C} : S_{F(x)} \leq p\}$.
 1416

1417 Then for a given \mathbf{y} , let $\mathbf{x}^{(q)} = \arg \min_{x \in \mathcal{Q}} \|\mathbf{y} - F(x)\|_2$, and $\|\mathbf{y} - F(\mathbf{x}^{(q)})\|_2 = t$.
 1418

1419 For any randomly selected $\{\mathbf{x}^{(i)}\}_{i=1}^{M_2}$ samples in P2, let $A'_m = \max_{i \in [M_2]} \|F(\mathbf{x}^{(q)}) - F(\mathbf{x}^{(i)})\|_2$ and
 1420 $B'_m = \min_{i \in [M_2]} \|F(\mathbf{x}^{(q)}) - F(\mathbf{x}^{(i)})\|_2$.
 1421

1422 Then, there are $A_m = \max_{i \in [M_2]} \|\mathbf{y} - F(\mathbf{x}^{(i)})\|_2 \geq \max_{i \in [M_2]} \|F(\mathbf{x}^{(q)}) - F(\mathbf{x}^{(i)})\|_2 - \|\mathbf{y} - F(\mathbf{x}^{(q)})\|_2 = A'_m - t$, similar, there are $B_m \leq B'_m + t$. So, we have $B_m - C(A_m - B_m) \leq B'_m - C(A'_m - B'_m) + t(1 + 2C)$.
 1423

1424 As shown in the proof of theorem 3, with probability $1 - e^{-2N\delta^2} - \beta$ of P1, there is $C \geq p$, and
 1425 then, using $\mathbf{x}^{(q)} \in \mathcal{Q}$, we have $P_{P2}(B'_m - C(A'_m - B'_m) \leq 0) \geq 1 - 2(1 - \epsilon)^{M_2}$, which can imply
 1426 that $P_{P2}(B_m - C(A_m - B_m) \leq t(1 + 2C)) \geq 1 - 2(1 - \epsilon)^{M_2}$ by the above result.
 1427

1428 And when $B_m - C(A_m - B_m) \leq t(1 + 2C)$ holds, there are $t \geq \frac{B_m - C(A_m - B_m)}{(1+2C)} = d_{\min}$, and
 1429 hence $B(\mathbf{y}, d_{\min}) \cap \mathcal{Q} = \emptyset$ by the definition of t , which implies that $V(\mathbf{y}, d_{\min}) \leq \alpha$, this is what
 1430 we want. □
 1431

K THE PART THREE FOR SMALL NETWORKS

1435 To demonstrate the superiority of our method in Section 4 and compare it with existing approaches,
 1436 we show how we can apply Part Three on small-scale object detection based on the feed-forward
 1437 ReLU neural networks. In this case, the problem in Part Three can be formulated as follows:
 1438

$$\begin{aligned} \min_{\mathbf{x}, \hat{\mathbf{x}}} \quad & \|\mathbf{y} - \mathbf{x}^{(L)}\|_2 \\ \text{s.t.} \quad & \text{(i) } \mathbf{x} \in \mathcal{C}, \quad \hat{\mathbf{x}}^{(0)} = \mathbf{x}; \\ & \text{(ii) } \mathbf{x}^{(i)} = \mathbf{W}^{(i)} \hat{\mathbf{x}}^{(i-1)} + \mathbf{b}^{(i)}, \quad i \in [L]; \\ & \text{(iii) } \hat{\mathbf{x}}^{(i)} = \max(0, \mathbf{x}^{(i)}), \quad i \in [L-1] \end{aligned}$$

1444 Where $\mathbf{W}^{(i)}$ is the transition matrix of i -th layer in network, $\mathbf{b}^{(i)}$ is the bias vector of i -th layer in
 1445 network. Unfortunately, finding an exact solution to this problem is NP-complete(Katz et al., 2017).
 1446 So, we consider bounds on the outputs of hidden-layers: $l_j^{(i)} \leq x_j^{(i)} \leq u_j^{(i)}$. Based on these bounds,
 1447 let $\mathcal{I}^{-(i)} = \{j : u_j^{(i)} \leq 0\}$, $\mathcal{I}^{+(i)} = \{j : l_j^{(i)} \geq 0\}$ and $\mathcal{I}^{\pm(i)} = \{j : l_j^{(i)} < 0 < u_j^{(i)}\}$, the
 1448 condition (iii) can be replaced by the following constraints: $\hat{x}_j^{(i)} \geq 0$, $\hat{x}_j^{(i)} \geq x_j^{(i)}$, $(u_j^{(i)} - l_j^{(i)})\hat{x}_j^{(i)} \leq$
 1449 $u_j^{(i)}x_j^{(i)} - l_j^{(i)}u_j^{(i)}$, $j \in \mathcal{I}^{\pm(i)}$; $\hat{x}_j^{(i)} = x_j^{(i)}$, $j \in \mathcal{I}^{+(i)}$; $\hat{x}_j^{(i)} = 0$, $j \in \mathcal{I}^{-(i)}$. To solve this problem,
 1450 we prove that such minimum value is equal to the maximum value of the square root of $d(\boldsymbol{\alpha}, \boldsymbol{\nu})$
 1451 which is defined in the following theorem. So, we can use the gradient to estimate the maximum of
 1452 $d(\boldsymbol{\alpha}, \boldsymbol{\nu})$, and use it to be the minimum distance in the part three.
 1453

1454 **Theorem 4.** *Under the setting in this section, we have that:*
 1455

$$\min_{\mathbf{x} \in \mathcal{C}} \|F(\mathbf{x}) - \mathbf{y}\|_2 = \max_{\boldsymbol{\alpha} \in [0, 1]} \sqrt{d(\boldsymbol{\alpha}, \boldsymbol{\nu})}$$

1456 , which is defined as below:
 1457

$$\begin{aligned}
d(\boldsymbol{\alpha}, \boldsymbol{\nu}) = & \mathbf{y}^\top \boldsymbol{\nu}^{(L)} - \frac{\boldsymbol{\nu}^{(L)\top} \boldsymbol{\nu}^{(L)}}{4} - [\boldsymbol{\nu}^{(1)\top} \mathbf{W}^{(1)}]_+ \mathbf{u}^{(0)} + [\boldsymbol{\nu}^{(1)\top} \mathbf{W}^{(1)}]_- \mathbf{l}^{(0)} \\
& - \sum_{i=1}^L \boldsymbol{\nu}^{(i)\top} \mathbf{b}^{(i)} + \sum_{i=1}^{L-1} \sum_{j \in \mathcal{I}^{\pm(i)}} \left[\frac{u_j^{(i)} l_j^{(i)} [\hat{\nu}_j^{(i)}]_+}{u_j^{(i)} - l_j^{(i)}} \right]
\end{aligned} \tag{6}$$

where

$$\begin{aligned}
\hat{\nu}_j^{(i)} &= \boldsymbol{\nu}^{(i+1)\top} \mathbf{W}_{:,j}^{(i+1)}, \hat{\nu}_j^{(i)} = [\hat{\nu}_j^{(i)}]_+ - [\hat{\nu}_j^{(i)}]_-, \forall i \in \{1, 2, \dots, L-1\} \\
\nu_j^{(i)} &= \begin{cases} \hat{\nu}_j^{(i)} & , j \in \mathcal{I}^{+(i)} \\ 0 & , j \in \mathcal{I}^{-(i)} \\ \frac{u_j^{(i)} l_j^{(i)} [\hat{\nu}_j^{(i)}]_+}{u_j^{(i)} - l_j^{(i)}} - \alpha_j^{(i)} [\hat{\nu}_j^{(i)}]_- & , j \in \mathcal{I}^{\pm(i)} \end{cases} \quad \forall i \in \{1, 2, \dots, L-1\}
\end{aligned}$$

L THE PROOF OF THEOREM 4

We mainly follow the proof idea in (Kotha et al., 2023).

Proof. Consider the $\mathcal{I}^{-(i)} = \{j : u_j^{(i)} \leq 0\}$, $\mathcal{I}^{+(i)} = \{j : l_j^{(i)} \geq 0\}$ and $\mathcal{I}^{\pm(i)} = \{j : l_j^{(i)} < 0 < u_j^{(i)}\}$, such optimization problem tends to the:

$$\begin{aligned}
\min_{\mathbf{x}, \hat{\mathbf{x}}} \quad & (\mathbf{x}^{(L)} - \mathbf{y})^\top (\mathbf{x}^{(L)} - \mathbf{y}) \\
\text{s.t.} \quad & \mathbf{l}^{(0)} \leq \hat{\mathbf{x}}^{(0)} \leq \mathbf{u}^{(0)} \\
& \mathbf{x}^{(i)} = \mathbf{W}^{(i)} \hat{\mathbf{x}}^{(i-1)} + \mathbf{b}^{(i)}; i = \{1, 2, 3, \dots, L\} \\
& \hat{x}_j^{(i)} \geq 0; j \in \mathcal{I}^{\pm(i)} \\
& \hat{x}_j^{(i)} \geq x_j^{(i)}; j \in \mathcal{I}^{\pm(i)} \\
& (u_j^{(i)} - l_j^{(i)}) \hat{x}_j^{(i)} \leq u_j^{(i)} x_j^{(i)} - l_j^{(i)} u_j^{(i)}, j \in \mathcal{I}^{\pm(i)} \\
& \hat{x}_j^{(i)} = x_j^{(i)}, j \in \mathcal{I}^{+(i)} \\
& \hat{x}_j^{(i)} = 0, j \in \mathcal{I}^{-(i)}
\end{aligned} \tag{7}$$

Then we use the Lagrange dual of the optimization problem to solve it, the Lagrange dual of the optimization problem is given by:

1512
 1513
 1514
 1515
$$\min_{\mathbf{x}, \hat{\mathbf{x}}} \max_{\boldsymbol{\lambda}, \boldsymbol{\mu}, \boldsymbol{\nu}, \boldsymbol{\tau}} (\mathbf{x}^{(L)} - \mathbf{y})^\top (\mathbf{x}^{(L)} - \mathbf{y})$$

 1516
$$+ \sum_{i=1}^L \boldsymbol{\nu}^{(i)\top} (\mathbf{x}^{(i)} - \mathbf{W}^{(i)} \hat{\mathbf{x}}^{(i-1)} - \mathbf{b}^{(i)})$$

 1517
$$+ \sum_{i=1}^{L-1} \sum_{j \in \mathcal{I}^{\pm(i)}} \mu_j^{(i)} (-\hat{x}_j^{(i)})$$

 1518
$$+ \sum_{i=1}^{L-1} \sum_{j \in \mathcal{I}^{\pm(i)}} \tau_j^{(i)} (x_j^{(i)} - \hat{x}_j^{(i)})$$

 1519
$$+ \sum_{i=1}^{L-1} \sum_{j \in \mathcal{I}^{\pm(i)}} \left[\lambda_j^{(i)} \left((u_j^{(i)} - l_j^{(i)}) \hat{x}_j^{(i)} - u_j^{(i)} x_j^{(i)} + l_j^{(i)} u_j^{(i)} \right) \right]$$

 1520
 1521
 1522
 1523
 1524
 1525
 1526
 1527
 1528
 1529
$$\text{s.t. } \mathbf{l}^{(0)} \leq \hat{\mathbf{x}}^{(0)} \leq \mathbf{u}^{(0)};$$

 1530
$$\hat{x}_j^{(i)} = 0, j \in \mathcal{I}^{-(i)}; \hat{x}_j^{(i)} = x_j^{(i)}, j \in \mathcal{I}^{+(i)}$$

 1531
 1532
$$\boldsymbol{\mu} \geq 0; \boldsymbol{\tau} \geq 0; \boldsymbol{\lambda} \geq 0;$$

 1533
 1534
 1535

1536 According to it's strong duality, the solution of the dual problem is the same as the primal problem.
 1537 The dual problem is given by:

1538
 1539
 1540
$$\max_{\boldsymbol{\lambda}, \boldsymbol{\mu}, \boldsymbol{\nu}, \boldsymbol{\tau}} \min_{\mathbf{x}, \hat{\mathbf{x}}} (\mathbf{x}^{(L)} - 2\mathbf{y} + \boldsymbol{\nu}^{(L)})^\top \mathbf{x}^{(L)} + \mathbf{y}^\top \mathbf{y} - (\boldsymbol{\nu}^{(1)})^\top \mathbf{W}^{(1)} \hat{\mathbf{x}}^{(0)}$$

 1541
$$+ \sum_{i=1}^{L-1} \sum_{j \in \mathcal{I}^{+(i)}} (\nu_j^{(i)} - \boldsymbol{\nu}^{(i+1)\top} \mathbf{W}_{i,j}^{(i+1)}) x_j^{(i)}$$

 1542
$$+ \sum_{i=1}^{L-1} \sum_{j \in \mathcal{I}^{-(i)}} \nu_j^{(i)} x_j^{(i)}$$

 1543
$$+ \sum_{i=1}^{L-1} \sum_{j \in \mathcal{I}^{\pm(i)}} \left[(\nu_j^{(i)} + \tau_j^{(i)} - \lambda_j^{(i)} u_j^{(i)}) x_j^{(i)} \right.$$

 1544
$$\left. + (-\boldsymbol{\nu}^{(i+1)\top} \mathbf{W}_{:,j}^{(i+1)} - \mu_1^{(i)} - \tau_j^{(i)} + (u_j^{(i)} - l_j^{(i)}) \lambda_j^{(i)}) \hat{x}_j^{(i)} \right]$$

 1545
$$- \sum_{i=1}^L \nu_i^{(i)\top} \mathbf{b}_i^{(i)} + \sum_{i=1}^{L-1} \sum_{j \in \mathcal{I}^{(i)}} \lambda_j^{(i)} u_j^{(i)} l_j^{(i)}$$

 1546
 1547
 1548
 1549
 1550
 1551
 1552
 1553
 1554
 1555
 1556
$$\text{s.t. } \mathbf{l}^{(0)} \leq \hat{\mathbf{x}}^{(0)} \leq \mathbf{u}^{(0)}; \hat{x}_j^{(i)} = 0, j \in \mathcal{I}^{-(i)}; \hat{x}_j^{(i)} = x_j^{(i)}, j \in \mathcal{I}^{+(i)}$$

 1557
 1558
$$\boldsymbol{\mu} \geq 0; \boldsymbol{\tau} \geq 0; \boldsymbol{\lambda} \geq 0;$$

 1559
 1560

1561 Here, we adjust the order of each term in the formula and directly incorporate the constraints
 1562 $\hat{x}_j^{(i)} = 0, j \in \mathcal{I}^{-(i)}; \hat{x}_j^{(i)} = x_j^{(i)}, j \in \mathcal{I}^{+(i)}$ into the objective function. Then we can minimize
 1563 $-(\boldsymbol{\nu}^{(1)})^\top \mathbf{W}^{(1)} \hat{\mathbf{x}}^{(0)}$ subject to $\mathbf{l}^{(0)} \leq \hat{\mathbf{x}}^{(0)} \leq \mathbf{u}^{(0)}$ according to the each dimension of $\boldsymbol{\nu}^{(1)\top} \mathbf{W}^{(1)}$.
 1564 If $(\boldsymbol{\nu}^{(1)\top} \mathbf{W}^{(1)})_j > 0$, then $\hat{x}_j^{(0)} = \mathbf{u}_j^{(0)}$; Otherwise, $\hat{x}_j^{(0)} = \mathbf{l}_j^{(0)}$. Since no additional constraints
 1565 applied to $\mathbf{x}^{(L)}$, we can minimize $(\mathbf{x}^{(L)} - 2\mathbf{y} + \boldsymbol{\nu}^{(L)})^\top \mathbf{x}^{(L)}$ by setting $\mathbf{x}^{(L)} = \mathbf{y} - \frac{1}{2} \boldsymbol{\nu}^{(L)}$. Then

1566 we get:

$$\begin{aligned}
& \max_{\lambda, \mu, \nu, \tau} \min_{x, \hat{x}} \quad \mathbf{y}^\top \boldsymbol{\nu}^{(L)} - \frac{\boldsymbol{\nu}^{(L)\top} \boldsymbol{\nu}^{(L)}}{4} - [\boldsymbol{\nu}^{(1)\top} \mathbf{W}^{(1)}]_+ \mathbf{u}^{(0)} + [\boldsymbol{\nu}^{(1)\top} \mathbf{W}^{(1)}]_- \mathbf{l}^{(0)} \\
& + \sum_{i=1}^{L-1} \sum_{j \in \mathcal{I}^{+(i)}} (\nu_j^{(i)} - \boldsymbol{\nu}^{(i+1)\top} W_{i,j}^{(i+1)}) x_j^{(i)} \\
& + \sum_{i=1}^{L-1} \sum_{j \in \mathcal{I}^{-(i)}} \nu_j^{(i)} x_j^{(i)} \\
& + \sum_{i=1}^{L-1} \sum_{j \in \mathcal{I}^{\pm(i)}} \left[\left(\nu_j^{(i)} + \tau_j^{(i)} - \lambda_j^{(i)} u_j^{(i)} \right) x_j^{(i)} \right. \\
& \quad \left. + \left(-\boldsymbol{\nu}^{(i+1)\top} \mathbf{W}_{:,j}^{(i+1)} - \mu_j^{(i)} - \tau_j^{(i)} + (u_j^{(i)} - l_j^{(i)}) \lambda_j^{(i)} \right) \hat{x}_j^{(i)} \right] \\
& - \sum_{i=1}^L \nu^{(i)\top} b^{(i)} + \sum_{i=1}^{L-1} \sum_{j \in \mathcal{I}^{\pm(i)}} \lambda_j^{(i)} u_j^{(i)} l_j^{(i)} \\
\text{s.t.} \quad & \boldsymbol{\mu} \geq 0; \quad \boldsymbol{\tau} \geq 0; \quad \boldsymbol{\lambda} \geq 0;
\end{aligned} \tag{10}$$

Since variables x, \hat{x} are unconstrained, any of their coefficients are nonzero would make their value to $-\infty$ by the inner minimization. Therefore, the outer maximization requires setting all the coefficients of x, \hat{x} to zero. Then we get:

$$\begin{aligned}
& \max_{\lambda, \mu, \tau, \nu} \quad \mathbf{y}^\top \boldsymbol{\nu}^{(L)} - \frac{\boldsymbol{\nu}^{(L)\top} \boldsymbol{\nu}^{(L)}}{4} \\
& \quad - [\boldsymbol{\nu}^{(1)\top} \mathbf{W}^{(1)}]_+ \mathbf{u}^{(0)} + [\boldsymbol{\nu}^{(1)\top} \mathbf{W}^{(1)}]_- \mathbf{l}^{(0)} \\
& \quad - \sum_{i=1}^L \boldsymbol{\nu}^{(i)\top} \mathbf{b}^{(i)} + \sum_{i=1}^{L-1} \sum_{j \in \mathcal{I}^{\pm(i)}} \lambda_j^{(i)} u_j^{(i)} l_j^{(i)} \\
\text{s.t.} \quad & \boldsymbol{\mu} \geq 0; \boldsymbol{\tau} \geq 0; \boldsymbol{\lambda} \geq 0; \\
& \nu_j^{(i)} - \boldsymbol{\nu}^{(i+1)\top} \mathbf{W}_{:,j}^{(i+1)} = 0, j \in \mathcal{I}^{+(i)} \\
& \nu_j^{(i)} = 0, j \in \mathcal{I}^{-(i)} \\
& \nu_j^{(i)} + \tau_j^{(i)} - \lambda_j^{(i)} u_j^{(i)} = 0; j \in \mathcal{I}^{\pm(i)} \\
& \boldsymbol{\nu}^{(i+1)\top} \mathbf{W}_{:,j}^{(i+1)} = (u_j^{(i)} - l_j^{(i)}) \lambda_j^{(i)} - (\mu_j^{(i)} + \tau_j^{(i)}), j \in \mathcal{I}^{\pm(i)}
\end{aligned} \tag{11}$$

Define $\hat{\nu}_j^{(i)} = \nu^{(i+1)\top} \mathbf{W}_{:,j}^{(i+1)}$. Then, we define $(u_j^{(i)} - l_j^{(i)})\lambda_j^{(i)} = [\hat{\nu}_j^{(i)}]_+$ and $\mu_j^{(i)} + \tau_j^{(i)} = [\hat{\nu}_j^{(i)}]_-$, we get the following bound propagation procedure:

$$\begin{aligned}
& \max_{\boldsymbol{\alpha}, \boldsymbol{\nu}} \quad \mathbf{y}^\top \boldsymbol{\nu}^{(L)} - \frac{\boldsymbol{\nu}^{(L)\top} \boldsymbol{\nu}^{(L)}}{4} - [\boldsymbol{\nu}^{(1)\top} \mathbf{W}^{(1)}]_+ \mathbf{u}^{(0)} + [\boldsymbol{\nu}^{(1)\top} \mathbf{W}^{(1)}]_- \mathbf{l}^{(0)} \\
& \quad - \sum_{i=1}^L \boldsymbol{\nu}^{(i)\top} \mathbf{b}^{(i)} + \sum_{i=1}^{L-1} \sum_{j \in \mathcal{I}^{\pm(i)}} \left[\frac{u_j^{(i)} l_j^{(i)} [\hat{\nu}_j^{(i)}]_+}{u_j^{(i)} - l_j^{(i)}} \right] \\
\text{s.t.} \quad & \hat{\nu}_j^{(i)} = \boldsymbol{\nu}^{(i+1)\top} \mathbf{W}_{:,j}^{(i+1)}, \hat{\nu}_j^{(i)} = [\hat{\nu}_j^{(i)}]_+ - [\hat{\nu}_j^{(i)}]_-, \forall i \in \{1, 2, \dots, L-1\} \\
& \nu_j^{(i)} = \begin{cases} \hat{\nu}_j^{(i)} & , j \in \mathcal{I}^{+(i)} \\ 0 & , j \in \mathcal{I}^{-(i)} \\ \frac{u_j^{(i)}}{u_j^{(i)} - l_j^{(i)}} [\hat{\nu}_j^{(i)}]_+ - \alpha_j^{(i)} [\hat{\nu}_j^{(i)}]_- & , j \in \mathcal{I}^{\pm(i)} \end{cases} \quad \forall i \in \{1, 2, \dots, L-1\} \\
& 0 \leq \alpha_j^{(i)} \leq 1, j \in \mathcal{I}^{\pm(i)}
\end{aligned} \tag{12}$$

1620 Here $\alpha_j^{(i)}$ is the optimizable parameter controlling the relaxation of neuron j in layer i introduced in
 1621 (Xu et al., 2021). This is what we want. \square
 1622

1623 **M THE PROOF OF THEOREM 2**
 1624

1625 **Theorem.** *Using the notation from the three algorithms above. Given $\alpha, \beta, \delta, \epsilon \in (0, 1)$
 1626 satisfying $(1 - 2\epsilon)^M - \delta > 0$, $N \cdot ((1 - 2\epsilon)^M - \delta) > \frac{2}{\alpha} \ln(\frac{1}{\beta}) + 2 + \frac{2}{\alpha} \ln(\frac{2}{\alpha})$ and $N_2 \geq$
 1627 $[\frac{2 \ln 1/\beta}{\alpha} + 2 + \frac{2 \ln 2/\alpha}{\alpha}]$. Then, after executing the algorithms defined above, if, for a sample
 1628 \mathbf{x} , these algorithms output the 'safe' after T refinement turns, then with probability $1 -$
 1629 $T(e^{-2N\delta^2} + \beta + 2(1 - \epsilon)^{M_2}) - \beta$ of part one and three, there are $P_{\mathbf{x} \sim \mathcal{C}}(\mathbf{x} \text{ issafe}) >$
 1630 $1 - (1 + T)\alpha$.*

1631 *Proof.* We use the sample fact that $P(A \cap B) \geq P(A) + P(B) - 1$ to get the following result:
 1632

1633 From Theorem 1, after T refinement steps, the reduction in the probability of the system being
 1634 certifiably safe due to these refinements is at most $T\alpha$. This statement holds with a confidence of at
 1635 least $T \left(1 - (e^{-2N\delta^2} + \beta + 2(1 - \epsilon)^{M_2})\right) - (T - 1) = 1 - T \left(e^{-2N\delta^2} + \beta + 2(1 - \epsilon)^{M_2}\right)$.
 1636

1637 According to Proposition 1, we can get that the probability of the box is safe is $1 - T\alpha - \alpha$ with
 1638 probability $1 - T(e^{-2N\delta^2} + \beta + 2(1 - \epsilon)^{M_2}) + (1 - \beta) - 1 = 1 - T(e^{-2N\delta^2} + \beta + 2(1 - \epsilon)^{M_2}) - \beta$.
 1639

1640 Then we can get that the probability $P(\mathbf{x} \text{ is safe}) > 1 - (1 + T)\alpha$ with probability $1 - T(e^{-2N\delta^2} +$
 1641 $\beta + 2(1 - \epsilon)^{M_2}) - \beta$.
 1642

1643 Then we can get the final result. \square

1644 **Remark 6.** Note we do not assume that the Part 1 and Part 3 are independent, so we can reuse the
 1645 samples in Part 1 to Part 3.

1646 **N EXPERIMENT DETAILS**
 1647

1648 **Detailed Setting:** We use $N_1 = 30000$, $N_2 = 5000$, $N = 3000$, $M = 10$, $M_2 = 2000$, $\alpha = 0.0099$,
 1649 $\beta = 0.0099$, $\epsilon = 1/200$, $\delta = 0.1$ as our default setting. As we do not assume that the Part 1 and Part
 1650 3 are independent, samples from Part 1(Algorithm 2) can be also used in Part 3(Algorithm 4), so we
 1651 only need to sample $N_1 + N_2 + M_2 = 37000$ samples in total, where $N_1 = N \cdot M$. We use one
 1652 turn refinement($T = 1$) for all the experiments.

1653 **Attack Setting:** We use square attack with 5000 iterations for each box. For PGD, we use 20
 1654 iterations with step size 1/255 and 2/255. Each iteration, We find the box with the highest IoU and
 1655 same class with the ground truth box, then use the GIoU of them as the loss function. Note each
 1656 turn may attack a different box. We found that this is a strong attack for YOLO networks.

1657 **Server Setting:** We use a server with 8 NVIDIA V100 32G GPUs, 40 Intel(R) Xeon(R) Gold
 1658 5215 CPUs at 2.50GHz and 503GB memory. The code is implemented in Python with Gurobi and
 1659 PyTorch.

1660 **Sample Calculation:** According to the theorem 2, we can get that the sample number is $N_1 + N_2 +$
 1661 $M_2 = 37,000$ for each box. Note this is the sample number of full algorithm. **For RCP_N methods,**
 1662 **from Appendix C.1, we need:**

$$N \geq \left[\frac{2 \ln 1/\beta}{\alpha} + 2d_0 + \frac{2d_0 \ln 2/\alpha}{\alpha} \right]$$

1663 **to make sure that with $1 - \beta$ confidence, the range is over approximate the real range with
 1664 probability with probability $1 - \alpha$. Here we use $d_0 = 640 \times 640 \times 3$, $\alpha = 0.02$, $\beta = 0.02$ to
 1665 achieve comparable results, then we have $N \geq 568341303$. Note that this is the sample number
 1666 for Part**

1667 Our work (Part 1 only) aims to find a tight hyper-rectangle bound \mathcal{Z} for the d_L -dimensional vector
 1668 output space $\{\mathbf{F}(\mathbf{x})\}_{\mathbf{x} \in \mathcal{C}}$. In this context, a more appropriate application of RCP_N as a baseline for

1674 this task would be to directly estimate an upper bound for each dimension in this d_L -dimensional
 1675 space. The decision-variable dimension for this problem would be $d = d_L$ (i.e., the network output
 1676 dimension), corresponding to finding a vector $\mathbf{u} \in \mathbb{R}^{d_L}$ such that, for all inputs $\mathbf{x} \in \mathcal{C}$, the network
 1677 output $\mathbf{F}(\mathbf{x}) \leq \mathbf{u}$ element-wise. Based on this, the required sample count would be:
 1678

$$1679 N \geq \left[\frac{2 \ln 1/\beta}{\alpha} + 2d_L + \frac{2d_L \ln(2/\alpha)}{\alpha} \right] \approx 10^9$$

1682 Alternatively, if one were to use the RCP_N method to directly verify the entire problem,
 1683 this could be framed as computing an IoU lower bound for each predicted box against its
 1684 corresponding ground-truth (GT) box. The decision variable dimension in this case would be
 1685 $d = (80 \times 80 + 40 \times 40 + 20 \times 20) \times 3 = 25,200$ (i.e., the number of bounding boxes). Based
 1686 on this, the required sample count would be:
 1687

$$1688 N \geq \left[\frac{2 \ln 1/\beta}{\alpha} + 2d + \frac{2d \ln(2/\alpha)}{\alpha} \right] \approx 10^7$$

1691 The order of magnitude of the sample size under either estimation is still prohibitively large for any
 1692 practical application.

1694 For the PAC-based methods, according to (Li et al., 2022), to achieve $1 - \alpha$ probability with $1 - \beta$
 1695 confidence, we need N satisfies:

$$1697 N \geq \frac{2}{\beta} \times \left(\log\left(\frac{1}{\alpha}\right) + d_0 \right) \geq 122880391.$$

1699 Here we also use $\alpha = 0.02$, $\beta = 0.02$.

1700 In terms of randomized smoothing(Cohen et al., 2019), the number of samples required is strongly
 1701 correlated with the standard deviation (σ) and the certified radius. For example, to certify a radius
 1702 of $2/255$ against noise with a standard deviation of $\sigma = \frac{1}{255 \times 3}$, the randomized smoothing method
 1703 would require an impractical number of samples (approximately 3.9×10^9). This severely limits its
 1704 application in real-world scenarios.

1706 Our method, by introducing v_{\max} and the scalar c_1 , reduces the entire verification problem to a $d = 1$
 1707 scalar optimization (for c_1) plus a constrained optimization (MIQP). Thus the required sample size
 1708 is significantly reduced to a manageable level, making it feasible for practical applications.

1709 **Remark 7.** Note that without refinement (only Part 1 and Part 2), our method can achieve 99%
 1710 confidence and 99% probability with $\alpha = 0.0099$, $\beta = 0.0099$. After refinement, the true confidence
 1711 and probability are both 98%. For other two methods, we use error rate 0.02 and significance level
 1712 0.02, to get the same confidence and probability.

1713 **Clarification on Sample Complexity** There are two distinct sampling procedures used in our
 1714 experiments, which serve different purposes:

- 1716 • **Verification Samples (37,000):** This is the sample budget used by our algorithm to issue
 1717 the certificate. For each ground-truth box, we use 37,000 samples ($N_1 + N_2 + M_2$) to
 1718 construct \mathcal{Z} and the refinement constant C , as prescribed by Theorem 2.
- 1719 • **RCP_N Baseline Samples (10⁶ in Table 1):** For the RCP_N baseline in Table 1, we also
 1720 use 10⁶ samples to compute empirical robustness, but this does not yield comparable
 1721 theoretical guarantees. To achieve our target (98% robustness, 98% confidence), RCP_N
 1722 would theoretically require about 11.6 million samples. With only 10⁶ samples, RCP_N
 1723 can only provide an 86% robustness guarantee at 98% confidence.
- 1724 • **Evaluation Samples (10⁶ in Table 2):** Independently of the verification algorithm, we
 1725 draw 10⁶ additional uniform perturbations to empirically estimate the "ground truth"
 1726 robustness. These samples are only used to calculate evaluation metrics (TPR, FPR, TNR,
 1727 FNR, and CRA) and do not inform the certificate itself.

Table 3: Ground Truth Information for Table 2. #RB: Number of robust boxes; #NRB: Number of non-robust boxes

Model	ε	#RB($\tau = 0.5$)	#NRB($\tau = 0.5$)	#RB($\tau = 0.7$)	#NRB($\tau = 0.7$)
yolo11m	1/255	363	164	335	192
yolo11m	2/255	346	181	315	212
yolo11x	1/255	390	137	348	179
yolo11x	2/255	379	148	335	192
yolov3-sppu	1/255	364	163	332	195
yolov3-sppu	2/255	356	171	320	207
yolov3u	1/255	374	153	338	189
yolov3u	2/255	365	162	327	200
yolov5mu	1/255	354	173	316	211
yolov5mu	2/255	344	183	301	226
yolov5xu	1/255	387	140	354	173
yolov5xu	2/255	372	155	337	190
yolov8m	1/255	376	151	342	185
yolov8m	2/255	361	166	327	200
yolov8x	1/255	385	142	348	179
yolov8x	2/255	370	157	337	190

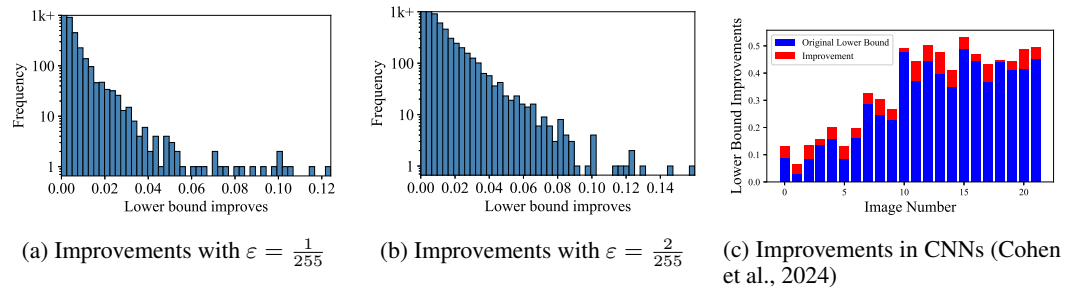


Figure 7: Verification bound improvement after Part 3

Ground Truth information of Table 2: Table 3 shows the ground truth information of Table 2. Here, #RB means the number of robust boxes, and #NRB means the number of non-robust boxes. The ground truth is calculated by 10^6 uniform perturbations for each box.

O THE EFFECTIVENESS OF NMS VERIFICATION

The NMS optimization step is highly efficient. Verifying one ground-truth box against all candidate boxes takes an average of only 4.9 seconds. This efficiency arises because we only perform sound verification: boxes that could potentially cause unsafe behavior are filtered out in advance, leaving only a small number of boxes to be verified.

P THE EFFECT OF PART 3

This section shows that Part 3 in Section 4 and Appendix K is effective for both large-scale networks (YOLO) and small-scale CNNs. For the LARD dataset, we use a six-layer CNN network provided in (Cohen et al., 2024). As seen in Figure 7c, with Part 3, the IoU lower bound we obtain is higher than the bound obtained without using Part 3. This improvement occurs because Part 3 reduces the over-approximation of the network’s output, implying our bound is closer to the true bound. Note that we use sound formal verification on small object detection, instead of probabilistic verification, so that the network can indeed achieve such a bound. For YOLO, we also show the effect of Part 3

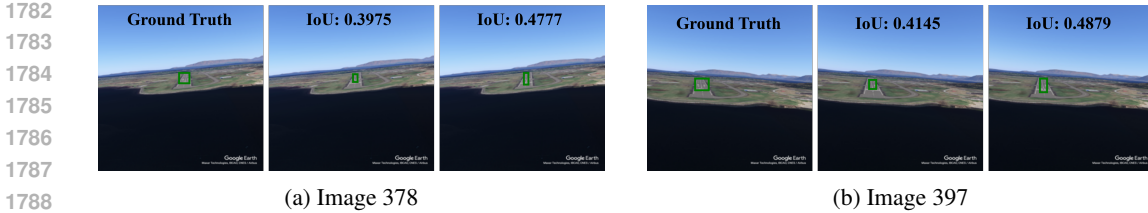


Figure 8: The effect of Part 3 in small object detection. The middle panel shows the bound from prior methods; the right panel shows our improved bound.

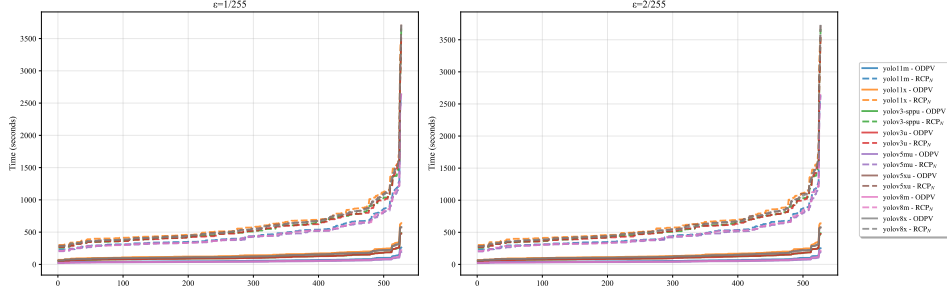


Figure 9: Verification time comparison

in Fig. 7a and Fig. 7b. After refinement, most of the lower bounds are improved, which means Part 3 is also helpful in YOLO networks.

We observe that the first iteration yields the most significant gains. Since further refinement linearly accumulates confidence loss as described in Theorem 2, employing $T = 1$ represents a favorable trade-off in most cases.

Q TIME COMPARISON

Fig. 9 shows the detailed time comparison of our method and RCP_N on different YOLO models with $\varepsilon = \frac{1}{255}$ and $\varepsilon = \frac{2}{255}$. The results show that our method is significantly faster than RCP_N in all images.

R REAL-WORLD EXAMPLES.

We take 40 images from sensor cameras of our autonomous vehicles and annotated ground truth by ourselves. Table 4 shows the results of our method on these images. The results show that our method can also work well in real-world scenarios. Our method still uses less time and achieve better bounds than RCP_N . Both CRA are high in these images, which means most boxes verified as robust by our method are reasonably robust.

S COMPARED WITH MEDIAN SMOOTHING

Table 5 compares our method with median smoothing (MS) (Cohen et al., 2019) under normal distribution on 50 images from the COCO dataset. We set the standard deviation of normal distribution as $\sigma = \frac{1}{255 \times 3}$ and $\sigma = \frac{2}{255 \times 3}$. The results show that our method significantly achieves a smaller mean absolute difference of IoU lower bounds relative to the worst-case input found by the PGD attack(Δ_{PGD}), indicating more precise IoU lower bounds. Besides, in most cases, the CRA of our method is higher than median smoothing. This also prove that our method works well in different distributions.

1836 Table 4: Real world examples of our method.
1837

1838 1839 1840 1841 1842 1843 1844	ε	method	time	Δ_{PGD}		CRA	
				$\tau = 0.5$	$\tau = 0.7$	$\tau = 0.5$	$\tau = 0.7$
1845 1846 1847 1848 1849 1850 1851 1852 1853 1854 1855 1856	1/(3 * 255)	RCP_N	571.0	0.53	0.52	1.00	1.00
		ODPV	32.1	0.47	0.44	1.00	1.00
	2/(3 * 255)	RCP_N	569.6	0.57	0.55	1.00	1.00
		ODPV	32.1	0.43	0.37	1.00	1.00

1845 Table 5: Comparison of our method with median smoothing. Δ_{PGD} denotes the mean absolute difference of IoU lower bounds relative to the PGD attack. Bold values indicate the best performance.
1846

1848 1849 1850 1851 1852 1853 1854 1855 1856	ε	method	Δ_{PGD}		CRA	
			$\tau = 0.5$	$\tau = 0.7$	$\tau = 0.5$	$\tau = 0.7$
1857 1858 1859 1860 1861 1862 1863 1864 1865 1866 1867 1868 1869 1870 1871 1872 1873 1874 1875 1876 1877 1878 1879 1880 1881 1882 1883 1884 1885 1886 1887 1888 1889	1/255	RCP_N	0.45	0.47	1.00	1.00
		ODPV	0.42	0.40	0.99	0.98
		MS	0.44	0.45	0.99	0.98
	2/255	RCP_N	0.59	0.56	1.00	1.00
		ODPV	0.54	0.47	1.00	1.00
		MS	0.59	0.53	0.96	0.97

T ABLATION STUDY OF PARAMETERS

Fig. 10 shows the ablation study of parameters η and ι . The results show that our method still maintains more accurate bounds than RCP_N under different parameters. Besides, the results show that a larger η and a larger ι will lead the bounds to be closer to the worst-case bound found by PGD attack. This is because a larger η and a larger ι will result in a stricter NMS condition, fewer boxes can remain and the resulting boxes will be more robust.

U BROADER IMPACT

Our method focuses on verifying the safety of the object detection model, which may help people to better understand the model and give a safety metric. We do not think there is a negative social impact of our method as our method is not used to attack the model.

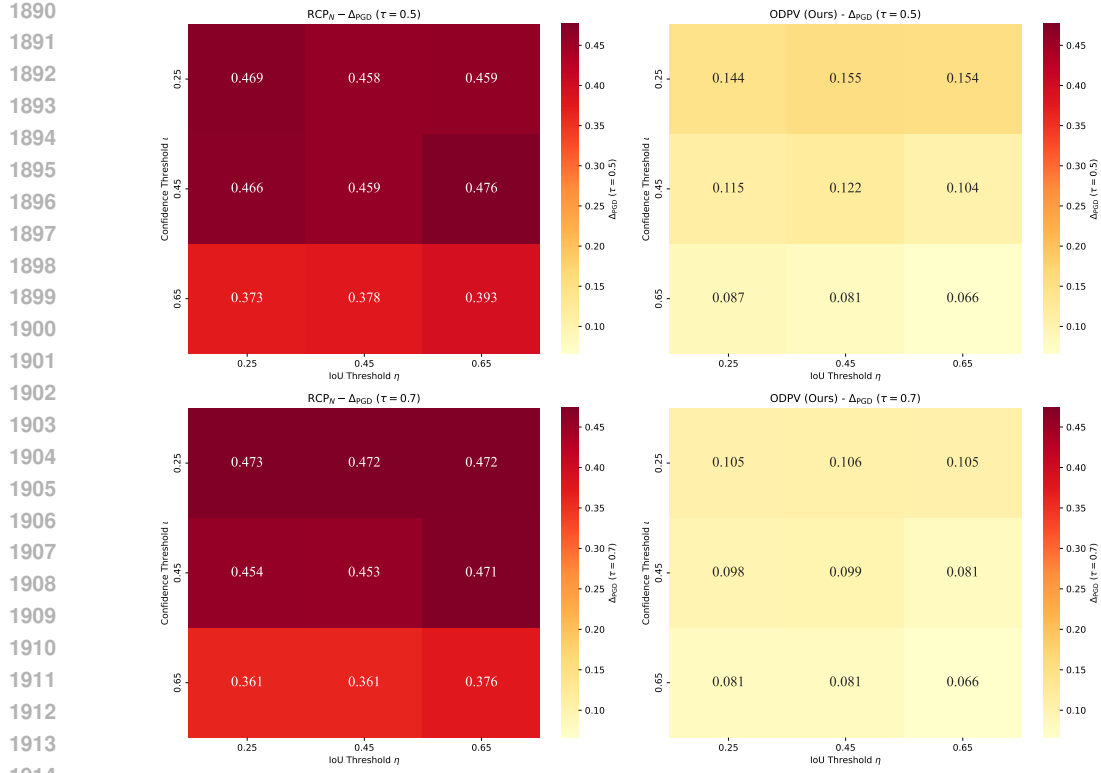
V LLM USAGE STATEMENT

In the preparation of this manuscript, a Large Language Model (LLM) was utilized as a writing assistance tool. Its use was strictly confined to language polishing, which includes proofreading for grammatical errors, improving sentence structure, and enhancing the overall clarity and readability of the text.

All core intellectual contributions—including the research ideation, paper structure, and the initial drafting of the content—are the original work of the authors. The LLM did not contribute to the formulation of any hypotheses, experimental results, or conclusions presented herein. The authors have reviewed all AI-generated suggestions and take full responsibility for the final content of this paper.

W DESCRIPTION OF HYPERPARAMETERS

Our framework consists of three parts (Algorithms 1-4): Part 1 (Output Approximation), Part 2 (NMS Verification), and Part 3 (Counterexample-Based Refinement). Only Parts 1 and 3 are probabilistic; Part 2 is based on sound MIQP constraints and introduces no additional probabilistic error.

Figure 10: Ablation study of parameters η, τ

W.1 ROLE OF PARAMETERS AND FAILURE EVENTS

We now describe the role of the four key parameters $\alpha, \beta, \delta, \epsilon$ used in our theoretical guarantees and experiments.

- α (Error Rate)
 - Appears in Definition 1 (OD PAC-Verification), Proposition 1 (Part 1), Theorem 1 (Part 3), and Theorem 2 (Overall Guarantee).
 - Controls the *allowable violation probability* of the OD property under the input distribution: In Theorem 2, if the algorithm returns “safe” after at most T refinement steps, we guarantee

$$P_{x \sim \mathcal{C}}(x \text{ is safe}) > 1 - (1 + T)\alpha.$$

- In our experiments, we set $\alpha = 0.0099$, so with $T = 1$ we obtain a lower bound on the safety probability for each certified box of approximately $1 - 0.0198 \approx 0.98$.

- β (Significance / Confidence)

- Used for the scenario-type bounds in Part 1 (Prop. 1) and Part 3 (Thm. 1), and combined in Theorem 2.
- Controls the *confidence* with which the above probabilistic claim holds, i.e., the probability that the inequality regarding $P(x \text{ is safe})$ is valid under the randomness of our sampling process. Theorem 2 gives the overall confidence:

$$P[P_{x \sim \mathcal{C}}(x \text{ is safe}) > 1 - (1 + T)\alpha] \geq 1 - T(e^{-2N\delta^2} + \beta + 2(1 - \epsilon)M_2) - \beta.$$

- We use $\beta = 0.0099$; with our default N, δ, ϵ, M_2 , and $T = 1$, this lower bound is ≈ 0.98 (reported in Appendix N).

- δ (Concentration slack in Part 3)

- 1944 - Appears only in Theorem 1 / Theorem 2. It is the slack term in the Hoeffding
 1945 bound, controlling how many of the N sampled points in Part 3 have “good” local
 1946 neighborhoods (i.e., have sufficient neighbors within the interval $[B_{F(x)}, A_{F(x)}]$).
 1947 - The condition

$$N((1 - 2\epsilon)M - \delta) > \frac{2}{\alpha} \ln \frac{1}{\beta} + 2 + \frac{2}{\alpha} \ln \frac{2}{\alpha}$$

1951 ensures that with probability at least $1 - \beta$, enough sample points are “good” to apply
 1952 the RCP_N -style scenario bound to the refinement constant C .

- 1953 - We fix $\delta = 0.1$ in all experiments (Appendix N).

1954 • ϵ (width of the local uncertainty interval in Part 3)

- 1956 - Used in Theorem 1 to define the probability mass of the local distance interval
 1957 $[B_{F(x)}, A_{F(x)}]$. For each x , at least a $1 - 2\epsilon$ fraction of the M local perturbations
 1958 fall into this interval.
 1959 - The term $2(1 - \epsilon)M_2$ in Theorem 2 bounds the probability that the empirical
 1960 estimation of this interval fails.
 1961 - We set $\epsilon = 1/200$ in all experiments.

1963 In practice, one needs to select appropriate $\alpha, \beta, \delta, \epsilon$ based on the desired probability thresholds
 1964 and then calculate the sample sizes N_1, N_2, N, M, M_2 . Below we discuss the relationship between
 1965 sample sizes and these parameters.

1966 W.2 SAMPLE SIZE RELATIONSHIPS

1968 The main sample size constraints appear in Theorem 2:

1970 • Part 1 Sampling:

$$N_2 \geq \frac{2}{\alpha} \ln \frac{1}{\beta} + 2 + \frac{2}{\alpha} \ln \frac{2}{\alpha}.$$

1974 For fixed α, β , we have $N_2 = O(\frac{1}{\alpha} \log \frac{1}{\beta})$. Importantly, there is no explicit dependency
 1975 on the output dimension d_L in this bound.

1977 • Part 3 Sampling: With fixed δ, ϵ, M , the bound on N can be written as

$$N \geq \frac{1}{(1 - 2\epsilon)M - \delta} \left(\frac{2}{\alpha} \ln \frac{1}{\beta} + 2 + \frac{2}{\alpha} \ln \frac{2}{\alpha} \right),$$

1981 Thus, for fixed δ, ϵ, M , we again have $N = O(\frac{1}{\alpha} \log \frac{1}{\beta})$.

1983 In the experiments, we instantiate these quantities with the following values:

$$N_1 = 30,000, \quad N_2 = 5,000, \quad N = 3,000, \quad M = 10, \quad M_2 = 2,000,$$

1986 and $\alpha = \beta = 0.0099$, $\epsilon = 1/200$, $\delta = 0.1$ (Appendix N). Because the samples from Part 1 are reused
 1987 in Part 3 (Remark 6), the total number of samples per box is:

$$N_{\text{total}} = N_1 + N_2 + M_2 = 37,000$$

1991 This quantity is independent of d_L and forms the basis for the claim “achieving 98% guarantee at
 1992 98% confidence with 37,000 samples” in Section 6.

1993 W.3 NOTATION FOR SAMPLING PARAMETERS

1996 Throughout Proposition 1, Theorem 1 and 2, the symbols $N_1, N_2, N, M, M_2, A'_x, B'_x, A_w, B_w$
 1997 and C are inherited from Algorithms 2 and 4 as follows. In Algorithm 2, N_1 denotes
 the number of samples used to estimate the per-coordinate scale vector v_{\max} , and N_2 is

1998 the number of samples used to compute the smallest scaling factor c_1 in the optimization
 1999 problem equation 1, which yields the output hyper-rectangle \mathcal{Z} . In Algorithm 4, N is the
 2000 number of reference points $\{\mathbf{x}^{(i)}\}_{i=1}^N$ drawn from \mathcal{C} in Step One, and M is the number
 2001 of auxiliary samples $\{\mathbf{x}^{(i,j)}\}_{j=1}^M$ drawn for each reference point. For each $i \in [N]$, we
 2002 define $A'_i = \max_{j \in [M]} \|\mathbf{F}(\mathbf{x}^{(i,j)}) - \mathbf{F}(\mathbf{x}^{(i)})\|_2$ and $B'_i = \min_{j \in [M]} \|\mathbf{F}(\mathbf{x}^{(i,j)}) - \mathbf{F}(\mathbf{x}^{(i)})\|_2$, and the
 2003 constant C is updated as $C \leftarrow \max\{C, B'_i / (A'_i - B'_i)\}$. In Step Two of Algorithm 4, M_2
 2004 denotes the number of additional samples $\{\mathbf{x}^{(i)}\}_{i=1}^{M_2}$ drawn from \mathcal{C} to estimate the distance from
 2005 a candidate output \mathbf{y} to the true output set $\{\mathbf{F}(\mathbf{x})\}_{\mathbf{x} \in \mathcal{C}}$, with $A_m = \max_{i \in [M_2]} \|\mathbf{F}(\mathbf{x}^{(i)}) - \mathbf{y}\|_2$
 2006 and $B_m = \min_{i \in [M_2]} \|\mathbf{F}(\mathbf{x}^{(i)}) - \mathbf{y}\|_2$. These quantities are then combined to form the estimator
 2007 $d_{\min} = \max\{(B_m - C(A_m - B_m)) / (1 + 2C), 0\}$ used in Part 3.
 2008

X EXTENDING OUR METHOD

We acknowledge that different architectures and threat models may necessitate distinct verification strategies, making a universal solution challenging. Nonetheless, for many common threats, our proposed method can be adapted by modifying only the encoding in Part 2, while keeping Parts 1 and 3 unchanged. The following describes how to adapt our method to verify two additional threats: class misidentification and false appearances.

X.1 EXTENDING TO CLASS MISIDENTIFICATION

Algorithm 6 Soundness Class Misidentification Verification for NMS

Require: Constraints $\mathcal{Z} = \mathcal{H} \setminus \mathcal{S}$; input \mathbf{x} ; output \mathbf{y} ; ground truth box_{gt} ; confidence threshold ℓ .
Ensure: Calculate per-box upper bounds $\{\tau_{\text{mis}}(i)\}_{i=1}^{n_{\mathbf{x}}}$ for class misidentification.

- 1: $\{\bar{box}_i\}_{i=1}^{n_{\mathbf{x}}} \leftarrow \text{CONSTRUCT_ABSTRACT_BOX}(\mathcal{Z})$
- 2: **for all** $box_i \in \{\bar{box}_k\}_{k=1}^{n_{\mathbf{x}}}$ **do**
- 3: $\tau_{\text{mis}}(i) \leftarrow 0$ ▷ Initialize upper bound for misidentification IoU of box i
- 4: **if** $\forall k \in [n] \setminus \{\text{Class}(box_{gt})\}$, $p_{i, \text{Class}(box_{gt})} \geq \bar{p}_{ik}$ **then**
- 5: **continue** ▷ Skip boxes that must match box_{gt} class (never misclassified w.r.t. this GT)
- 6: **end if**
- 7: **if** $\bar{c}_i \geq \ell$ **then** ▷ Box i may pass the confidence threshold in some realization
- 8: $\tau_{\text{mis}}(i) \leftarrow \text{IoU_UPPER_BOUNDS}(\bar{box}_i, box_{gt})$ ▷ Worst-case IoU to box_{gt} when box_i is potentially of a wrong class
- 9: **end if**
- 10: **end for**
- 11: **return** $\{\tau_{\text{mis}}(i)\}_{i=1}^{n_{\mathbf{x}}}$

Formalization of the property (bad Event): Given an input constraint set \mathcal{C} , if there exists an input $\mathbf{x} \in \mathcal{C}$ such that after processing by the network \mathbf{F} and NMS module, the output set $\mathbf{N}(\mathbf{F}(\mathbf{x}))$ contains a predicted box box_i that has an IoU $\geq \tau$ with some GT box box_{gt} , but their predicted and GT classes do not match, we consider this a class misidentification. Formally:

$$\exists \mathbf{x} \in \mathcal{C}, \exists box_i \in \mathbf{N}(\mathbf{F}(\mathbf{x})), \exists box_{gt} \in \mathcal{G} : \mathbb{I}(\text{class}(box_i) \neq \text{class}(box_{gt})) \cdot \text{IoU}(box_i, box_{gt}) \geq \tau.$$

We want to prove that class misidentification does **not** occur, which is the negation of the bad event, equivalently written as:

$$\forall \mathbf{x} \in \mathcal{C}, \forall box_i \in \mathbf{N}(\mathbf{F}(\mathbf{x})), \forall box_{gt} \in \mathcal{G} : \mathbb{I}(\text{class}(box_i) \neq \text{class}(box_{gt})) \cdot \text{IoU}(box_i, box_{gt}) < \tau.$$

To this end, we can define a worst-case function:

$$\Phi_{\text{cls}}(\mathbf{x}) = \max_{box_i \in \mathbf{N}(\mathbf{F}(\mathbf{x})), box_{gt} \in \mathcal{G}} (\mathbb{I}(\text{class}(box_i) \neq \text{class}(box_{gt})) \cdot \text{IoU}(box_i, box_{gt})),$$

2052 The property holds if and only if: $\sup_{x \in \mathcal{C}} \Phi_{\text{cls}}(x) < \tau$.

2053
 2054 Let \mathcal{Z} be the over-approximation of the pre-NMS network output range $\{F(x)\}_{x \in \mathcal{C}}$ obtained in Part
 2055 1. Since our NMS analysis in Part 2 is applied uniformly over all $y \in \mathcal{Z}$, we can compute an upper
 2056 bound of $\mathbb{I}(\text{class}(box_i) \neq \text{class}(box_{gt})) \cdot \text{IoU}(box_i, box_{gt})$ on \mathcal{Z} over all possible predicted boxes
 2057 and GT pairs:

$$U_{\text{cls}} = \sup_{box_i \in \mathcal{Z}, box_{\text{gt}} \in \mathcal{G}} (\mathbb{I}(\text{class}(box_i) \neq \text{class}(box_{\text{gt}})) \cdot \text{IoU}(box_i, box_{\text{gt}})) .$$

2061 If we can prove $U_{\text{cls}} < \tau$, then it is impossible for any $x \in \mathcal{C}$ and any prediction/GT pair to have an
2062 IoU $\geq \tau$ and a class mismatch. Thus, we can certify that no class misidentification occurs within \mathcal{C} ,
2063 and the property is verified.

Algorithm 6 shows how to compute per-box upper bounds on the misidentification IoU in Part 2.

X.2 EXTENDING TO FALSE APPEARANCES

Algorithm 7 Soundness False Appearance Verification for NMS

Require: Constraints $\mathcal{Z} = \mathcal{H} \setminus \mathcal{S}$; input x ; output y ; set of ground truth boxes \mathcal{G} ; confidence threshold ℓ .

Ensure: Calculate per-box lower bounds $\{\tau_{\text{FA}}(i)\}_{i=1}^{n_x}$ on $\max_{\text{box}_{\text{gt}} \in \mathcal{G}} \text{IoU}(\text{box}_i, \text{box}_{\text{gt}})$.

```

1:  $\{\underline{box}_i\}_{i=1}^{n_x} \leftarrow \text{CONSTRUCT\_ABSTRACT\_BOX}(\mathcal{Z})$ 
2: for all  $\underline{box}_i \in \{\underline{box}_k\}_{k=1}^{n_x}$  do
3:    $\tau_{\text{FA}}(i) \leftarrow 0$                                  $\triangleright$  Initialize lower bound for maximal IoU to GTs of box  $i$ 
4:   if  $\underline{c}_i < \underline{l}$  then
5:     continue                                 $\triangleright$  Box  $i$  can never become a high-confidence detection, ignore it for False
Appearance
6:   end if
7:    $lb \leftarrow 0$                                  $\triangleright$  Lower bound on  $\max_{box_{\text{gt}} \in \mathcal{G}} \text{IoU}(\underline{box}_i, box_{\text{gt}})$ 
8:   for all  $box_{\text{gt}} \in \mathcal{G}$  do
9:      $lb_{\text{gt}} \leftarrow \text{IOU\_LOWER\_BOUNDS}(\underline{box}_i, box_{\text{gt}})$ 
10:     $lb \leftarrow \max(lb, lb_{\text{gt}})$                  $\triangleright$  Aggregate lower bounds to over-approximate  $\max_{box_{\text{gt}}} \text{IoU}$ 
11:   end for
12:    $\tau_{\text{FA}}(i) \leftarrow lb$ 
13: end for
14: return  $\{\tau_{\text{FA}}(i)\}_{i=1}^{n_x}$ 

```

Formalization of the property (bad Event): Given an input constraint set \mathcal{C} , if there exists an input $x \in \mathcal{C}$ and a predicted box $box_i \in N(F(x))$ whose IoU with all GT boxes is less than τ , we consider this a False Appearance:

$$\exists \mathbf{x} \in \mathcal{C}, \exists box_i \in \text{N}(\text{F}(\mathbf{x})), \forall box_{\text{gt}} \in \mathcal{G}, \text{IoU}(box_i, box_{\text{gt}}) < \tau.$$

Equivalently, define the **maximum IoU** for each predicted box with all GT boxes:

$$\text{IoU}_{\max}(box_i, x) = \max_{box_{\text{gt}}} \text{IoU}(box_i, box_{\text{gt}}),$$

The bad event can be written as:

$$\exists \mathbf{x} \in \mathcal{C}, \exists box_i \in N(F(\mathbf{x})) : \text{IoU}_{\max}(box_i, \mathbf{x}) < \tau.$$

We want to prove "no false appearances occur", which is the negation of the bad event:

$$\forall \mathbf{x} \in \mathcal{C}, \forall \mathbf{box}_i \in \mathbf{N}(\mathbf{F}(\mathbf{x})) : \text{IoU}_{\max}(\mathbf{box}_i, \mathbf{x}) \geq \tau.$$

2106 We can further define:

2107
$$\Phi_{\text{FA}}(\mathbf{x}) = \min_{\text{box}_i \in \mathcal{N}(\mathcal{F}(\mathbf{x}))} \text{IoU}_{\text{max}}(\text{box}_i, \mathbf{x}),$$
 2108

2109 and the property holds if and only if $\inf_{\mathbf{x} \in \mathcal{C}} \Phi_{\text{FA}}(\mathbf{x}) \geq \tau.$

2110 Algorithm 7 shows how to compute per-box lower bounds on the maximum IoU to GT boxes in Part 2.

2111 For any given property, we first formalize the attack and verification objective as described in Section 2112 3 and the process above. Then, as in Section 4 and above, we adapt Part 2 of the algorithm (e.g., by 2113 adjusting the MIQP constraints) based on the specific verification objective. We will add a discussion 2114 of these and other potential extensions in the revised manuscript, and specify how Part 2 of the 2115 algorithm should be modified for these two threats.

2116

2117

X.3 EVALUATION

2118

2119 To assess the effectiveness of our proposed method under diverse noise conditions and threat 2120 types, we conduct experiments using four distinct noise models and verify the False Appearance 2121 (FA) detection performance of our YOLO11x model. We define a noise tensor \mathbf{N}_x and set the 2122 perturbation magnitude to $\varepsilon = 1/255$. The specific noise distributions and their corresponding 2123 real-world motivations are outlined below:

2124

- 2125
- **Uniform:** $\mathbf{N}_x \sim \mathcal{U}(-\varepsilon, \varepsilon)$ (Quantization/Uncertainty).
 - **Gaussian:** $\mathbf{N}_x \sim \mathcal{N}(0, (\varepsilon/3)^2)$ (Sensor Readout Noise).
 - **Salt-and-Pepper:** $\pm \varepsilon$ impulse noise with $p = 0.05$ (Transmission Faults).

2126

2127 We randomly select 10 images from the COCO validation set and apply each noise model with 2128 $\varepsilon = 1/255$ to generate noisy inputs. We then evaluate the FA detection verification performance of 2129 our YOLO11x model on these perturbed images. For each input, we draw 10^6 samples from the 2130 corresponding noise distribution to approximate the ground truth. The results are summarized in the 2131 table below:

2132

2133 Table 6: FA Detection Verification Performance under Diverse Noise Models

2134

Model	Noise type	CAR _{FA}	TPR _{FA}	TNR _{FA}	FPR _{FA}	FNR _{FA}
yolo11x	gaussian	100.00%	92.31%	100.00%	0.00%	7.69%
yolo11x	salt and pepper	100.00%	85.71%	100.00%	0.00%	14.29%
yolo11x	uniform	100.00%	92.31%	100.00%	0.00%	7.69%

2135

2136 A detection is considered positive if it remains robust under the corresponding noise model and 2137 negative otherwise. The results indicate that our method sustains a high Certified Accuracy Rate 2138 (CAR) across different noise types, demonstrating that it provides reliable guarantees under diverse 2139 real-world noise conditions and threat types. Moreover, the True Positive Rate (TPR) and True 2140 Negative Rate (TNR) remain consistently high, while the False Positive Rate (FPR) and False 2141 Negative Rate (FNR) stay low, underscoring the method's effectiveness in distinguishing between 2142 robust and non-robust detections.

2143

2144 Overall, these results demonstrate that our method remains reliable across heterogeneous noise 2145 distributions and diverse threat types. This confirms that the proposed framework is broadly 2146 applicable and provides trustworthy robustness guarantees under a wide range of real-world noise 2147 conditions. the algorithm (e.g., by adjusting the MIQP constraints) based on the specific verification 2148 objective. We will add a discussion of these and other potential

2149

2150

2151

2152

2153

2154

2155

2156

2157

2158

2159